

**Aus der Medizinischen Klinik und Poliklinik IV der Ludwig-Maximilians-
Universität München**

Vorstand: Prof. Dr. med. Martin Reincke

**CEACAM1 aggravates renal injury in heterologous
glomerulonephritis**

Dissertation

**zum Erwerb des Doktorgrades der Medizin
an der Medizinischen Fakultät der
Ludwig-Maximilians-Universität zu München**

vorgelegt von

Yao Bai

aus China

Jahr

2020

**Mit Genehmigung der Medizinischen Fakultät
der Universität München**

Berichterstatter: Prof. Dr. med. Markus Wörnle

Mitberichterstatter: Prof. Dr. med. Jens Waschke
Prof. Dr. med. Alexander Buchner

Mitbetreuung durch den
promovierten Mitarbeiter: Dr. med. Dr. Marc Weidenbusch

Dekan: Prof. Dr. med. dent. Reinhard Hickel

Tag der mündlichen Prüfung: 29.10.2020



LUDWIG-
MAXIMILIANS-
UNIVERSITÄT
MÜNCHEN

Dean's Office
Faculty of Medicine



Affidavit

Surname, first name

Street

Zip code, town

Country

I hereby declare, that the submitted thesis entitled

is my own work. I have only used the sources indicated and have not made unauthorised use of services of a third party. Where the work of others has been quoted or reproduced, the source is always given.

I further declare that the submitted thesis or parts thereof have not been presented as part of an examination degree to any other university.

Place, date

Yao Bai
Signature doctoral candidate

The research presented in this thesis was conducted between October 2017 and October 2019 in the department of Cancer Research Institute, Central South University and clinical biochemistry, Medizinischen Klinik und Poliklinik IV der Ludwig-Maximilians-Universität durchgeführt. (Direktor: Herr Prof. Dr. med. Martin Reincke).

Table of contents

1	Introduction.....	1
1.1	Anti-glomerular basement membrane disease.....	1
1.1.1	History.....	1
1.1.2	Epidemiology.....	3
1.1.3	Diagnosis.....	4
1.1.4	Treatment.....	4
1.1.5	Mouse model of anti-GBM nephritis.....	5
1.1.6	Molecular mechanisms of anti-GBM disease.....	6
1.2	Carcinoembryonic antigen-related cell adhesion molecule 1 biology.....	6
1.2.1	CEACAM1.....	6
1.2.2	CEACAM1 in vascular homeostasis.....	8
1.2.3	CEACAM1 in the immune system.....	11
1.2.4	CEACAM1 in kidney disease.....	13
1.3	Aims of this thesis project.....	16
1.4	Hypotheses.....	17
2	Materials and methods.....	18
2.1	Animal experiments.....	18
2.1.1	Mice.....	18
2.1.2	Mice housing.....	18
2.1.3	Mice genotyping.....	18
2.1.4	Narcosis, injectables, sacrifice.....	19
2.1.5	Mice blood collecting.....	19
2.1.6	Organ removal.....	19
2.1.7	Serum tests.....	20
2.1.8	Histological staining and analyses.....	20
2.1.9	Cell culture.....	21
2.1.10	Reverse-transcriptase-quantitative polymerase chain reaction.....	22
2.1.11	Chemicals.....	23

Table of contents

2.1.12	Western blotting	23
2.1.13	Murine primer sequences.....	24
2.1.14	Machines for experiment.....	25
2.1.15	Machine for centrifuges.....	26
2.2	Animal experiments.....	28
2.2.1	Mice housing.....	28
2.2.2	Genotyping.....	28
2.2.3	Anti-GBM disease.....	29
2.2.4	Sacrifice	31
2.2.5	Colorimetric serum test	31
2.2.6	Histological analysis	31
2.2.7	Western blotting.....	36
2.2.8	RNA isolation.....	36
2.2.9	cDNA preparation	37
2.2.10	Quantitative real-time RT-PCR (qPCR).....	37
2.2.11	Cell culture	38
2.2.12	Transwell permeability assay.....	38
2.2.13	Epithelial barrier testing via electric cell–substrate impedance sensing (ECIS)	39
2.2.14	Statistical analyses	40
3	Results	41
3.1	CEACAM1 expression in murine and human kidneys.....	41
3.2	CEACAM1 is upregulated in murine experimental glomerulonephritis.....	43
3.3	CEACAM1 expression in human renal disease	44
3.4	<i>Ceacam1</i> deficiency ameliorates glomerular basement damage in murine glomerulonephritis.....	47
3.4.1	<i>Ceacam1</i> deficiency reduces albuminuria without affecting glomerular filtration rate	47
3.4.2	<i>Ceacam1</i> -deficient mice show less glomerular crescents and tubular cast formation.....	49
3.5	<i>Ceacam1</i> -deficient mice show less intra-renal injury	50

Table of contents

3.6	<i>Ceacam1</i> deficiency decreases intra-renal expression of inflammatory markers and fibrosis	52
3.7	CEACAM1 mediates podocyte loss during murine Anti-GBM disease	55
3.8	<i>Ceacam1</i> deficiency attenuates renal leukocyte recruitment	56
3.9	<i>Ceacam1</i> ^{-/-} enhances barrier function of human epithelial cells	57
3.10	CEACAM1 effects on Anti-GBM disease are likely mediated by expression on endothelial cells	58
3.10.1	CEACAM1 increases endothelial cell loss in anti-GBM mouse model	58
3.10.2	<i>Ceacam1</i> deficiency attenuates glomerular endothelial cell death	61
3.10.3	CEACAM1 expression is upregulated in endothelial cells after stimulation with lipopolysaccharide or histones.....	64
3.10.4	Endothelial cell death leads to increased permeability <i>in vitro</i>	66
3.10.5	Endothelial cell death activates vascular endothelial growth factor and AKT signaling pathways leading to vascular permeability	67
3.10.6	Tight junction proteins decrease in endothelial cells after stimulation with histone and LPS	70
4	Discussion	72
4.1	CEACAM1 is mainly expressed on endothelial cells in the kidney	73
4.2	CEACAM1 aggravates kidney injury in anti-GBM nephritis.....	75
4.3	The VEGF/AKT pathway in the downstream signaling of CEACAM1 in anti-GBM nephritis	76
4.4	CEACAM1-mediated endothelial cell death in anti-GBM nephritis	78
4.5	Limitations of this study	80
5	Summary.....	82
6	Zusammenfassung.....	83
7	List of abbreviations	84
8	References	86
9	Acknowledgement	102

List of Figures and tables

Figure 1 Schematic of the pathogenic mechanisms involved in anti-GBM disease	2
Figure 2 The structure of CEACAM1 protein (modified from [42])	8
Figure 3 CEACAM1 mediates angiogenesis through vascular endothelial growth factor	10
Figure 4 Functions of CEACAM1 in the immune system (modified from [68])	13
Figure 5 NOD-like receptor family CARD domain containing 5 aggravates acute kidney injury by regulating CEACAM1 the signaling pathway.....	15
Figure 6 Mouse model of anti-GBM and the study design	30
Figure 7 Crescent formation in anti-GBM nephritis.....	33
Figure 8 Electric cell-substrate impedance sensing experiments.....	39
Figure 9 The distribution of CEACAM1 expression on normal mice kidney and healthy human kidney (From KIT database)	43
Figure 10 <i>Ceacam1</i> expression in mice kidney after induced anti-GBM disease.....	44
Figure 11 CEACAM1 expression in human kidney	45
Figure 12 The location of CEACAM1 in human Anti-GBM kidney disease	46
Figure 13 Effect of CEACAM1 on albuminuria, BUN, creatinine and GFR	48
Figure 14 Glomerular crescent formation after induced Anti-GBM disease.....	49
Figure 15 Tubular casts formation after induced Anti-GBM disease	50
Figure 16 Injury marker expression was upregulated after being induced in anti-GBM disease.....	51
Figure 17 Inflammation and fibrosis biomarker expression was upregulated after being induced in anti-GBM disease	53
Figure 18 Fibrosis formation after induced in nephritis mice model	54
Figure 19 WT1 ⁺ staining for podocytes after induced in Anti-GBM disease in mice.....	55
Figure 20 Macrophage infiltration in mice model in nephritis	56
Figure 21 Neutrophil infiltration in mice model in nephritis.....	57
Figure 22 Effects of CEACAM1 in human epithelial cell culture model of barrier function	58

List of Figures and tables

Figure 23 CD31 ⁺ staining for endothelial cells after induced in Anti-GBM disease in mice	59
Figure 24 Image from electron microscopy of anti-GBM nephritis.....	60
Figure 25 Endothelial cell death in nephritis	62
Figure 26 Kidney tissue western blots of RIP3 in WT and <i>Ceacam1</i> ^{-/-} mice in nephritis..	63
Figure 27 Endothelial cell death after stimulated with LPS and histone.....	64
Figure 28 <i>Ceacam1</i> expression on endothelial cell after stimulated with LPS and histone	65
Figure 29 Transwell permeability assay with bovine serum albumin.....	66
Figure 30 Gene expression of <i>Vegf</i> and <i>Vegf</i> receptor in GN.....	67
Figure 31 Kidney tissue western blots in WT and <i>Ceacam1</i> ^{-/-} mice in GN.....	68
Figure 32 Angiopietins-1,2 and receptor kinase Tie-1,2 expression on kidney of nephritis	69
Figure 33 Tight junction proteins expression on endothelial cells	71

Declaration

I hereby declare that all of the presented work embodied in this thesis was carried out by me from 10/2017 until 10/2019 under the supervision of Dr. Dr. med. Marc Weidenbusch, Nephrologisches Zentrum, Medizinische Klinik und Poliklinik IV, Innenstadt Klinikum der Universität München. This thesis has not been applied to all or part to any other university for any degree or diploma.

Part of the work was supported by others, as mentioned below:

Tehyung Kim: support for electric cell-substrate impedance sensing experiments

John Hoppe: support for western blotting experiments

Chongxu Shi: support for immunofluorescence imaging.

Viviane Gnemmi, MD PhD: electron microscopy of murine kidney tissues

Date: 02.11.2020

Signature: Yao Bai

Place: Changsha, China

1 Introduction

1.1 Anti-glomerular basement membrane disease

1.1.1 History

Anti-GBM (Anti-glomerular basement membrane) disease is an autoimmune disease presenting as small vessel vasculitis that affects kidney glomerular as well as pulmonary capillaries [1], [2]. In 1958, Stanton *et al.* published a case series of patients suffering from lung hemorrhage and glomerulonephritis and first used the term "Goodpasture's syndrome" in honor of Ernest Goodpasture, who published the first case report already in 1919 [3]–[5]. With the introduction of immunofluorescence techniques, a characteristic GBM deposition of antibodies in a linear fashion was found [6], [7]. Anti-GBM disease manifests in the kidneys and lungs because the antibodies bind to a specific basement membrane antigen shown to be the non-collagenous domain of the alpha 3 chain (Collagen, type IV)[8]–[11]. Anti-GBM disease, which only impacts the kidneys, is known as anti-GBM glomerulonephritis. In addition, rapidly progressive type 1 glomerulonephritis, Goodpasture disease and anti-GBM nephritis point to the same type of disease, though they have different definitions [12]. The term "Goodpasture disease" was first used in 1958 by Tange [4] and is used to refer to patients with anti-GBM antibodies. The co-presentation of anti-GBM and pulmonary hemorrhage from any cause is referred to as "Goodpasture syndrome" whereas "anti-GBM disease" includes a wider range of kidney and lung diseases [1], [13], [14]. The general disease blueprint is shown in Figure 1.

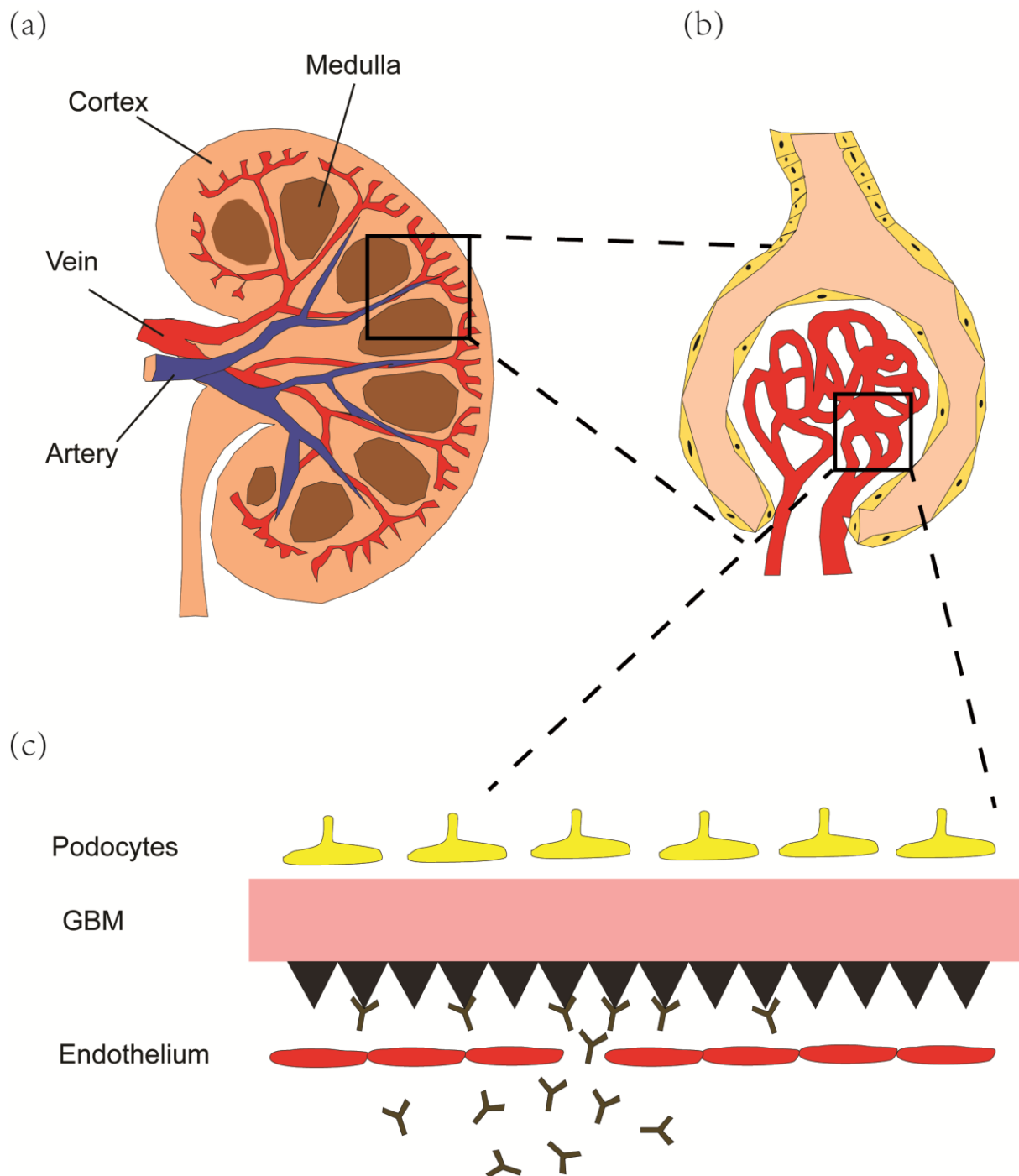


Figure 1 Schematic of the pathogenic mechanisms involved in anti-GBM disease

Anatomy of the longitudinal section of the kidneys, showing the medulla, cortex, vein, and artery (a). Magnified glomerulus, the main filtration unit of the kidney (b). Detailed ultrastructure of the glomerular basement membrane (c). Antibodies in the serum pass through the endothelium and bind to the GBM membrane; antibody deposition in the GBM causes inflammation and injury thereby initiating and promoting disease progression.

1.1.2 Epidemiology

The incidence and prevalence of anti-GBM diseases in the population are limited [15], [16]. Although there are no definite epidemiological data on the incidence of the disease, it is estimated to be less than one case per million per year [15]. The incidence rates in Europe and Asia are higher than in African, supporting a genetic susceptibility to the disease [1], [15], [17]. Some studies indicate that disease outbreaks and epidemics are seasonal, so environmental factors may play a role, especially influenza A, for which an association with the development of anti-GBM disease has been shown [8], [18]–[22].

Resistance to anti-GBM disease has been shown to be closely related to certain genetic factors. Despite limited big data-related epidemiological studies, genetic analyses have confirmed this relationship; for example, anti-GBM disease susceptibility is related to the Fc gamma receptors [22]–[24]. The association between human HLA (leukocyte antigen) and anti-GBM disease is better defined, as the HLA-DR2 haplotype is found in almost 80% of patients [25]. A hierarchy of associations has been recognized by genotyping studies with specific DRB1 alleles, revealing the protective effects of the DRB1*01 allele and the susceptibility associated with the DRB1*03 and DRB1*04 alleles [21], [22]. These alleles are common in the general population and are related to many other autoimmune diseases including Sjogren syndrome, explaining why genotyping is not usually performed in clinical practice. Anti-GBM disease is one cause of the clinical entity “rapidly progressive glomerulonephritis”. Anti-GBM antibodies and the classical histologic presentation of anti-GBM disease are detected in almost 10%-15% of patients who have rapidly progressive glomerulonephritis; again, the percentages vary between different populations [26], [27].

1.1.3 Diagnosis

AKI (Acute kidney injury) is characterized by a rapid kidney function loss and an increase in serum creatinine concentration, mainly due to a decrease in the glomerular filtration rate [28]. In the case of AKI, early serological detection of anti-GBM antibodies can guide the onset of treatment and improve patient outcomes [29]. Many clinicians increasingly rely on this test to affirm the diagnosis and some believe that kidney biopsy has possibly become obsolete for establishing the diagnosis [30]. There are certain shortcomings in this strategy, firstly, in anti-GBM disease the amount of histological injury rather than the titer of autoantibodies determines kidney recovery and hence prognosis, as well as the likelihood of recurrence [30]. Secondly, in polyclonal activation states, for example, HIV infection and multiple kidney pathologies, false positive detection of anti-GBM antibodies may occur [30]. Ultimately, diagnosis may be postponed until a renal biopsy is performed in rare patients who have no circulating anti-GBM antibodies [30]. The diagnosis of serologic diseases is based upon enzyme-related immunosorbent assays that are now standard antibody detection methods. The specificity and sensitivity of such assays is high, ranging from 90% to 100% and 94.7% to 100%, respectively [31].

1.1.4 Treatment

Considering that the main pathogenic mechanism of anti-GBM disease is antibody-specific binding to the basement membrane, rapid removal of antibodies from the blood by plasma exchange is the main treatment method for this disease [1]. Other treatment options used in clinical practice include corticosteroids and cyclophosphamide [1]. The main therapeutic principles are to ameliorate end-organ inflammation and inhibit autoantibody production, respectively [1] [32]. Often, doctors do not treat patients with one method exclusively, but use a combination of two methods with complementary functions to

optimize treat outcomes [32]. For example, plasma exchange combined with immunosuppressants improves renal function and survival compared with the use of immunosuppressants alone [8]. Patients with moderate renal impairment experienced significant recovery after treatment with plasma exchange and immunosuppression, but patients with severe renal failure experienced limited therapeutic benefit [8], [27], [33]. In one study, 19 patients with anti-GBM disease received plasma exchange, prednisolone and cyclophosphamide. The data demonstrated that patients who have a creatinine concentration of less than 500 $\mu\text{mol/L}$ showed “100% patient survival and 95% renal survival at 1 year and 84% patient survival and 74% renal survival at last follow-up (median 90 months)” [8]. Therefore, patients who have severe renal function failure should be treated with plasma exchange combined with immunosuppressive agents as soon as possible to restore the renal function of patients early in the disease; the possibility of renal recovery in patients requiring immediate dialysis is almost zero.

1.1.5 Mouse model of anti-GBM nephritis

The anti-GBM mouse model was established in 1932 by Masugi *et al.* [34]. It should be noted that the mouse model can acutely be established both by a single large dose of antibodies causing to crescent GN (known as the “heterologous model”) or by repetitive small doses of anti-GBM antibodies sub-acutely causing to immune complex GN (known as the “autologous mode) [35]. In addition, the dose of antibody administered, animal species used for the model, as well as the intensity of the host's immune response, all affect the severity of the model. For example, chronic glomerulonephritis frequently develops in the rat during the heterologous phase showing predominantly exudative lesions [34]. The heterologous model was used in our experiments as it causes actual anti-GBM disease rather than immune-complex disease observed using the autologous model.

In this research, 24 hours and 7 days time-points were used. Serum and urine were collected on days -1, 0, 1 and 7. Anti-GBM serum or phosphate-buffered saline were injected on day 0, and mice were euthanized on days 1 and 7. The disease pathology is expected to peak around days 1 or 2 after serum injection, then slowly recover [36].

1.1.6 Molecular mechanisms of anti-GBM disease

It is well-established that nephritis can cause AKI. Although anti-GBM nephritis is a rare disease, it can cause kidney damage at a rapid rate and lead to end stage renal disease within weeks of onset. This is because anti-GBM antibodies can rapidly bind to the basement membrane, thereby activating the complement system of the immune system, and glomerular basement membrane endothelial cells and podocytes are subsequently damaged and vascular permeability is increased, causing albuminuria as well as hematuria as clinical manifestations of AKI. Although not fully elucidated, the mechanisms involved include podocyte loss [37][38], increased vascular permeability [39][40] and inflammation [41].

Thus, to tackle this problem, we need to explore molecular mechanisms that can prevent the production of antibody or antibody binding and further aggravate kidney damage. More basic research on the mechanism of the disease needs to be done to ultimately achieve better treatment outcomes for anti-GBM nephritis.

1.2 Carcinoembryonic antigen-related cell adhesion molecule 1 biology

1.2.1 CEACAM1

CEACAM1 (Carcinoembryonic antigen-related cell adhesion molecule 1), also called CD66a, is a highly glycosylated cellular adhesion molecule and a known carcinoembryonic antigen [42]–[44]. CEACAM1 has several distinguishable isoforms in mice, two of which

contain four extracellular domains, respectively, one significantly longer (CEACAM1-4L) than the other (CEACAM1-4S) [42]. The extracytoplasmic Ig-like domains and long and short cytoplasmic domains of the different CEACAM1 isoforms are shown in Figure 2 [45], [46]. Additionally, the human CEACAM1-L isoform contains ITIMs (Two immunoreceptor tyrosine receptor inhibition motifs), whereas ITSMs (Two immunoreceptor tyrosine-based switch motifs) in mouse CEACAM1-L result in a distinctive CEACAM1-L structure, which is the structural basis for CEACAM1 function and signal transduction (AKT, RIPK3) [47], [48]. As described above, negative signaling is mediated by ITIM-containing CEACAM1 (CEACAM1-L), whereas CEACAM1-S isoforms mediate positive signaling, and different quantitative relations of CEACAM1-L to CEACAM1-S expression are related to the development of different diseases [49]. CEACAM1 is expressed in a variety of cells, such as hematopoietic cells, epithelial cells as well as endothelial cells, which have different biological functions, such as cell adhesion as well as cell signaling. CEACAM1 impacts the immune response of the host and the integrity of epithelial cells and homeostasis, which is connected to cell proliferation and differentiation [50], [51].

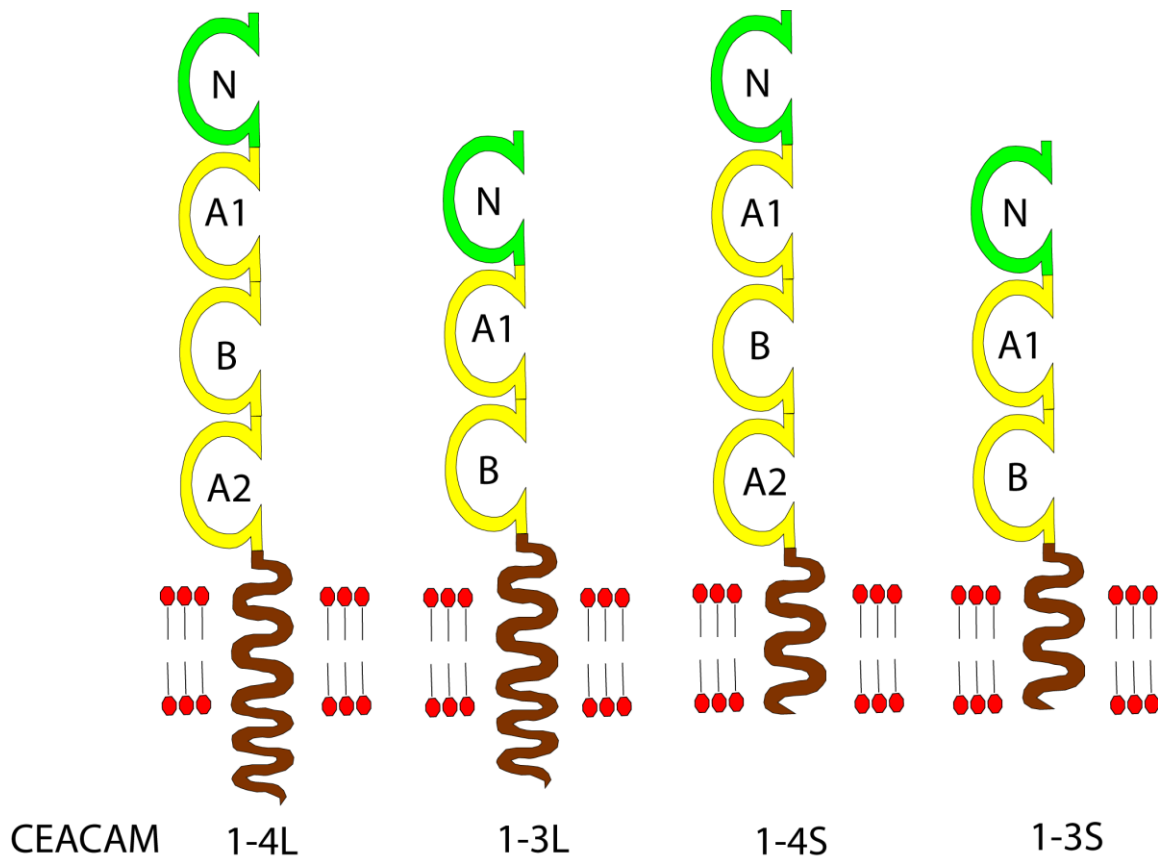


Figure 2 The structure of CEACAM1 protein (modified from [42])

From left to right are the various major isoforms of CEACAM1, 1-4L, 1-4S, 1-3L and 1-3S. Red indicates the membrane, brown indicates the transmembrane domain long cytoplasmic tail (two regions on the left) and short cytoplasmic tail (two regions on the right), green indicates the N-terminal IgV-like domain and yellow indicates the IgC-like domains of A1, B and A2.

1.2.2 CEACAM1 in vascular homeostasis

CEACAM1 is also expressed in a lot of cells and tissues, such as immune cells and activated endothelial cells [42] [52]. During the last decade, a lot of evidence in vascular homeostasis has revealed that CEACAM1 plays a role in vascular remodeling, controlling the function of the endothelial barrier and in the formation of blood vessels [45][53].

Vasculogenesis refers to the process by which undifferentiated mesodermal precursor cells form blood vessels [54]. VEGF (vascular endothelial growth factor) and the VEGFR1/2 (vascular endothelial growth factor receptor 1/2) ratio are critical for the

formation and differentiation of hemangioblasts into endothelial cells [55]. Some other vital molecules in vasculogenesis are cell adhesion molecules such as CEACAM1, as illustrated in research showing that CEACAM1 is expressed in rat brain vessels [56]. More recently, it has been shown that CEACAM1 is a potent stimulant of VEGF-mediated angiogenesis [57], [58] (Figure 3). The loss of CEACAM1 could, therefore, be expected to have serious implications for the growth of the vascular system; however, it has been demonstrated that vasculogenesis is unimpaired in *Ceacam1*^{-/-} mice [59]. This may be because there is another molecule that can substitute for CEACAM1 function during development *in vivo*. Taken together, this demonstrates a crucial role of CEACAM1 during vasculogenesis, while at the same time its role during development is redundant to some extent as *Ceacam1*^{-/-} mice are viable.

VEGF is an essential angiogenic regulator, therefore, CEACAM1 also plays an important role in the stimulation of endothelial cell proliferation and enhancing vascular permeability, which is an integral part of VEGF-mediated angiogenesis [59]–[61]. The regulation of vascular permeability is crucial for normal tissue integrity, hence, one of the pathological characteristics associated with tumor angiogenesis is abnormal vascular permeability. Cell adhesion molecules is very important to vascular morphogenesis as well as endothelial signaling in complex angiogenic systems. CEACAM1 is an adhesion molecule with pro-angiogenic activity and a major effector of VEGF. VEGF can upregulate the expression of CEACAM1, and anti-CEACAM1 antibodies block VEGF-induced angiogenesis [62]. Previous research revealed that the exogenous application of soluble CEACAM1 has angiogenic characteristics and can be used as a morphological effector of VEGF [57]. CEACAM1 also has an crucial function in the formation of vascular integrity as well as vascular networks *in vivo*, especially during normal neovascularization and is expressed in neovascularization during physiological angiogenesis, including endometrial hyperplasia and immature

neovascularization of different tumors [63], [64]. In a study in murine *Ceacam1*^{-/-} lung endothelial cells (MLECs), the VEGF-induced signaling pathway exposed a defective endothelial nitric oxide synthase signaling pathway with reduced nitric oxide production. “CEACAM1 is tyrosine-phosphorylated upon VEGF treatment in a SHP-1- and Src-dependent manner, and the ITIM motif of CEACAM1 is key to CEACAM1 phosphorylation and NO production” [65]. In summary, this links CEACAM1 to important VEGFR2/Akt/eNOS-mediated vascular permeability pathways.

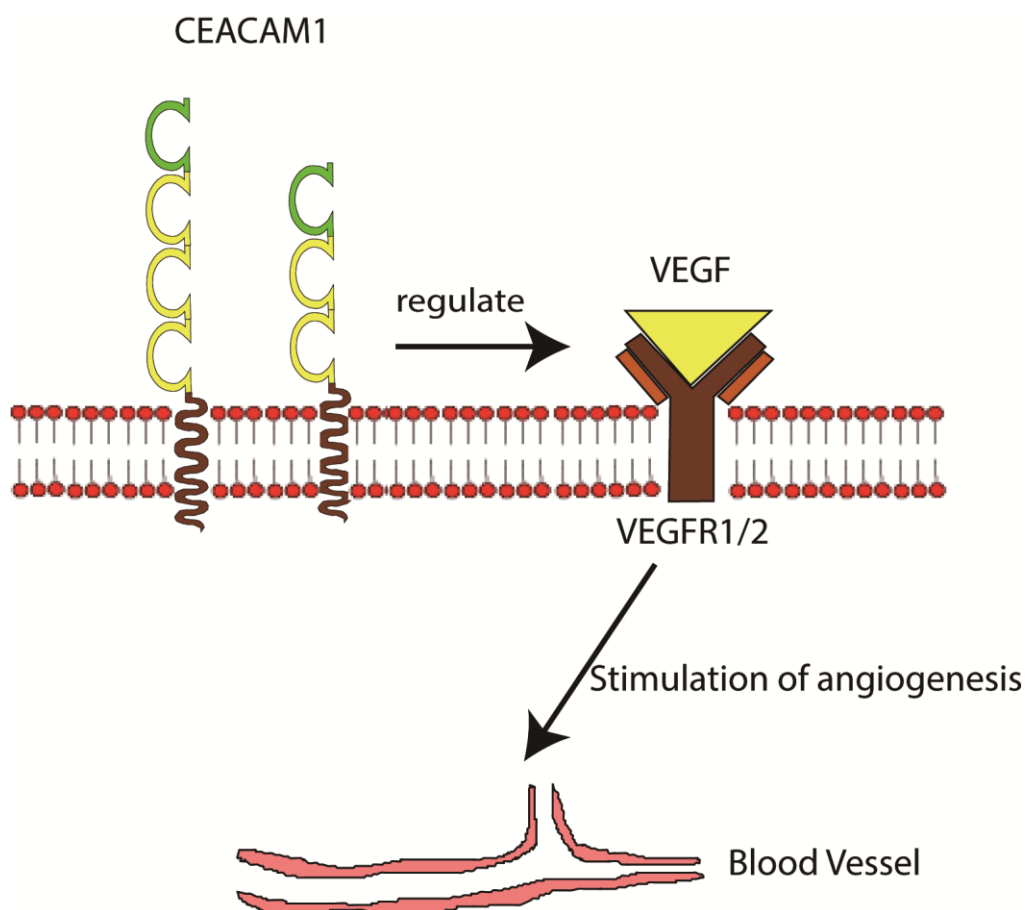


Figure 3 CEACAM1 mediates angiogenesis through vascular endothelial growth factor

The effects of CEACAM1 in angiogenesis. CEACAM1 can regulate the VEGF signaling pathway promoting angiogenesis.

1.2.3 CEACAM1 in the immune system

Numerous research have investigated the function of CEACAM1 in the immune system, including its role macrophages, neutrophils, in particular, in T cells and natural killer cells [66]–[69]. Function of CEACAM1 in the immune system is summarized in Figure 4.

CEACAM1 plays a regulatory function in some immune cells, particularly activated T cells where it is highly expressed in response to interleukin-2 (IL-2) stimulation [70], [71]. As outlined above, CEACAM1 comprises two subtypes, CEACAM1-L and CEACAM1-S. The main function of CEACAM1-L is to inhibit T cell activation, while CEACAM1-S promotes T cell activation [72], [73]. CEACAM1-L domain ITIMs mediate the inhibitory function of CEACAM1-L, which do not exist in CEACAM1-S [74]. Above ITIMs are phosphorylated by a lot of Src-associated tyrosine kinases, such as the recruited tyrosine phosphatases, SHP-1 (Src-homology 1 domain-containing protein tyrosine phosphatase) as well as SHP-2 (Src-homology 1 domain-containing protein tyrosine phosphatase). In summary, it has been shown that CEACAM1-L is an inhibitor of T cells through ITIM motifs and mediates its function via SHP-1 and SHP-2. CEACAM1 also functions along with TIM-3 (T-cell immunoglobulin and mucin-domain containing-3) in T cells. The exhausted phenotype of T cells is also demonstrated by CEACAM1 and TIM-3 co-expression [75]. TIM-3 and CEACAM1 is co-expressed on T cells during tolerance induction, exhibits biochemical relationships with CEACAM1, as well as acts as a heterophilic CEACAM1 ligand [75]. CEACAM1 induces TIM-3 localization on the T cell by promoting TIM-3 maturation, with double expression of CEACAM1 and TIM-3 being a biomarker of exhausted T cells.

NK cells are important lymphocytes for innate immunity as well as the expression of CEACAM1 protects against NK-mediated tumor cell killing. Several CEACAM1-mediated NK inhibition models have been proposed. Silencing of *CEACAM1* in human cancer cells increases the level of NK cell surface activating ligands, whereas overexpression of

CEACAM1-3S prevents NK cells from being activated [76]. The expression of CEACAM1 on tumor cells leads to NK-mediated immune escape through shielding the ligand of the NK cell surface receptor, although CEACAM1-L inhibits NK cell activation is not fully understood, the impact is clear.

B cells are specialized antigen presenting cells (APC), the primary role of which is to secrete antibodies. CEACAM1 is engaged in the function of B cells, although there is some controversy on the role of CEACAM1 in this cell type [52], [77], [78]. Recent studies have shown that CEACAM1 is a crucial factor for the survival of B cells, affecting not only the number of B cells, but also their functionality as antibody producers [77], [79]. The effect of CEACAM1 on naive B cells is limited, whereas there is significant reduction in the number of mature B cells in CEACAM1 knockout mice [80]. CEACAM1 may therefore have crucial function in the survival of B cells specifically during the propagation of an immune response. The expression of CEACAM1 on human B cells is less clear; whereas, CEACAM1 does play a vital role in the human B cell line [78].

In neutrophils, CEACAM1 plays an inhibitory role, although its role is more complicated in neutrophils than in other immune cells. CEACAM1 is expressed in a small proportion of resting neutrophils, where it is transferred from the intracellular environment to the cell surface after neutrophils have been activated [81], [82]. In addition, *CEACAM1* silencing can induce apoptosis of human neutrophils using the SHP1-mediated pathway. Consistent with this result, in tongue squamous cell carcinoma, CEACAM1 upregulation has been linked to neutrophil infiltration that is associated with poor clinical outcomes [83]. In addition, *Ceacam1*-deficient mice showed accelerated mortality compared with wild-type mice in neutrophil induced immunopathologies, indicating that neutrophil-induced immunopathological modifications occur without sufficient CEACAM1 expression, and indeed this phenotype is reversed by a restored expression of CEACAM1 [68].

The function of CEACAM1 in macrophages has been investigated and CEACAM1 can bind to macrophages to prevent apoptosis via the PI3K / AKT pathway [68].

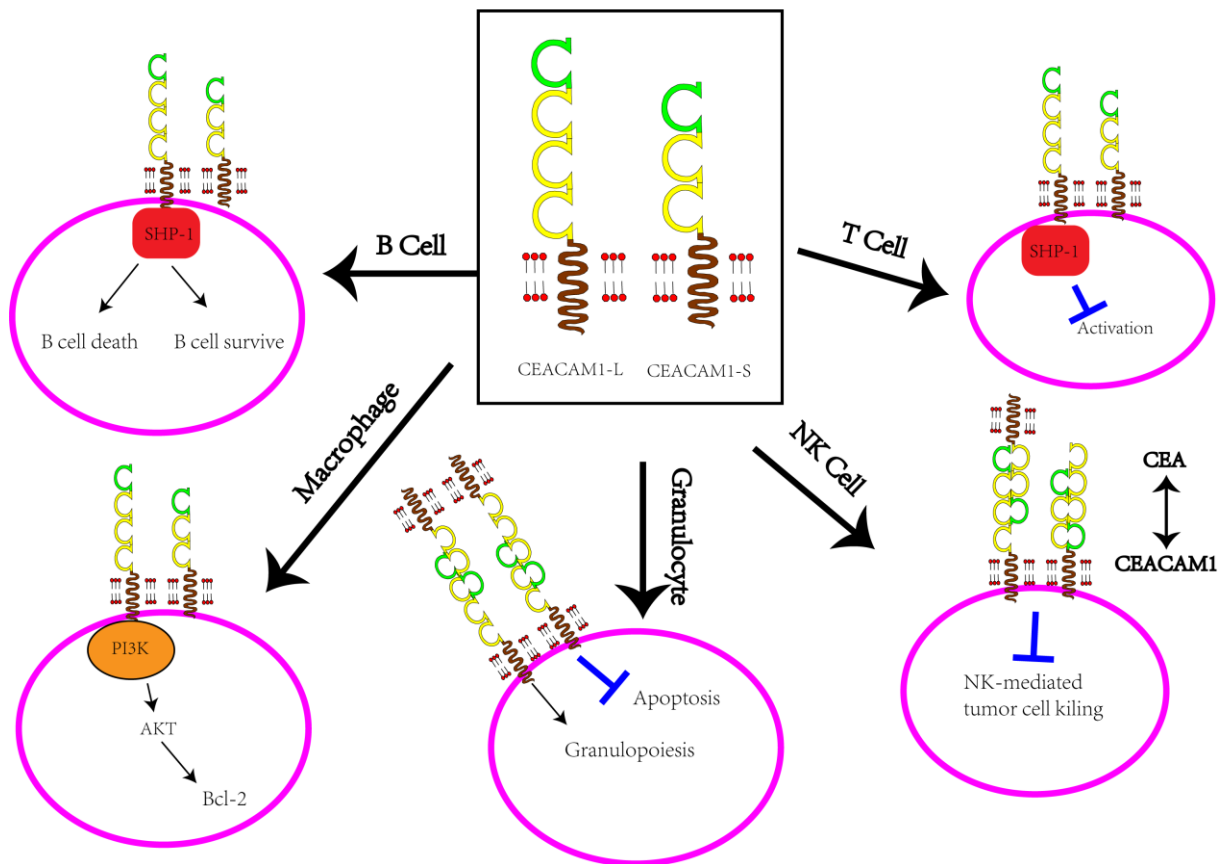


Figure 4 Functions of CEACAM1 in the immune system (modified from [68])

B cell: B lymphocyte, SHP-1: Src homology region 2 domain-containing phosphatase-1, PI3K: phosphatidylinositol 3-kinases, AKT: Protein kinase B, Bcl-2: B-cell lymphoma 2, NK cell: Natural killer cells, T cell: T lymphocytes, CEA: Carcinoembryonic antigen.

1.2.4 CEACAM1 in kidney disease

Most data on the functions of CEACAM1 in the kidney are derived from studies on renal cell carcinoma. Initial studies have demonstrated that CEACAM1 is expressed in renal epithelial cells (proximal tubular), whereas clear cell carcinoma is generated from proximal renal tubules [84]. Therefore, CEACAM1 can be considered to regulate the immunogenicity of renal cell carcinoma and expression was downregulated in almost all patients with renal cell carcinoma, and this type of downregulation was comparable to other cancers [85], [86].

Importantly, the complete loss of CEACAM1 expression has also been noted in renal adenomas, indicating that CEACAM1 downregulation or loss is an early occurrence in the development of renal cell carcinoma [85]. This observation strongly indicates that CEACAM1 plays a vital role in tumor suppression in renal cell carcinoma.

Acute renal injury (AKI) often caused by ischemia / reperfusion (IRI), sepsis and toxins, is a prevalent medical complication globally with high morbidity and mortality [83], [87]. AKI is related to a poor prognosis despite advancements in kidney replacement therapy. AKI is a condition of rapid renal excretion failure, frequently accompanied by oliguria that usually occurs within hours or days. Recovery of renal function is common in most patients; however, many still require dialysis or have severe renal impairment. Because high mortality rates are associated with serious AKI, this pathology should not be overlooked clinically. To date, there is limited research on the role of CEACAM1 in kidney nephritis. Recently, one study [88] showed that the NLRC5 (NOD-like receptor family CARD domain containing 5) negatively regulates CEACAM1 and leads to tubular epithelial cell death through the PI3K/AKT pathway, ultimately leading to AKI, as shown in Figure 5. However, there is insufficient knowledge about CEACAM1 and its function in the kidney, other than during tumorigenesis [89]–[93]. Therefore, the role of CEACAM1 in renal biology, especially under inflammatory conditions such as anti-GBM disease needs further clarification.

CEACAM1 has been found to play a vital role in the immune response, but to date, no research has been reported on the involvement of CEACAM1 in anti-GBM nephritis. My thesis will focus on the function of CEACAM1 in anti-GBM nephritis.

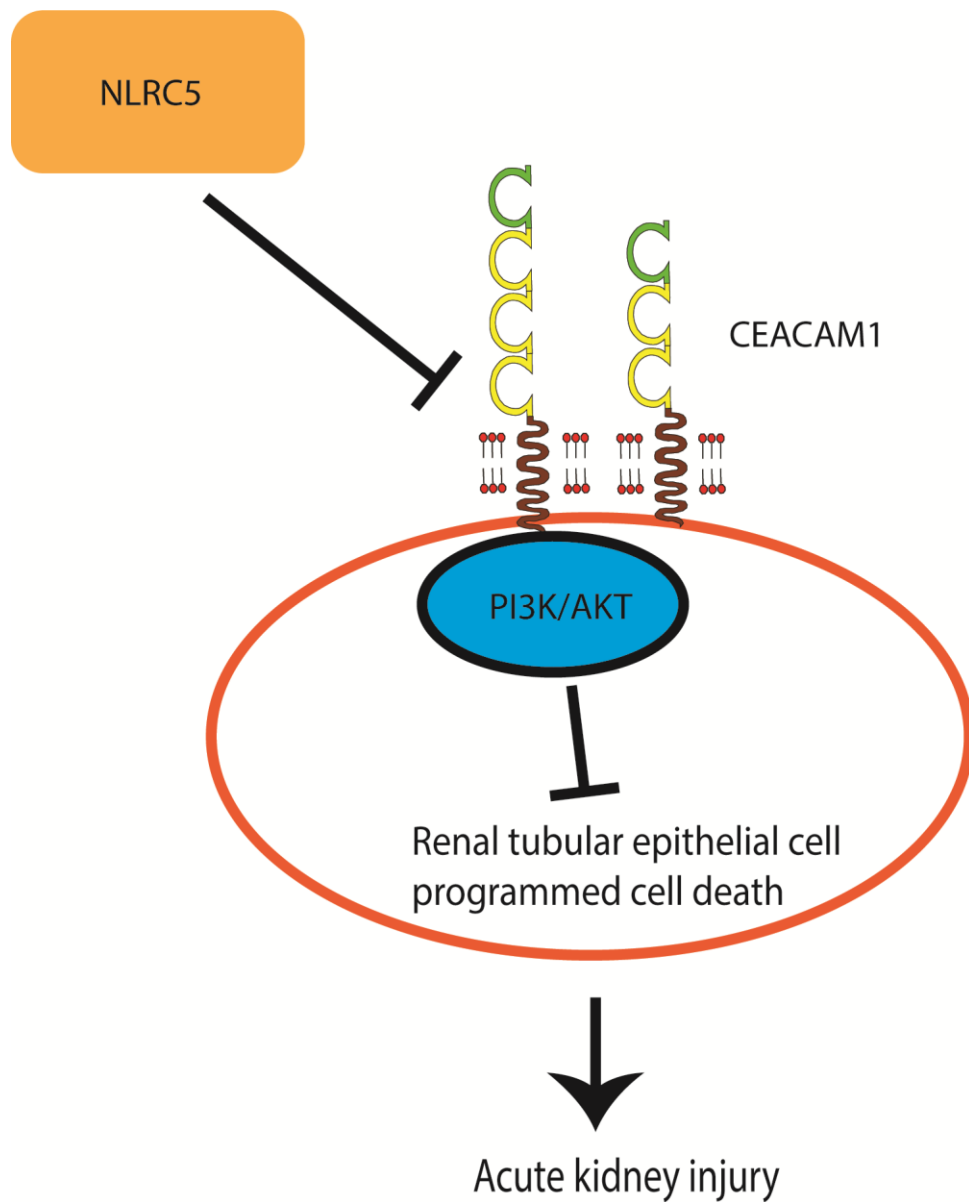


Figure 5 NOD-like receptor family CARD domain containing 5 aggravates acute kidney injury by regulating CEACAM1 the signaling pathway

NOD-like receptor family CARD domain containing 5 leads to renal injury through promoting tubular epithelial cell programmed cell death through PI3K/AKT signaling, which is related to the negative regulation of CEACAM1.

1.3 Aims of this thesis project

As described in previous studies, CEACAM1 plays a role in many physiological settings, such as tumor and vascular homeostasis. We aimed here to characterize its role during kidney inflammation by using human and murine tissue sections from normal and inflammatory conditions as well as *Ceacam1*^{-/-} mice and the use of anti-GBM disease.

First, the expression of CEACAM1 in normal mouse and human kidneys was compared to diabetic nephropathy as well as anti-GBM disease.

To further explore the function of CEACAM1 in anti-GBM disease, anti-GBM disease was induced in *Ceacam1*^{+/+} and *Ceacam1*^{-/-} mice and their phenotypes were compared. Finally, In vitro experiments were performed to investigate the deeply mechanisms of the phenotypes discovered in *Ceacam1*^{-/-} mice.

1.4 Hypotheses

Anti-GBM disease is a rare vasculitis that affects the renal and pulmonary capillary beds. This is a typical autoimmune disease induced by direct pathogenic autoantibodies that target a specific autoantigen expressed in the basement membrane of these organs; however, the reasons for, and the mechanisms by which, these autoantibodies are produced remain unclear. Clinically, the means of controlling GBM are still limited, with the current main methods being plasma exchange and immunosuppressive therapy.

CEACAM1 plays a different role in various inflammatory reactions and diseases, functioning as an anti-inflammatory factor or a pro-inflammatory factor depending on the cellular context.

However, the role of CEACAM1 in anti-GBM disease remains unclear. My project aimed to explore the role of CEACAM1 in anti-GBM nephritis to test the hypotheses below:

I hypothesized that

1. CEACAM1 plays a pathogenic role in the heterologous anti GBM disease mouse model of crescentic anti-GBM nephritis.
2. CEACAM1 deficiency protects against anti-GBM nephritis and prevents further development of the disease and this effect is likely mediated by CEACAM1 on endothelial cells.

2 Materials and methods

2.1 Animal experiments

2.1.1 Mice

C57/BL6/J	SJA Laboratory Animal company/ Changsha/C
<i>Ceacam1</i> ^{-/-} C57/BL6/J	PD Dr. Bernhard B. Singer/ UK Essen

2.1.2 Mice housing

Standard chow	SJA Laboratory Animal company/ Changsha/ C
Bedding	SJA Laboratory animal company/ Changsha/C
Nestlets	SJA Laboratory animal company/ Changsha/C
Makrolone cages (type 2)	SJA Laboratory animal company/ Changsha/ C
Polycarbonate retreats	SJA Laboratory animal company/ Changsha/C

2.1.3 Mice genotyping

Magnesium-chloride hexahydrate	Merck/ Darmstadt/ G
Potassium-chloride MSDS	Merck/ Darmstadt/ G
Gelatine solution	Sigma-Aldrich/Munich/ G
Proteinase K	Merck/ Darmstadt/ G
TRIS hydrochloride	Roth/ Karlsruhe/ G
NP-40	Sigma/ Munich/ G
10 XThermopol buffer	New England BioLabs/ Frankfurt/ G
Tween20	Sigma/ Munich/ G
Taq/DNA/Polymerase	New England BioLabs/ Frankfurt/ G
dNTP Mix (1,25mM)	Fermentas/ St. Leon-Rot/ G
Agarose	Invitrogen/ Karlsruhe/ G

Ethidium bromide solution	Sigma/ Munich/ G
Bromophenol/blue	Roth/ Karlsruhe/ G
Glycerine (1L)	Fermentas/ St. Leon-Rot/
Xylene-cyanol FF	G Roth/ Karlsruhe/ G
DNA/ladder	Sigma/ Munich/ G
TRIS (500g)	Roth/ Karlsruhe/ G
Boric-acid powder	Roth/ Karlsruhe/ G

2.1.4 Narcosis, injectables, sacrifice

Revertor	CP-Pharma/ Burgdorf/ G
Isofluran-Forene	Abbott/ Wiesbaden/ G
Vaporizer for Forene (100 Series)	Smiths Medical PM/ Norwell/ America
Surgical/forceps	Medicon/ Tuttlingen/ G
Anatomical/forceps	Medicon /Tuttlingen/ G
Scalpel	Pfm medical ag/ Cologne/ G
Scissors (Surgical)	Medicon/ Tuttlingen G
Sheep anti-rat GBM serum	Probetex Inc./ San Antonio/ America
Clip/Applying/Forceps	Medicon/ Tuttlingen/ G

2.1.5 Mice blood collecting

Eppendorf-tubes (1,5 ml)	TPP/ Trasadingen/ Switzerland
Micropipettes(20µl)	Brand/ Wertheim/ G
EDTA	Biochrom KG/ Berlin/ G

2.1.6 Organ removal

Shandon-Formal-Fixx (10%)	Thermo Fisher Scientific/ Waltham/ America
Cassettes	NeoLab/ Heidelberg/ G
RNAlater®Storage Solution	life Technologies/ Darmstadt/ G

2.1.7 Serum tests

Mouse Albumin ELISA Kit	Bethyl Laboratories/ Montgomery/ American
BUN kit	DiaSys Diagnostic Systems/ Holzheim/ G
Creatinine kit	DiaSys Diagnostic Systems/ Holzheim/ G

2.1.8 Histological staining and analyses

Ethanol Solution	Merck/ Darmstadt/ G
Ammoniumpersulfate	Bio-Rad Munich G
Xylenes	Merck/ Darmstadt/ G
Periodic acidSchiff	Bio-Optica/ Mailand/ Italy
Paraffin Powder	Merck/ Darmstadt/ G
Masson Goldner's Trichrom kit	Morphisto/ Frankfurt/ G
Methanol Solution	Merck/ Darmstadt/ G
H2O2	Biosciences/ San Diego/ America
Weigert's iron hematoxylin	Morphisto/ Frankfurt/ G
Hematoxylin	Merck/ Darmstadt/ G
Eosin	Sigma/Aldrich/ St. Louis America
Thiosemicarbazide	Sigma/Aldrich/ St. Louis/ America
Methenamine	Sigma/Aldrich/ St. Louis/America
Disodium Tetraborate	Carl Roth/Karlsruhe/ G
Silver-nitrate	Sigma/Aldrich/ St. Louis/America
Formaldehyde Solution	Fisher/ Waltham/America
Hydrogen-Nitrate	Sigma/Aldrich/ St. Louis/ America
Avidin powder	Vector/ Burlingame/ America
GoldChloride	Sigma/ St. Louis/ America
Antigen/unmasking	Vector/ Burlingame/America
Periodic/acid	Sigma/Aldrich/ St. Louis/America
Methyl green	Sigma/ Munich/ G
ABC substrate solution kit	Vector/ Burlingame/ America
VectaMount® mounting medium	Vector/ Burlingame/ America
Biotin powder	Vector/ Burlingame/ America

Anti-F4/80 -Antibody	Bio-Rad / Hercules/ America
Lotus tetragonolobus lectin (LTL)	Vector Labs/ Burlingame/ America
Anti-CEACAM1 -Ab	Prof. B. Singer/ Essen/ G
Anti-neutrophil/Ly6B.2-Antibody	BioRad/ Munich/ G
Fibrinogen	Abcam/ Cambridge/ UK
SuperFrost® adhesion slides	Menzel / Braunschweig/ G
TUNEL kit	Roche/ Mannheim/ G
Anti-CD31-Antibody	Dianova/ Hamburg/ G
WT-1	Cell signaling/ Danvers/ MA
Mac-2	Cedarlane/ ON/ Canada
Anti-THP-Antibody	Cedarlane/ Burlington/ Canada
Nephrin	Acris Antibodies GmbH/ Herford/ G

2.1.9 Cell culture

96-well plates	TPP/ Trasadingen/ Switzerland
24-well plates	Nunc/ Wiesbaden/ G
6-well plates	Costar Corning/ Schiphol/ Netherlands
RIPM-medium	GIBCO/Invitrogen/ Paisley/ UK
DMEM-medium	Invitrogen/ Karlsruhe/ G
8-well arrays (ECIS)	Ibidi/ Martinsried/ G
Tubes (1.5, 2 mL)	TPP/ Trasadingen/ Switzerland
Ultrapure- FCS	Hyclone/ Logan/ America
Cell culture dishes (35x10mm)	Becton Dickinson/ Franklin Lakes/ America
PBS Solution(1x)	PAN Biotech/ Aidenbach/ G
Fetal bovine serum	Biochrom KG/ Berlin/ G
Tubes (15, 50 mL)	TPP/ Trasadingen/ S
Tissue culture flasks 150 cm ²	TPP/ Trasadingen/ S
Penicillin - Streptomycin	PAA Laboratories/ Pasching/ Austria
Plastic histocassettes	NeoLab/ Heidelberg/ G
Cell culture dishes (100x20mm)	TPP/ Trasadingen/ S
Cell culture dishes (150x20mm)	TPP/ Trasadingen/ S

Needles	Drogheda/ Ireland
Pipette's tip (1-1000 μ L)	Eppendorf/ Hamburg/ G
Microscope slides	Menzel-Gläser/ Braunschweig/ G
Syringes	Becton Dickinson/ Heidelberg/ G
Preseparation Filters	Miltenyl Biotec/ Bergish Gladbach/ G

2.1.10 Reverse-transcriptase-quantitative polymerase chain reaction

2.1.10.1 RNA Isolation

100 % Ethanol	Merck/ Darmstadt/ G
RNase/free DNase	Qiagen- Strasse 1 / Hilden/ G
RNA Kit	Ambion/ Darmstadt/ G
β -Mercaptoethanol	Roth/ Karlsruhe/ G

2.1.10.2 cDNA Synthesis

Reverse Transcriptase "SS-II"5	Invitrogen/ Karlsruhe/ G
Diethylpyrocarbonate	Sigma/ München/ G
0,1 M Dithiothreitol	Invitrogen/ Karlsruhe/ G
Hexanucleotide-Mix	Roche/ Mannheim/ G
linear acrylamide	Ambion/ Darmstadt/ G
25 mM dNTPs	GE Healthcare/ Munich/ G
RNAsin	Promega/ Mannheim/ G
x FS buffer solution	Invitrogen/ Karlsruhe/ G

2.1.10.3 Quantitative polymerase-chain reaction

Bovine serum albumin	Fermentas/ St. Leon-Rot/ G
PCR optimization kit	Bitop-AG/ Witten/ G
dNTPs/25 mM	Fermentas/ St. Leon-Rot/ G
Taq-buffer/10x	Fermentas/ St. Leon-Rot/ G
SYBRgreen I	Sigma/ Munich G
96-well plates/LightCycler	Roche/ Mannheim/ G

PCR-Primer/300 nM	Metabion/ Martinsried/ G
MgCl ₂ /25 mM	Fermentas/ St. Leon-Rot/ G

2.1.11 Chemicals

Bovines Serum Albumin	Roche Diagnostics/ Mannheim/ G
Potassium-dihydrogenphosphate	Merck/ Darmstadt/ G
DEPC	Fluka/ Buchs/ Switzerland
Sodium-acetate	Merck/ Darmstadt/ G
TEMED	SCBT/ Santa Cruz/ CA
Sodium-citrate	Merck/ Darmstadt/ G
Penicillin	Sigma/ Deisenhofen/ G
Disodium-hydrogenphosphate	Merck/ Darmstadt/ G
Tissue Freezing Medium	Leica/ Nussloch/ G
Potassium-hydroxide	Merck/ Darmstadt/ G
DMSO	Merck/ Darmstadt/ G
EDTA	Calbiochem/ SanDiego/ America
Sodium-chloride	Merck/ Darmstadt/ G
Ethanol	Merck/ Darmstadt/ G
Formalin	Merck/ Darmstadt/ G
NAOH (5N)	Merck/ Darmstadt/ G
Sodium-dihydrogenphosphate	Merck/ Darmstadt/ G
Calcium hydroxide	Merck/ Darmstadt/ G
Calcium dihydrogenphosphate	Merck/ Darmstadt/ G
Calcium chloride	Merck/ Darmstadt/ G
Isopropanol	Merck/ Darmstadt/ G
Streptomycin	Sigma/ Deisenhofen/ G
Potassium-chloride powder	Merck/ Darmstadt/ G
HCl (5N)	Merck/ Darmstadt/ G

2.1.12 Western blotting

Bradford reagent	BioRad/ Munich/ G
------------------	-------------------

Protein standard	BioRad/ Munich/ G
Complete™ Protease-Inhibitor	Roche Life Science/ Basel/ Switzerland
Rabbit anti-mouse p-AKT Ab	Cell Signaling/ Danvers/ America
RIPA buffer solution	Sigma/Aldrich/ St. Louis/ America
Goat anti-rabbit IgG/HRP-linked	Cell Signaling/ Danvers/America
Beta-mercaptoethanol	GE Healthcare/ Amersham/ UK
ECL-WB Detection Kit	Millipore/ Schwalbach/ G
TEMED	BioRad/ Munich/ G
Filter Whitman papers	Millipore/ Schwalbach/ G
Acrylamide	Carl Roth/ Karlsruhe/ G
Agarose	MP Biomedicals/ Eschwege/ G
TAE	Sigma/ St. Louis/American
Nonfat dried milk powder	RanReac-AppliChem/ Poligon/ Spain
Ammoniumperoxodisulfate	BioRad/ Munich/ G
Protein-Marker IV	PeqLab/ Erlangen/ G
Stripping-Buffer Restore™	ThermoFisher/ Waltham/America
Immobilon®-PVDF membrane	Carl Roth/ Karlsruhe/ G
Bromphenolic blue	Merck/ Darmstadt/ G
Rabbit anti-mouse beta-actin Ab	Cell Signaling/ Danvers/America
SDS	BioRad/ Munich/ G
Rabbit anti-mouse RIPK3 antibody	Cell Signaling/ Danvers/America

2.1.13 Murine primer sequences

Murine	Forward (5'-3')	Reverse (5'-3')
18s	GCAATTATCCCCATGAACG	AGGGCCTCACTAAACCATCC
NGAL	ATGTCACCTCCATCTGG	GCCACTTGACATTGTAG
KIM1	TGGTTGCCTCCGTGCTCT	TCAGCTCGGGAATGCACAA
TIMP2	GCAACAGGCGTTTTGCAATG	AGGTCCTTGAACATCTTTATCTGC
COL1A1	ACATGTTGAGCTTTGTTGAC	TAGGCCATTGTGTATGCAGC
TNF- α	AGGGTCTGGGCCATAGAACT	CCACCACGCTCTTCTGTCTAC
CEACAM1	CCTCTATTCCAGGAAGTCTGGC	G TTCAGGACAGTGTATGCGACG

2.1.14.3 Microscopy system and microtome

Digital camera (DC 300F)	Leica Microsysteme/ Cambridge/ UK
Light microscope Leica Wild (MPS52)	Leica Microsystems/ Wetzlar
Light microscope Leica (DMRBE)	Leica Microsystems/ Wetzlar
Microtome Jung (CM 3000)	Leica/ Solms

2.1.14.4 Nucleic acid analysis

Rotilabo®-Mikropistill	Carl Roth GmbH/ Karlsruhe/ G
Thermomixer (5436)	Eppendorf/ Hamburg/ G
PCR-Gelchamber	PeqLab Biotechnologie/ Erlangen/ G
Photometer-Ultrospec (1000)	Amersham/ Freiburg/ G
Photometer-DU (530)	Beckman Coulter/ Fullerton/America
PCR machine (LightCycler 480)	Roche Diagnostics/ Mannheim/ G
Thermo cycler (UNO-II)	Biometra/ Saxony/ G

2.1.15 Machine for centrifuges

Heraeus/ Biofuge primo	Kendro Laboratory Products GmbH/ G
Centrifuge-5415 C	Eppendorf/ Hamburg/ G
Heraeus/ Minifuge T	VWR International/ Darmstadt/ G
Centrifuge-5418	Eppendorf/ Hamburg/ G
Centrifuge-Megafuge (1.0R)	Heraeus Sepatech/ Osterode/ G

2.1.15.1 Smaller balances

Benchtop Mettler(PJ 3000)	Mettler Toledo/ Giessen/ G
Benchtop BP (110S)	Sartorius/ Saxony/ G

2.1.15.2 Other devices

Olympus (BX50)	Olympus Microscopy/ Hamburg/ G
Pipet-Pipetman	Gilson/ Middleton/America
Tecan/ GENios Plus	Tecan/ Crailsheim/ G
pH meter	WTW GmbH/ Weilheim/ G

Water bath (HI1210)	Leica Microsysteme/ Solms
Pipet tips	Peske/ Aindling-Arnhofen
Leica (DC 300F)	Leica Microsystems/ Cambridge/ UK
Vortex	Scientific Industries/ Bohemia/ America

2.1.15.3 Software

Inkscape 0.92.3	Inkscape
CellQuest	BD Biosciences/ Heidelberg/ G
Adobe-Illustrator (cc 2017)	Microsoft/ Redmond/America
Windows 10 Software	Microsoft/ Redmond/America
QWinows	Leica Microsystems/ Wetzlar
Office (2017)	Adobe/ California/America
Adobe-photoshop (cc 2017)	Adobe/ California/ America
Endnote (x8)	Thomson-Reuters/ New York/ America
Mendeley	Mendeley/ London/ UK
Acrobat-Writer	Adobe Systems/ Dublin/ Ireland

2.2 Animal experiments

2.2.1 Mice housing

It more diffuse that the care followed the standards of the institution (The department of Cancer Research Institute, Central South University). Before use, mouse retreats, nestlets, bedding, cages, water and food were autoclaved for sterilization. Mice were housed in a maximum of five in filter-top cages with unlimited access to water and food under specific pathogen free conditions as well as a 12-h dark-light cycle. All experimental procedures detailed below were conducted in strict compliance with China's equivalent of the National Institutes of Health's Guide for the use of mice, and with approval from the Ethics Committee of Cancer Research Institute of Central South University.

2.2.2 Genotyping

Ear punch biopsies, obtained from mice using the earhole punching technique, were used to isolate DNA. The tissue was lysed on a shaker in 200 μ l of PBD buffer (2.5 ml of 2 M KCl, 1 ml of 1 M Tris-HCl (pH-8.3), 0.25 ml of 1 M MgCl₂, 10 ml of 0.1% gelatine, 0.45 ml of NP-40 (100%), 0.45 ml of Tween-20 (100%), and H₂O up to 100 ml) containing 1 μ l of proteinase K (20 mg/ml) for 4 hours at 56°C. Then the supernatant containing DNA was centrifuged for 2 min (12,000 \times g), and the supernatant (1 μ l) was used in PCR, along with 2 μ l of either the CEACAM1 wild-type or CEACAM1 knockout primers (1 μ l of forward and reverse primer) and PCR master mix (2.5 μ l-10 \times PE buffer, 2.0 μ l-1.25 mM dNTPs, 0.5 μ l of Taq polymerase, 17.0 μ l of H₂O) in a reaction volume of 25 μ l. Two reactions were set up per animal. Samples from known knockout and wild-type (WT) animals were used as controls and H₂O was used as a no-template control instead of DNA. The reaction conditions were

94°C for 15 minutes, then 30 cycles of 94°C for 30 seconds, 61°C for 60 second and 72°C for 90 seconds, finally extension step at 72°C for 10 minutes. Next, 4 µl of the PCR reaction was mixed with 6× loading buffer (3 ml of glycerol, 0.5 ml of 5% bromphenol blue, 0.5 ml of 5% xylenecyanol and 6 ml of H₂O) by gentle pipetting and the samples were then loaded onto an gel consist of ethidium bromide in TBE buffer (Tris: 108 g, boric acid: 55 g, EDTA: 5.84 g, H₂O:10 L). Finally, gels were run at 200 V for 30 minutes, and a DNA ladder is used to estimate adequate separation of the fragments.

2.2.3 Anti-GBM disease

The anti-GBM mouse model (Figure 6) was established following a previously described protocol [94]. Anti-GBM serum for experiment was purchased from a company (Probetex Inc., San Antonio, USA) and was prepared in accordance with their protocol. A kit (Roche Diagnostics GmbH, Mannheim, G) was used to isolate the glomerulus, which was then injected into sheep to activate their immune system to produce anti-mouse glomerulus antibody. Serum was then gathered from the animals and stored at -80°C for future use. In experiments, 200 µl of serum was injected per mouse to induce anti-GBM disease and the same dose of PBS was injected for control mouse.

To induce anti-GBM glomerulonephritis, male mice aged 8–10 weeks were injected with 200 µl of anti-GBM serum intravenously at day 0. The urinary protein concentration was evaluated at 24 h to confirm that the model had been successfully established. Urine and blood samples were collected at day -1, day 1 (d1) and day 7 (d7) to evaluate kidney damage. Mice were euthanized at the end and the kidneys were harvested. The anti-serum contained GBM antibodies, which bind GBM directly to the glomerular, causing the

supplementary system to be activated and glomerular and endothelial cell death at the two time points are shown in Figure 6.

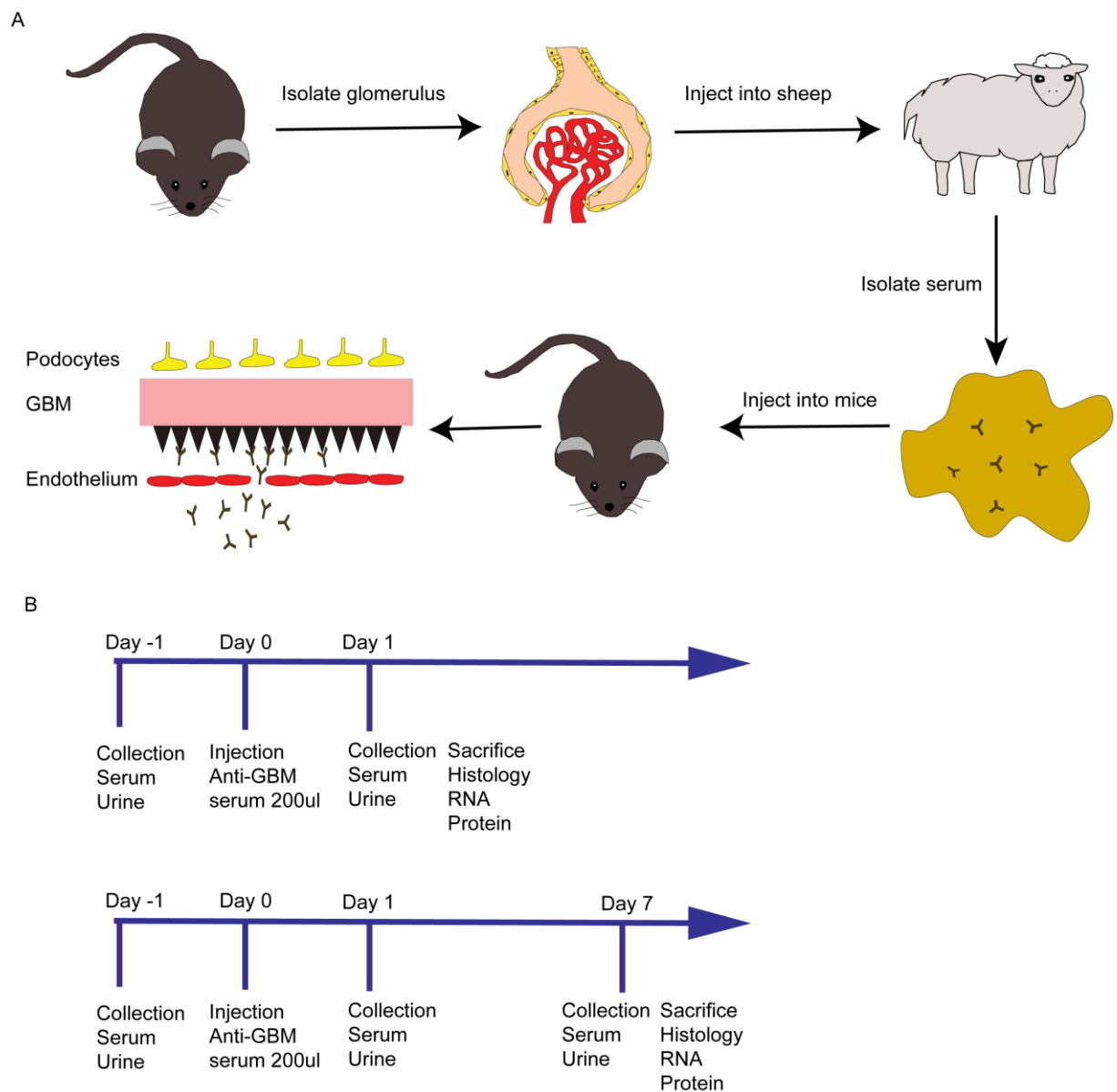


Figure 6 Mouse model of anti-GBM and the study design

The mouse model of anti-GBM. Step 1: the glomerulus is isolated from rats, then antibody is injected into sheep. Step 2: serum is collected from sheep that contains anti-rat glomerulus antibody and this antibody is injected into mice to induce anti-GBM disease (A). Design of the mouse model. Two time points were selected for analysis, 24 h and 7 days. Mice were sacrificed at the end of the experiment (B).

2.2.4 Sacrifice

At the respective endpoints (24 h and 7 days after anti-GBM serum injection), mice were anesthetized in a chamber (200 cm³, oxygen flow:1 L/minutes, alveolar concentration:2%–3%). Upon induction of surgical tolerance (no reaction to forceps stimulation of the paw), blood was drawn from the mouse's tail into an Eppendorf tube coated with 8 µl of EDTA. The mice were then euthanized by cervical dislocation. Mice were placed in a supine position; their limbs were fixed with syringe needles and 70% alcohol was sprayed evenly onto the skin. The kidneys were harvested after peritoneal cavity was opened. Next, the kidney was divided into three sections, the center portion was immersed in 4% formalin, the upper pole was snap/frozen (in liquid nitrogen) and transferred to -80°C storage for later protein analysis, while the lower pole was immersed in RNAlater for -20°C storage and subsequent RNA extraction.

2.2.5 Colorimetric serum test

Measurements of serum creatinine, urinary albumin/creatinine ratios, and blood urea nitrogen levels were performed according to the manufacturer's instructions [95].

2.2.6 Histological analysis

Paraffinization of tissues

The tissues that were already in histology cassettes were fixed overnight in 4% formalin and were then sequentially immersed in an increasing ethanol series (2× 70%, 80% and 95%, and 3× 100% ethanol) for 1 h each. Histology cassettes were then sequentially immersed in xylene (1.5 hours), three times, then two paraffin immersions at 60°C for 2 hours each. For optimal sectioning results, tissues were then repositioned in the histology cassettes and integrated into a paraffin block, that was refrigerated at 0°C. The block was

sectioned in a water bath using a microtome into 2- μ m-thick sections. Swimming sections were then carefully mounted onto slides covered with ammonium persulfate and were dried at 37°C for 12 h.

PAS staining and scoring

- a) Deparaffinization in xylene as well as rehydration in ethanol solution (100% ethanol: 3 times X 3 minutes, 95% ethanol: 2 times X 3 minutes, 70% ethanol: 1 time X 3 minutes).
- b) Tissue sections (of 2- μ m thickness) were stained under full immersion (10 minutes with 0.5% periodic acid) then rinsed in distilled water (2 times X 5 minutes).
- c) Sections were immersed in Schiff reagent (20 minutes), then rinsed in distilled water (2times X 5 minutes).
- d) Slides were covered in 0.55% potassium metabisulfite for 2 minutes, then rinsed with distilled water (2 times X 5 minutes), counterstained in Mayer's hemalaun reagent (3 minutes) then washed with running water (10 minutes).
- e) Slides were dehydrated in ethanol solution (2X 70%, 80%, 95% and 3X 100% ethanol), then covered in VectaMount media and sealed with a coverslip after rapidly immersed in xylene.

All of the kidney slides were scored according to the following protocol and scores in the results section are expressed as the mean \pm SD. Tubular injury was assessed by digital limorphometry using the ImageJ software. Tubular casts were evaluated on sections in 20 high-powered cortical fields per mouse. In total, 50 glomerular were assessed per mouse and the number of crescents was counted as shown in Figure 7.

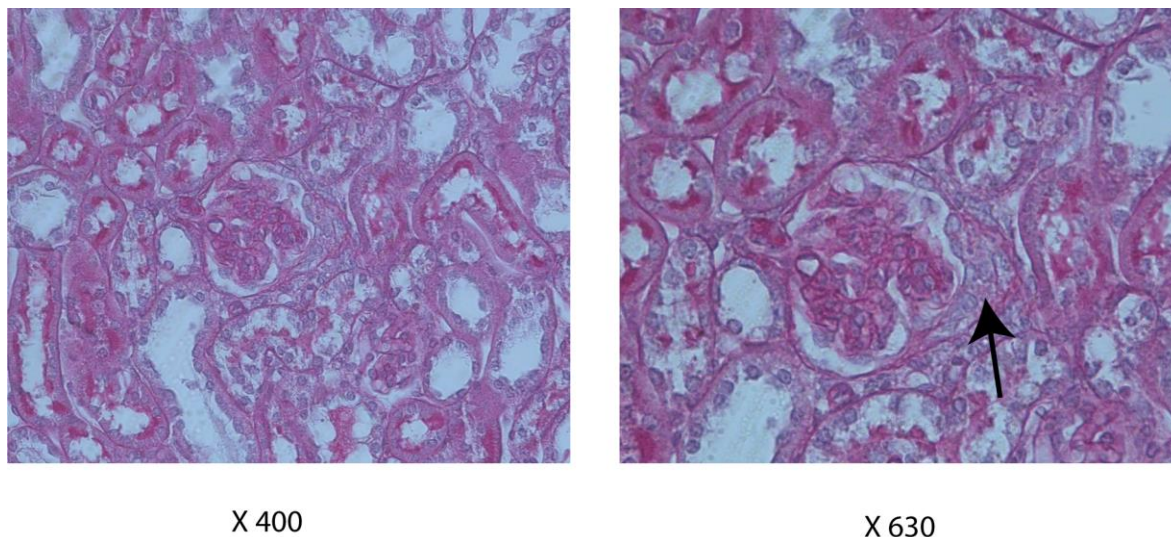


Figure 7 Crescent formation in anti-GBM nephritis

Panels show different magnifications: 400× (Left) and 630× (Right). The black arrow represents the crescent.

Masson-Goldner-Trichrom-staining and scoring

The steps below were followed for Masson-Goldner-Trichrom staining and scoring:

- a) Deparaffinization in xylene as well as rehydration in ethanol solution (100% ethanol: 3 times X 3 minutes, 95% ethanol: 2 times X 3 minutes, 70% ethanol: 1 time X 3 minutes).
- b) Weigert's iron hematoxyline: 2 μ m tissue sections were stained (3 minutes), then rinsed with running water (10 minutes).
- c) Goldner solution I (Ponceau Acid Fuchsin): tissue sections were stained (10 minutes), then rinsed (1% acetic acid: 30 seconds) and analyzed after around 2 min.
- d) Goldner solution II (Phosphomolybic Acid-Orange) was used for complete collagen bleaching, then slides were rinsed I (1% acetic acid: 30 seconds) then stained in Goldner solution III (5 minutes).
- e) After more than 5-minutes rinse (1% acetic acid), slides were dehydrated in ethanol solution (2 X 70%, 80%, 95%, and 3 X 100% ethanol), then covered in VectaMount media and sealed with a coverslip after rapidly immersed in xylene.

All slides were assessed by digital morphometry using ImageJ software. For each kidney, 20 images were recorded per slide and the percentage positive area per side was quantified after threshold quantitation.

Immunohistochemistry and scoring

The steps below were followed for immunohistochemistry and scoring:

- a) Tissue was deparaffinized in xylene as well as rehydrated in ethanol solution (100% ethanol: 3 times X 3 minutes, 95% ethanol: 2 times× 3 minutes, 70% ethanol: 1 time× 3 minutes).
- b) Tissue sections of 2 µm were washed with PBS (7 minutes) and blocked in methanol containing 3% H₂O₂ for 20 min.
- c) Sections were immersed in 1% antigen-unmasking solution and heated 4× for 2.5 min each in a microwave.
- d) After washing with PBS for another (7 minutes), sections were blocked in avidin (15 minutes) and biotin (15 minutes).
- e) Primary antibody staining was performed overnight (4°C) . Sections were incubated in secondary antibodies (30 minutes) , After washing under PBS.
- f) After washing with PBS for another (7 minutes), each section was incubated with 0.1% PBS ABC substrate solution (30 minutes), followed by further washing under PBS then by Tris-HCl.
- g) Staining was visualized under incubation in DAB substrate then methyl green was used as a counterstain.
- h) Slides were dehydrated in ethanol solution (2× 70%, 80%, 95%, and 3× 100% ethanol), then covered in VectaMount media and sealed with a coverslip after rapidly immersed in xylene.

All slides were assessed by digital morphometry using ImageJ software. For each kidney, 20 images were recorded per section, and Mac-2 and WT-1 positive cells were counted manually (20 glomeruli/each kidney section). The percentage of the area that was positive per slide was quantified after the threshold quantitation.

Co-Immunofluorescence and scoring

The steps below were followed for co-immunofluorescence and scoring:

a) Tissue was deparaffinized in xylene as well as rehydrated in ethanol solution (100% ethanol: 3 times X 3 minutes, 95% ethanol: 2 times× 3 minutes, 70% ethanol: 1 time× 3 minutes).

b) Tissue sections of 2 μm were washed under PBS (7 minutes), immersed in 1% antigen-unmasking solution and heated 4 \times , for 2.5 min each, in a microwave.

c) Slides were then washed under PBS for another (7 minutes), and sections were blocked in avidin and biotin (15 minutes, each solution).

e) Sections were stained with primary antibody for 1 hour at room temperature. Sections were incubated in secondary antibodies (30 minutes), after washing under PBS.

d) For immunofluorescence co-staining with (CD31 or TUNEL, then antibody staining was followed by CD31 or TUNEL enzyme incubation in accordance with the manufacturer's instructions.

f) Slides were dehydrated in ethanol solution (2 \times 70%, 80%, 95%, and 3 \times 100% ethanol), then covered in VectaMount media and sealed with a coverslip after rapidly immersed in xylene.

All slides were assessed by digital morphometry using ImageJ software. For each kidney, 20 images were recorded per slide, and the percentage of the positive cells was quantified after the threshold quantitation.

2.2.7 Western blotting

Total protein was extracted from kidney using RIPA buffer with phosphatase and protease inhibitor for western blotting as described previously [96]. Gel castings were prepared according to previous protocols [96]. Proteins were separated slowly by polyacrylamide gel electrophoresis using 10% sodium dodecyl sulfate buffer, then transferred to PVDF (polyvinylidene fluoride) membranes. All membranes were blocked at room temperature (5% skim milk:2 hours), then membranes were incubated with primary antibodies against mouse AKT, p-AKT, RIPK3 and β -actin at 4°C overnight. Then membranes were washed with TBST buffer three times, they were incubated in peroxidase-conjugated anti-rabbit IgG secondary antibodies (1 hour at room temperature). After washing three times, protein bands were detected using an ECL kit as described previously [97]. Images were normalized and analyzed by ImageJ software.

2.2.8 RNA isolation

a) PureLink RNA Mini kits were used for RNA isolation in accordance with the manufacturer's guidelines [36].

b) Tissue (1/3 of each kidney) was lysed by homogenization in RNeasy Lysis Solution containing 1% beta-mercaptoethanol. Homogenates were vortexed to lyse cells and lysates were mixed 1:1 with 70% ethanol.

c) The sample (700 μ l) was then centrifuged at room temperature (1200 \times g, 15 seconds). The flow-through was discarded and this was repeated until all of the sample had been processed.

d) Washing buffer, I was used to wash the membranes once, then with washing buffer II twice, and then centrifuged to dry the membrane (12000 \times g, 2 minutes).

- e) Membranes were incubated with RNase-free water at room temperature for 1 min.
- f) Membranes were then centrifuged to elute the RNA into the recovery tube (12000 ×g, 2 minutes).
- g) The quality and quantity of the total RNA was determined using the UV absorbance at 260 nm.

2.2.9 cDNA preparation

- a) To prepare cDNA, 2 µg of RNA (in RNase-free water up to a total volume of 15 µl) was reverse transcribed.
- b) To achieve this, the 15 µl RNA solution was added to 7.5 µl of master mix (4.5 µl 5× superscript II buffer, 0.45 µl 25 mM dNTPs, 1 µl 0.1 M DTT, 0.25 µl linear acylamide, 0.25 µl hexanucleotides, 0.5 µl RNasin and 0.5 µl SuperScript II enzyme) and the mixture was incubated at 42°C for 90 min, followed by 5 min at 95°C.
- c) Then, 200 µl of RNase-free water was used to dilute the concentration to a working concentration of 1:10, which was stored at -20°C for subsequent use.

2.2.10 Quantitative real-time RT-PCR (qPCR)

- a) Samples were prepared for PCR by adding 2 µl of template to a well, followed by 18 µl of qPCR master mix (0.16 µl of 10× Taq buffer; 10 µl of 2× SYBRgreen, 0.6 µl of each specific primer (diluted 1:10) and 6.64 µl of H₂O).
- b) cDNA amplification and detection were processed on a thermal cycler (LC480, Roche) using below standard protocol: 95°C initiation phase (10 minutes), 60°C annealing phase (20 seconds) and 72°C amplification phase (20 seconds) for a total of 40 amplification cycles.

c) Efficiency corrected quantitation was conducted by the thermal cycler relay on external standard curves describing the target's PCR efficiencies and reference genes (ratio= $E_{\text{target}}\Delta C_{\text{Ptarget}}(\text{control} - \text{sample})/E_{\text{ref}}\Delta C_{\text{Pref}}(\text{control} / \text{sample})$).

2.2.11 Cell culture

The GEC cells [98] as well as the Caco2 cells [99] were cultured under standard sterile conditions at 37°C and 5% CO₂ in DMEM or RPMI-1640 media, 1% penicillin/streptomycin and 10% fetal bovine serum. All cells were tested routinely every 6 months for mycoplasma contamination as described previously [100]. Cells were split for later experiment before growing to around 80%–90% confluency, and for the same experiment approximately the same passage cells were used.

2.2.12 Transwell permeability assay

- a) Endothelial cells (5×10^4) in 500 μl of DMEM were grown on the membrane of each transwell insert in a 24well plate.
- b) Then, 1 ml of endothelial growth medium was added to per well.
- c) Forceps were used to move the inserts into the medium and a lid was placed on the plate.
- d) The plate was incubated of 37°C until a cell monolayer had formed.
- e) Stimulator and bovine serum albumin were added to the transwell insert then the plate was incubated (37°C) for the desired time period.
- f) The medium was aspirated from the lower chambers, then the OD of the sample was measured at 485 nm and emission at was measured at 520 nm according to standard protocols.

2.2.13 Epithelial barrier testing via electric cell–substrate impedance sensing (ECIS)

Caco2 cells (50,000 cells/well) were incubated at ECIS 8-well arrays with serum-free DMEM and were incubated overnight at 37°C. When the cells reached confluence, they were stimulated with histones (100 µg/ml) or PBS. Cell damage was examined under a microscope and the histones were removed after 6 h when the medium was changed. Then 40 µg/ml of CEACAM1 antibody or PBS solution was added to well. The capacitance value was set as 0 or 1 just before the histones were added and immediately after medium exchange. The set-up for the ECIS assay is shown in Figure 8.

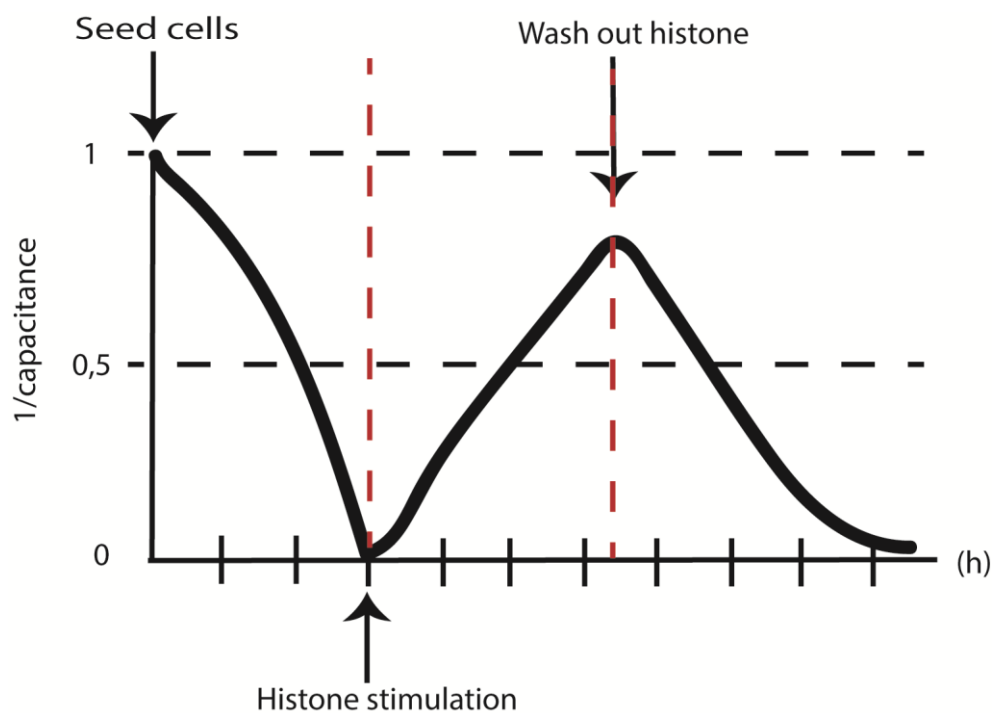


Figure 8 Electric cell-substrate impedance sensing experiments

Histone stimulation experimental set-up from human colon epithelial cells. Cells were seeded ECIS 8-well arrays, when the cells reached confluence, stimulate the cells with histone for 6 hours then wash out histone.

2.2.14 Statistical analyses

The data are shown as the mean \pm SD, unless otherwise indicated. A Student's t-test was used to compare the differences between groups and one-way ANOVA was used to compare the differences between more than two groups. GraphPad Prism software, version 8.0, was used for these comparisons. A p value <0.05 was considered to indicate statistical significance.

3 Results

3.1 CEACAM1 expression in murine and human kidneys

To characterize the renal expression CEACAM1 in mice and human, the online Kidney Interactive Transcriptomics (KIT) database built on healthy mice and human kidneys was assessed. Interestingly, CEACAM1 was expressed in murine healthy kidneys in a lot of different cell types including podocytes, macrophages and endothelial cells in mice, with about 4-6% of cells expressing CEACAM1 and the highest expression found in endothelial cells. (Figure 9A, B, C, D). In the human kidney, CEACAM1 is mainly expressed on distal tubule cells and proximal tubule cells (Figure 9E, F, G, H). Compared with mice, CEACAM1 shows a lower expression in the human kidney. Taken together, CEACAM1 is expressed both in healthy murine and human kidneys, albeit in different cell types and at low levels.

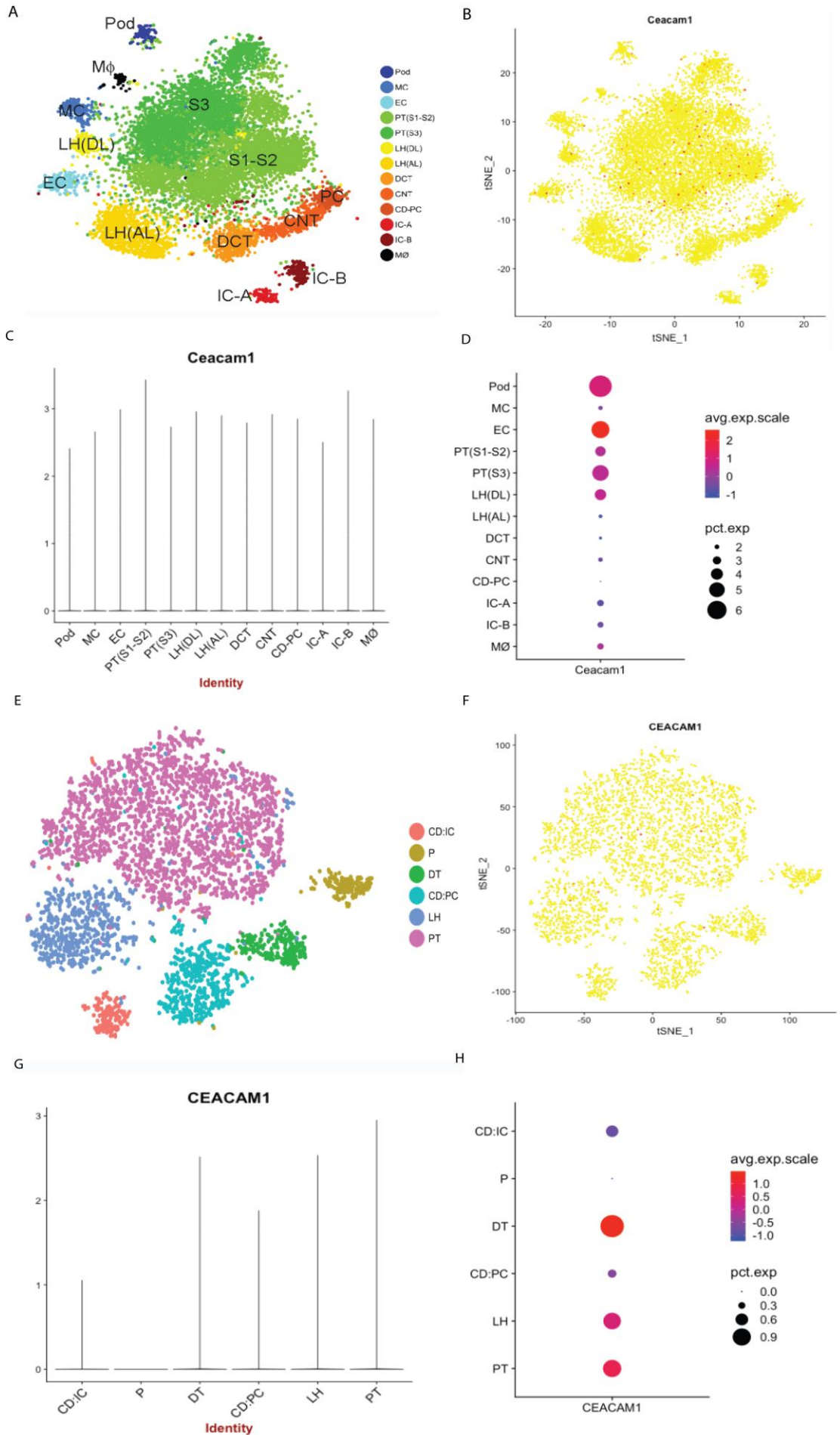


Figure 9 The distribution of CEACAM1 expression on normal mice kidney and healthy human kidney (From KIT database)

The total cells which they already analysis in this database (A, E), CEACAM1 distribution on those cells (B, F), the average percentage scale and percentage expression of CEACAM1 on those cells (C, D, G, H). EC, endothelial cell; t-SNE, t-Distributed Stochastic Neighbor Embedding; LOH (DL), loop of Henle, distal limb; P, one podocyte population; PT, proximal tubule; DT, distal tubule; Mono, monocyte; IC, intercalated cells; LOH (AL), loop of Henle, ascending limb; Pod, podocytes; CD, collecting duct;

3.2 CEACAM1 is upregulated in murine experimental glomerulonephritis

To further characterize the role of CEACAM1 in glomerulonephritis, CEACAM1 expression was analysed in kidneys at day 1 and day 7 after the induction of anti-GBM disease. *Ceacam1* mRNA levels were significantly upregulated at day 7 compared to healthy kidneys (about six-fold) and there was also a non-significant trend towards upregulation on day 1 (Figure 10).

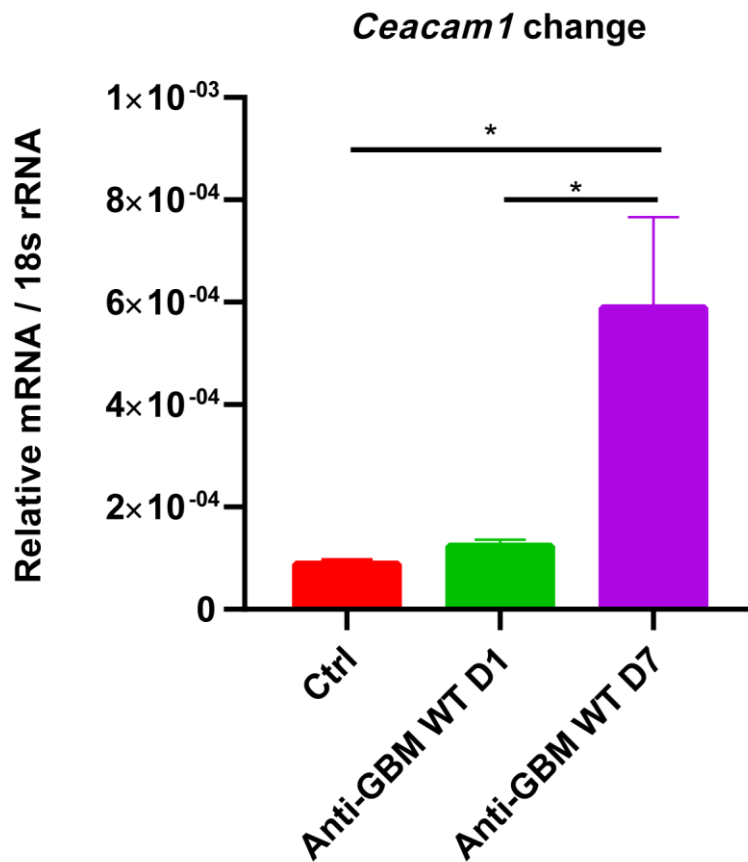


Figure 10 *Ceacam1* expression in mice kidney after induced anti-GBM disease

Ceacam1 expression change in kidneys after induced Anti-GBM disease and normal mice kidneys. * $p < 0.05$.

3.3 CEACAM1 expression in human renal disease

As CEACAM1 expression is upregulated during murine anti-GBM disease, CEACAM1 expression was assessed in human anti-GBM disease. In order to use histology specimens, a CEACAM1 immunohistochemistry staining was established. Indeed, CEACAM1 staining was significantly increased in human anti-GBM disease compared to healthy kidneys (Figure 11A+C). Interestingly, this effect seems to be somewhat disease-specific, as diabetic kidneys did not show any significant expression change compared to healthy control (Figure 11A+C). CEACAM1 is expressed in endothelial cells (white arrow, Figure 12 D) rather than other cells

such as podocytes (black arrow, Figure 12 D). Taken together, these results are consistent with the finding of CEACAM1 upregulation in mice during anti-GMB disease.

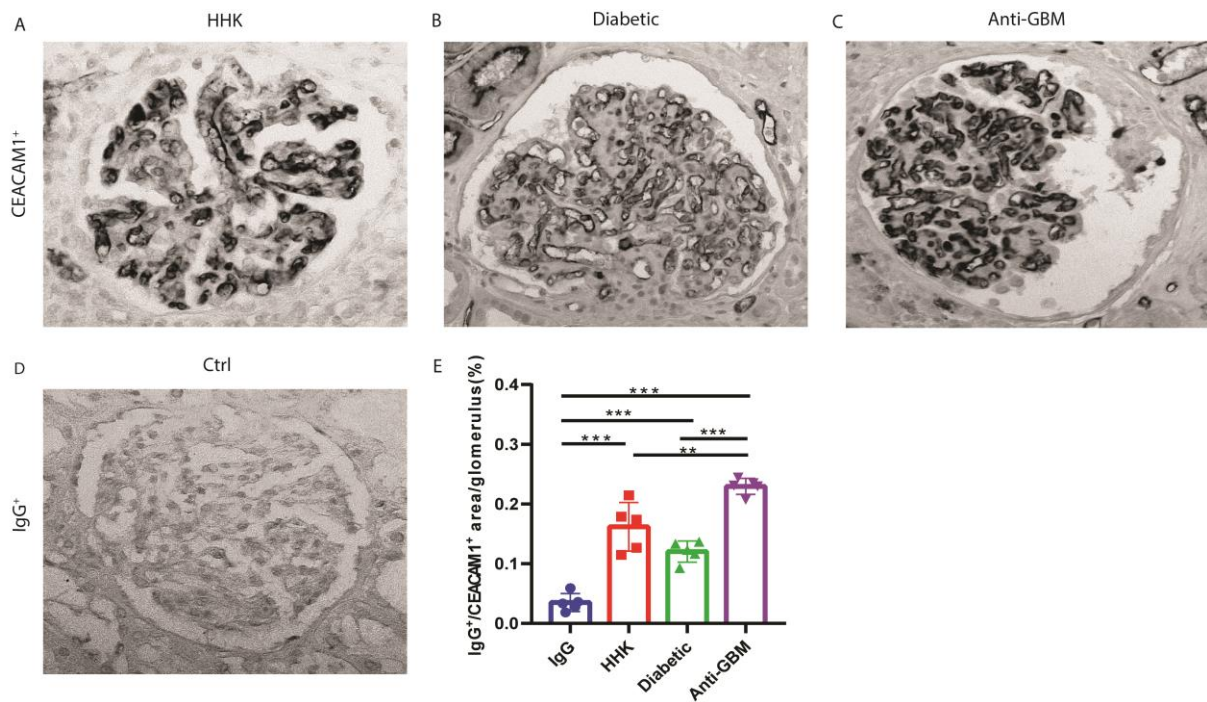


Figure 11 CEACAM1 expression in human kidney

(A) CEACAM1 staining on human healthy kidney (HHK). (B) the picture of CEACAM1 staining of human diabetic kidney. (C) CEACAM1 expression staining on human Anti-GBM disease from biopsy. (D) IgG staining as negative control (ctrl) for normal human kidneys. (E) Quantification statistics for CEACAM1 staining (n=5 for healthy kidney, diabetic kidney, and anti-GBM disease kidney, respectively). **P<0.01, ***P<0.001.

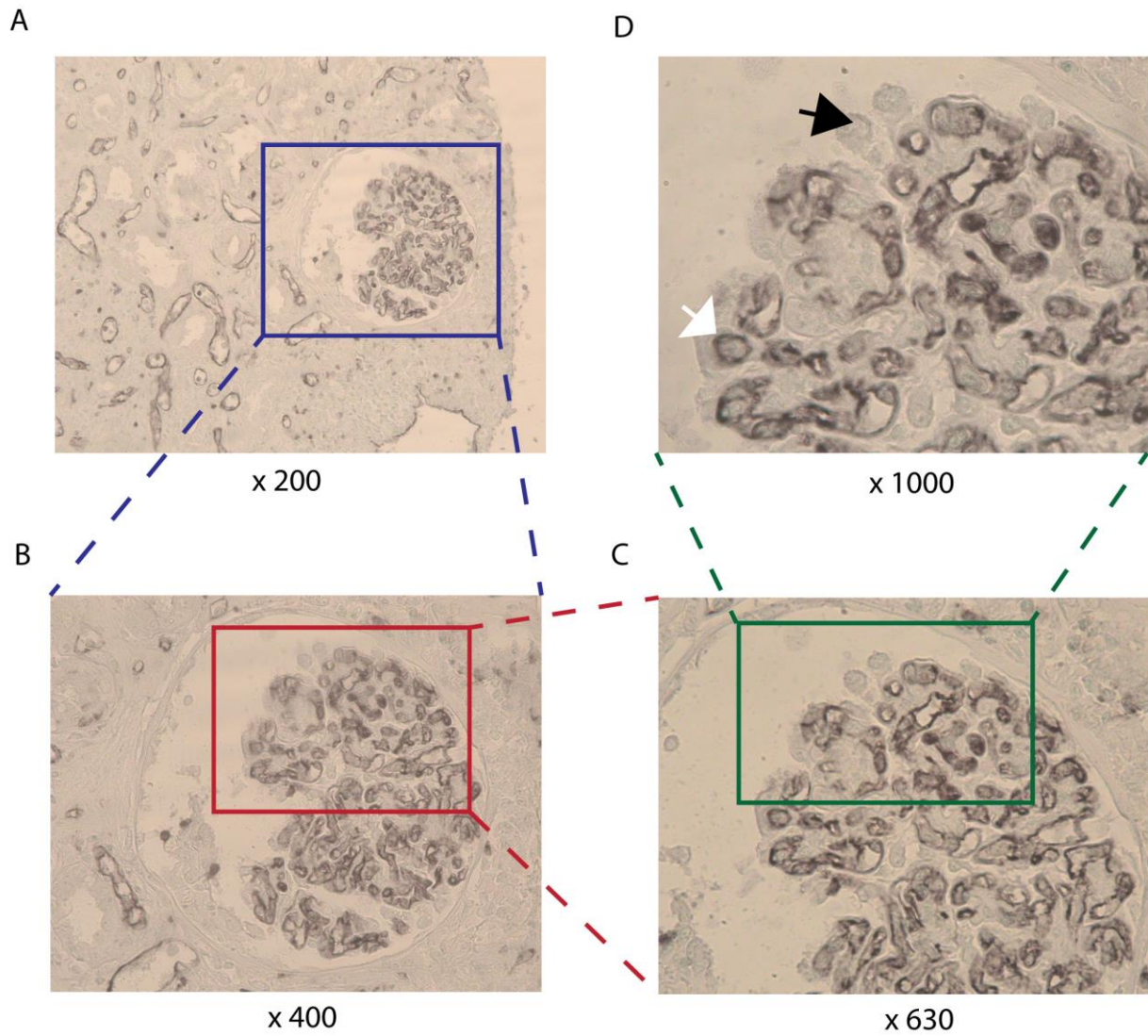


Figure 12 The location of CEACAM1 in human Anti-GBM kidney disease

The amplifying picture of CEACAM1 in human Anti-GBM disease kidneys, from A to D is x200, x400, x630 and x1000 times. (D) Endothelial cells (white arrow) and podocytes cells (black arrow).

3.4 *Ceacam1* deficiency ameliorates glomerular basement damage in murine glomerulonephritis

3.4.1 *Ceacam1* deficiency reduces albuminuria without affecting glomerular filtration rate

To establish the exact role of *Ceacam1* in glomerulonephritis, Anti-GBM disease was induced in both wild type and *Ceacam1*^{-/-} mice. Of note, *Ceacam1*^{-/-} mice showed significantly decreased albuminuria both at day 1 and day 7 compared to wild-type controls (Figure 13a). When serum BUN was significantly increased in wild-type mice compared to *Ceacam1*^{-/-} mice at day 7 (Figure 13B). However, serum creatinine was measured, no difference was found according to the *Ceacam1* genotype at either d1 or d7 (Figure 13C). As there was a small difference in baseline serum creatinine values, glomerular filtration rate (GFR), which is the most sensitive marker for acute renal injury also in GN, was additionally measured. GFR results show that CEACAM1 does not affect GFR decline as well as recovery (Figure 13D). Together, *Ceacam1* deficiency prevents renal injury in GN as evident by albuminuria while not affecting serum retention parameters and GFR.

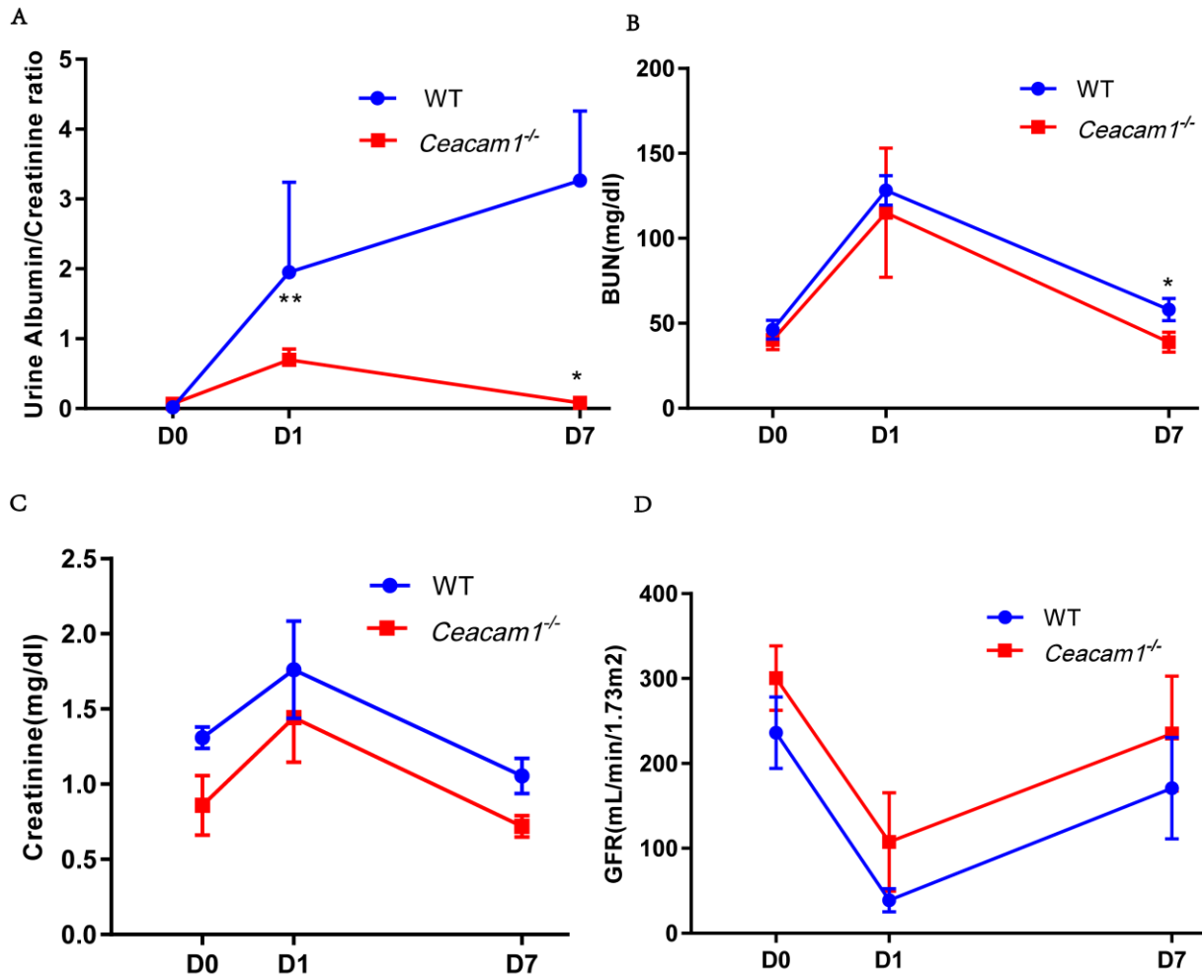


Figure 13 Effect of CEACAM1 on albuminuria, BUN, creatinine and GFR

(A) CEACAM1 deficiency reduce the albuminuria of mice and (B) reduce the blood urea nitrogen of mice. (C) but there is no effect on creatinine and GFR. * $P < 0.05$, ** $p < 0.01$.

3.4.2 *Ceacam1*-deficient mice show less glomerular crescents and tubular cast formation

To investigate the effect of CEACAM1 on crescent and tubular cast formation, the number of crescents per 50 glomeruli and the area of the tubular casts per kidney were measured. Compared to wild-type mice, *Ceacam1*^{-/-} mice show significantly less crescent and tubular cast formation at day 7 (Figure 14,15). Consistent with a previous study [36], no crescents or tubular casts were found at day 1. Thus, *Ceacam1* deficiency prevents the formation of crescents and tubular cast in murine GN.

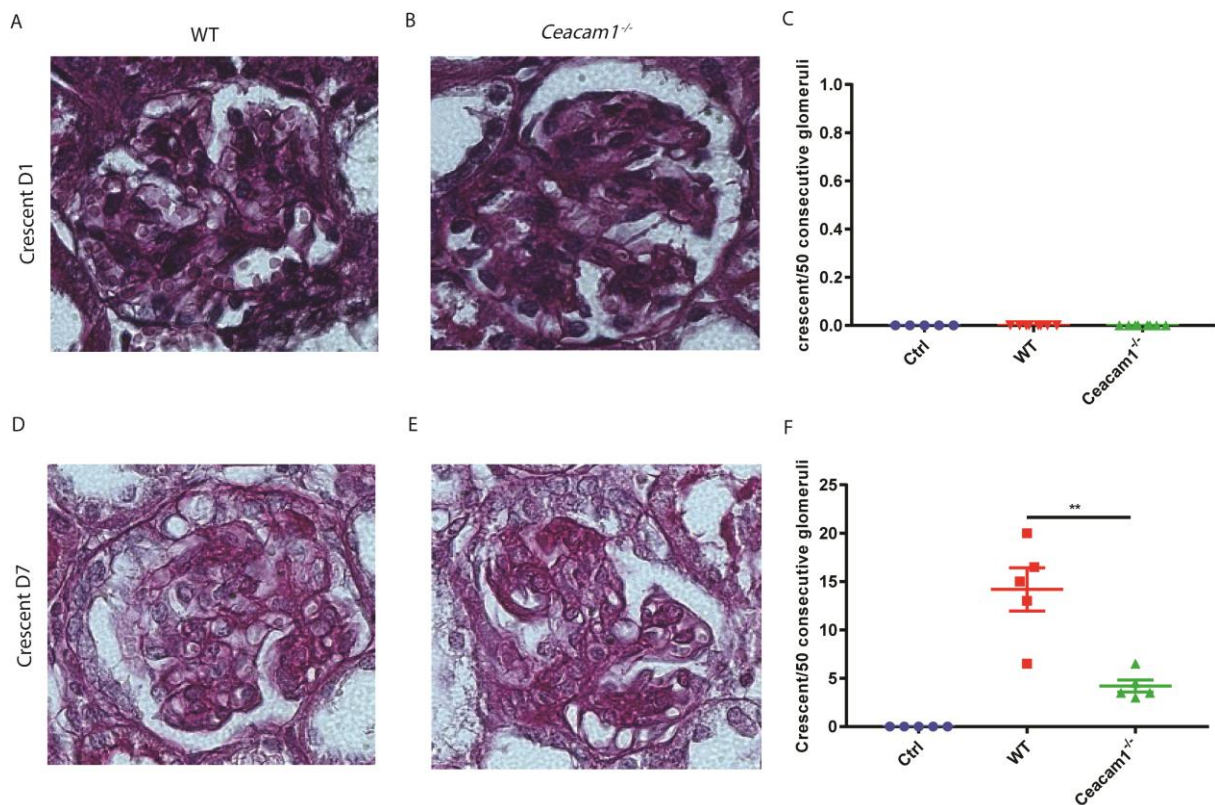


Figure 14 Glomerular crescent formation after induced Anti-GBM disease (A, B, D and E) represent section for wild-type day1, *Ceacam1*^{-/-} day 1, wild-type day 7 and *Ceacam1*^{-/-} day 7, respectively. Quantification data for day 1 (C) and day 7 (F). ** p<0.01.

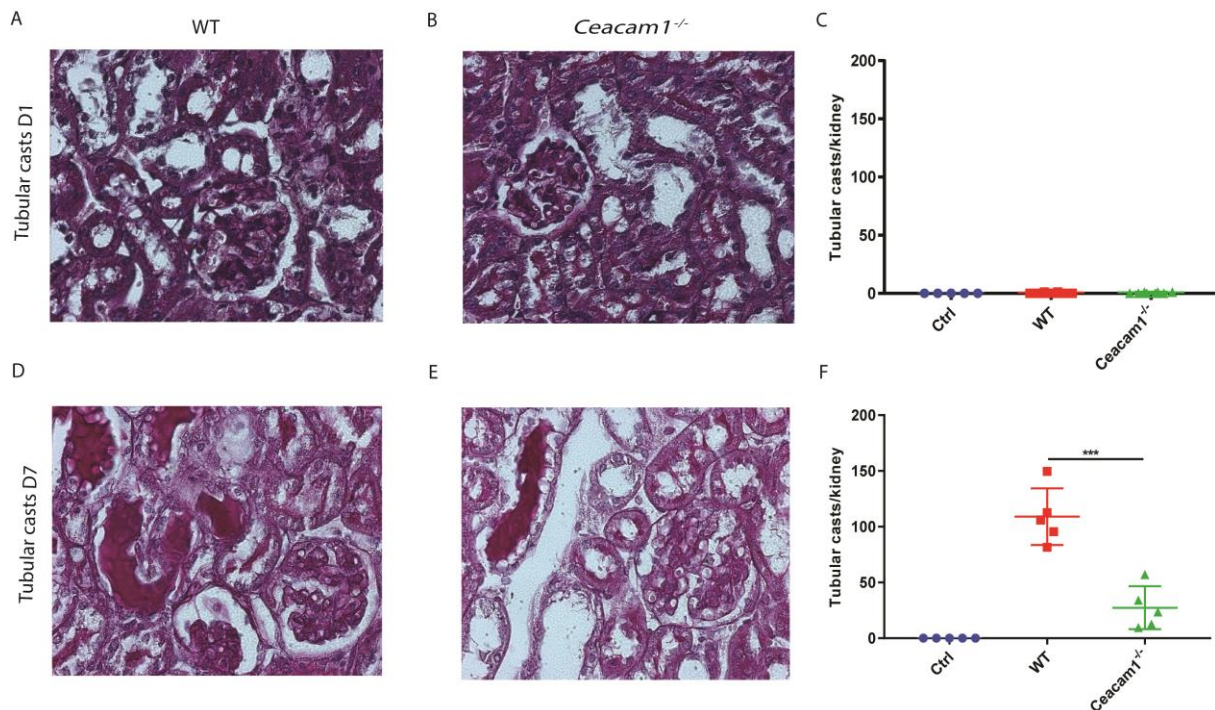


Figure 15 Tubular casts formation after induced Anti-GBM disease

A, B, D and E represent section for wild-type day1, *Ceacam1*^{-/-} day 1, wild-type day 7 and *Ceacam1*^{-/-} day 7, respectively. Quantification data for day 1 (C) and day 7 (F). *** $p < 0.0001$.

3.5 *Ceacam1*-deficient mice show less intra-renal injury

Serum creatinine is a noticeable indicator of renal function and has become a significant indicator of kidney disease and injury. However, it is not a sensitive marker because serum creatinine concentrations do not dramatically change until renal damage is widespread [101]. NGAL, KIM-1, TIMP2 and IGFBP7 are currently accepted biomarkers for kidney injury. *Ngal*, *Kim-1*, *Timp2* and *Igfbp7* mRNA levels were significantly upregulated at day 7 (but not day 1) after GN induction, with wild-type mice generally expressing higher levels than *Ceacam1*^{-/-} mice: *Ngal* and *Kim-1* nearly five-fold, *Timp2* about two-fold and *Igfbp7* about 1.3-fold (Figure 16). By and large, CEACAM1 aggravates kidney damage as measured by intra-renal injury marker expression during Anti-GBM disease progression.

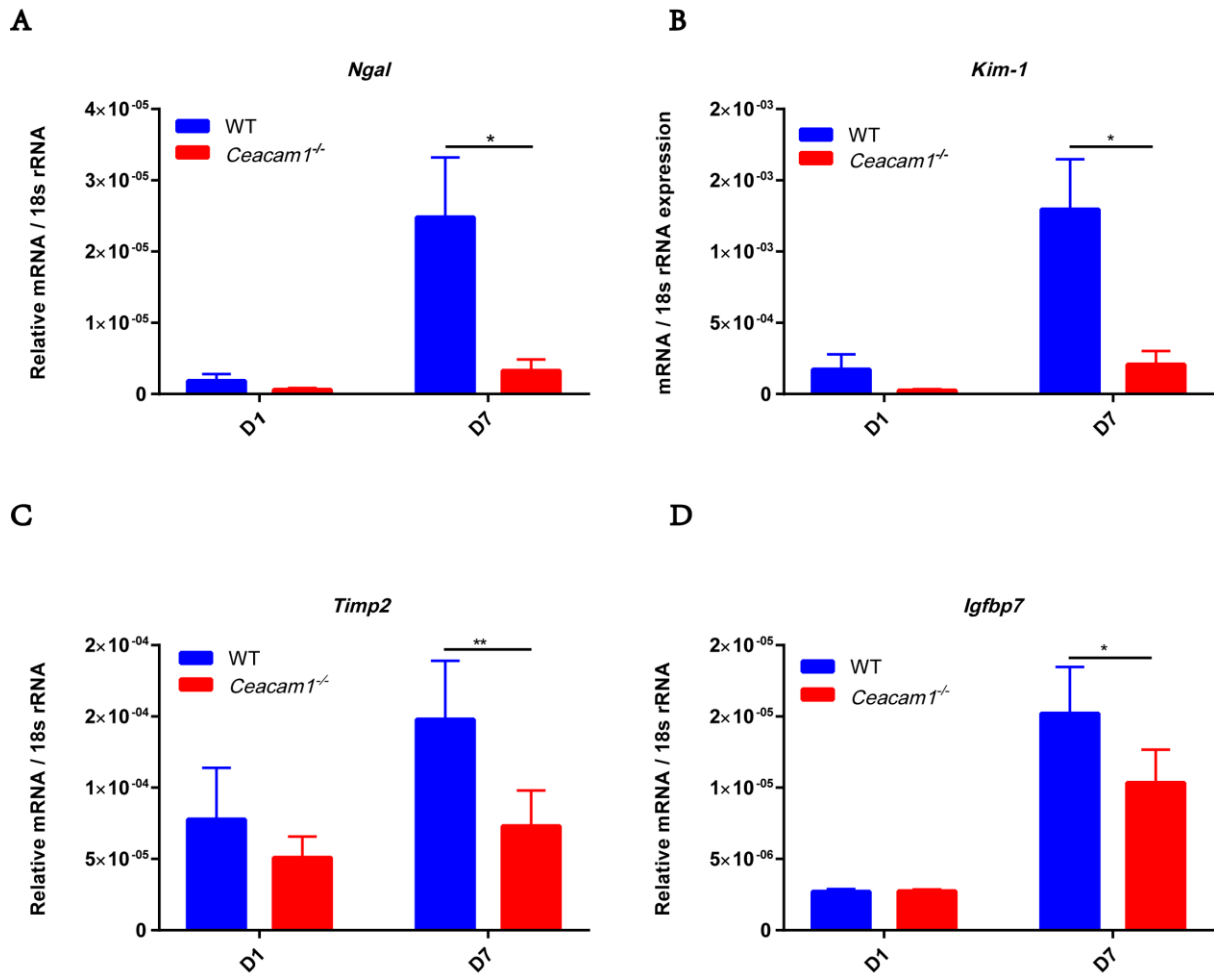


Figure 16 Injury marker expression was upregulated after being induced in anti-GBM disease

Ngal, *Kim-1*, *Timp2* and *Igfbp7* are increased more in the wild-type group on day 7. (A) kidney injury biomarker neutrophil gelatinase-associated lipocalin (NGAL) enhanced in GN, (B) kidney injury biomarker kidney injury molecule-1 (KIM-1) enhanced in GN. (C) The G1 cell cycle inhibitors tissue inhibitor metalloproteinase-2 (TIMP2) and (D) Insulin-like growth factor-binding protein 7 (IGFBP7) * $p < 0.05$, ** $p < 0.01$.

3.6 *Ceacam1* deficiency decreases intra-renal expression of inflammatory markers and fibrosis

As GN is primarily an inflammatory disease, the expression of the inflammatory cytokines CCL2, TNF-alpha, CCL5, CXCL1 and CXCL2 was assessed next. In keeping with the previous findings, *Ceacam1*^{-/-} mice showed significantly less intra-renal inflammatory cytokine expression, and for *CCL2* and *TNF-alpha* the difference reached statistical significance already on day 1 (Figure 17). While I did not observe any difference in intrarenal CD3+ or CD19+ cells between *Ceacam1*^{-/-} and *Ceacam1*^{+/+} mice (Data not show).

To assess the fibrosis induced by GN induction, intra-renal COL1A1 expression was assessed along with Sirius red staining of renal tissue sections. While a significant reduction on intra-renal *COL1A1* expression was observed in *Ceacam1*^{-/-} mice (Figure 17F), no difference was found between *Ceacam1*^{-/-} and *Ceacam1*^{+/+} mice in Sirius red staining of glomeruli (Figure 18). This suggests that differences in diffuse tubulointerstitial fibrosis secondary to renal inflammation account for the difference in *COL1A1* expression rather than glomerulosclerosis.

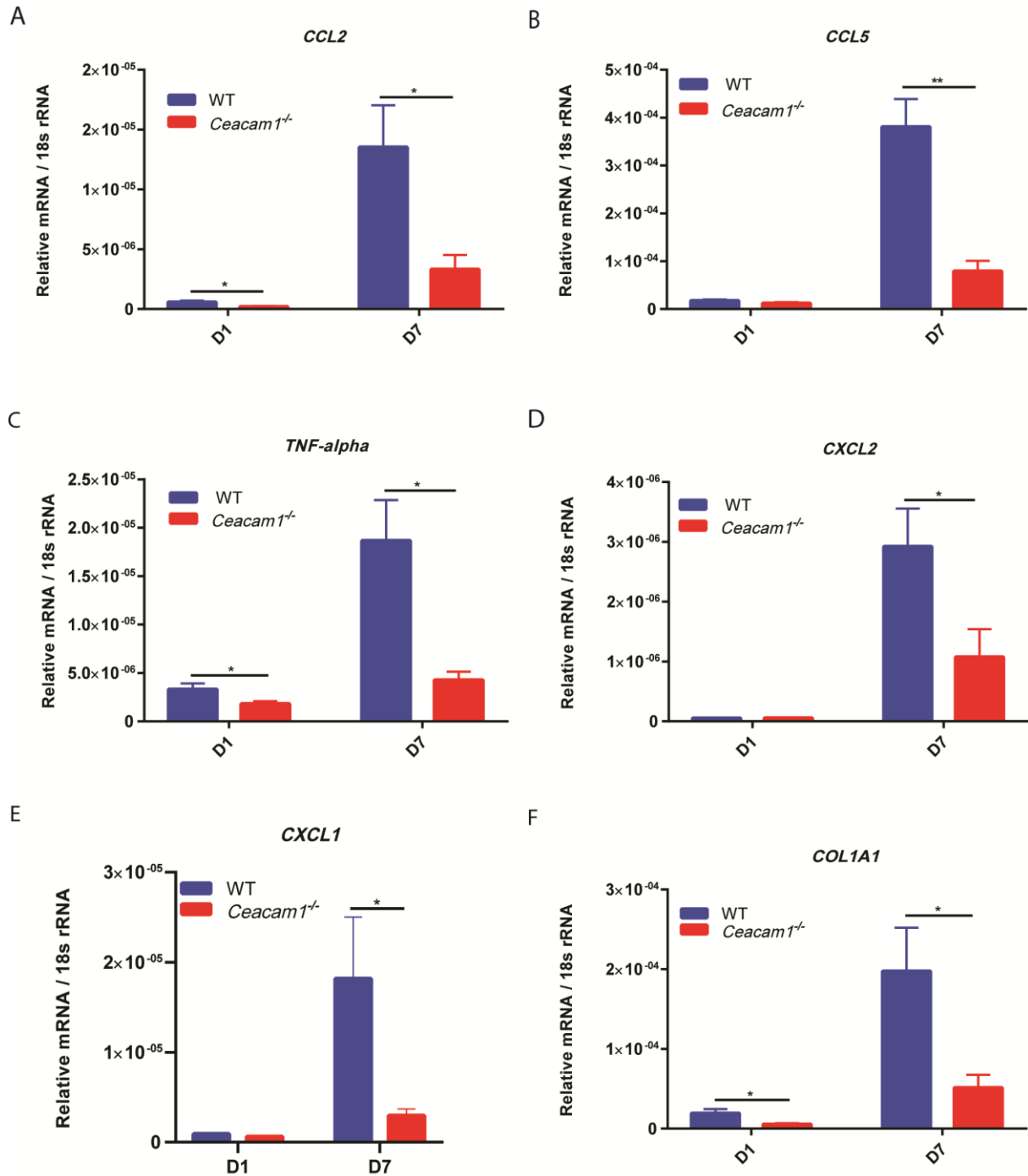


Figure 17 Inflammation and fibrosis biomarker expression was upregulated after being induced in anti-GBM disease

CCL2, *TNF-alpha* and *COL1A1* maker are increased more in wild- type group on both day1 and day 7, *CCL5*, *CXCL2* and *CXCL1* are enhanced more in the wild type group on day7. A: Chemokine (C-C motif) ligand 2 (CCL2) increased in GN, B: Chemokine (C-C motif) ligand 5 (CCL5) increased in GN, C: Tumor Necrosis Factor alpha (TNF-alpha) increased in GN, D: Chemokine (C-X-C motif) ligand 2 (CXCL2) increased in GN, E: Chemokine (C-X-C motif) ligand 1 (CXCL1) increased in GN, F: Collagen Type I, alpha 1 (COL1A1) increased in GN. *p<0.05, **p<0.01.

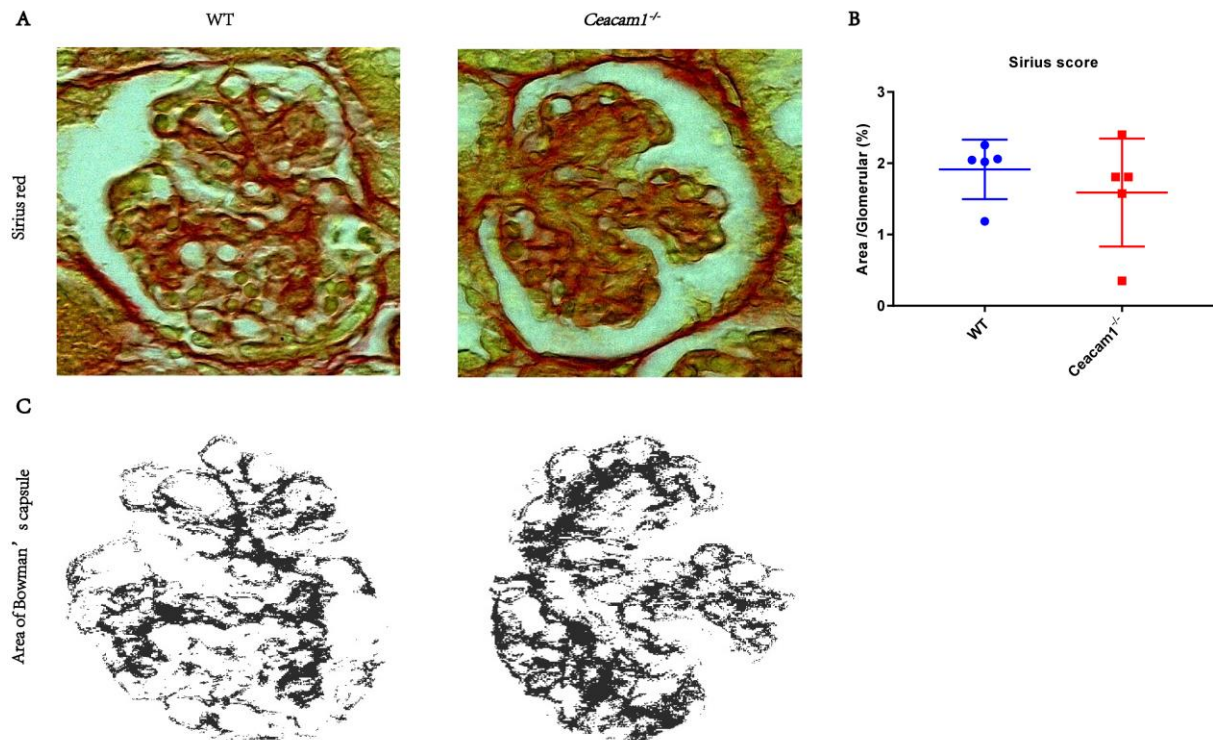


Figure 18 Fibrosis formation after induced in nephritis mice model

(A) Sirius red staining of section for fibrosis at day 7, and quantitation score of those section, (C) area of Bowman's capsule.

3.7 CEACAM1 mediates podocyte loss during murine Anti-GBM disease

Podocytes play an vital role in glomerular function which form a filtration barrier with the glomerular capillary loop endothelial cells and the glomerular basement membrane [102]. Albuminuria was found in after induction of Anti-GBM disease, indicating filtration barrier damage. To further understand which part of the filtration barrier is damaged, podocytes were counted (based on WT1 positivity). Again, while no difference could be seen at day 1, *Ceacam1*^{-/-} mice show less podocyte loss compared to wild-type mice at day 7 (Figure 19). Thus, CEACAM1 signaling may influence the survival of podocytes in Anti-GBM disease.

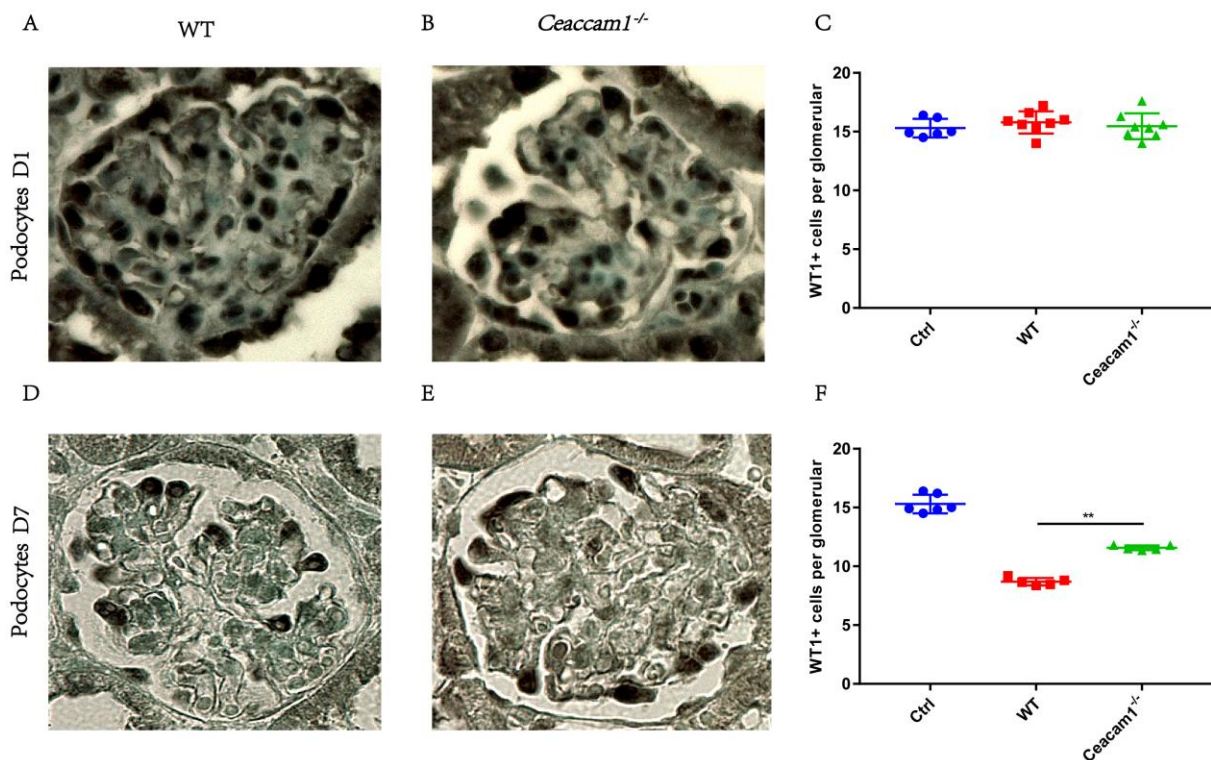


Figure 19 WT1⁺ staining for podocytes after induced in Anti-GBM disease in mice

(A, B, C and D) WT1⁺ staining for podocytes of WT day 1, *Ceacam1*^{-/-} day 1, WT day 7 and *Ceacam1*^{-/-} day 7, respectively. (C and F) quantitation data of those section. **p<0.01.

3.8 *Ceacam1* deficiency attenuates renal leukocyte recruitment

Another significant source of pro-inflammatory cytokines in glomerular diseases are activated mononuclear phagocytic cells, such as macrophages. CEACAM1 increases the number of macrophages (Mac-2 positive cells) infiltration in glomeruli as is shown in Figure 17, wild-type mice have more macrophage and a significant difference was only observed at day 7 (Figure 20). Neutrophils as another important leukocyte subset, did not show any difference according to *Ceacam1* genotype (Figure 21). Thus, CEACAM1 increases the renal leukocyte recruitment, namely of macrophages in GN.

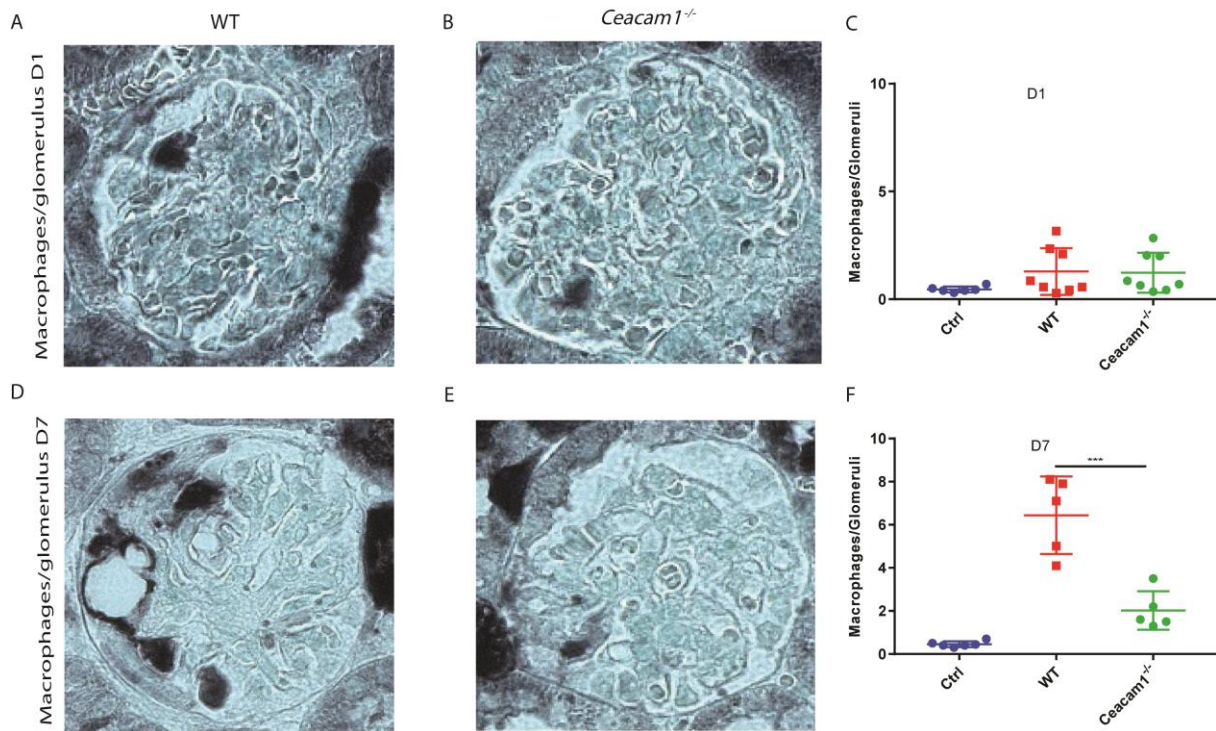


Figure 20 Macrophage infiltration in mice model in nephritis

(A, B, D, E) Immunohistochemical Mac-2 staining and (C, F) Mac-2 staining quantitation in WT and *Ceacam1*^{-/-} mice in GN. ***p<0.001.

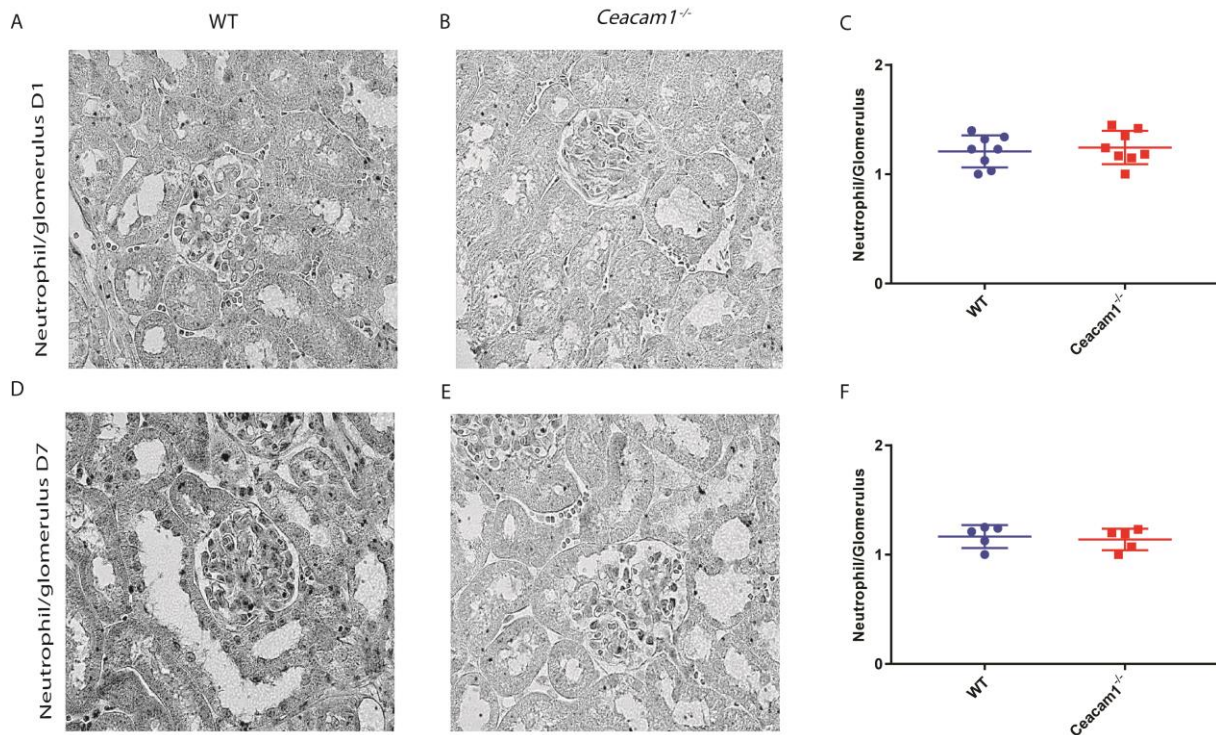


Figure 21 Neutrophil infiltration in mice model in nephritis

(A, B, D, E) Immunohistochemical Ly-6G staining and (C, F) Ly-6G staining quantitation in WT and *Ceacam1*^{-/-} mice in GN.

3.9 *Ceacam1*^{-/-} enhances barrier function of human epithelial cells

To further understand the association between CEACAM1 and GN, next ECIS experiment were performed using human epithelial cells and stimulating them with CEACAM1 activating antibody vs. PBS after damaging the cells with histones for 6h. Cells treated with the CEACAM1 antibody recovered slower than cells treated with PBS after histone damage (Figure 22), suggesting that CEACAM1 ligation prevents the recovery of cells after injury.

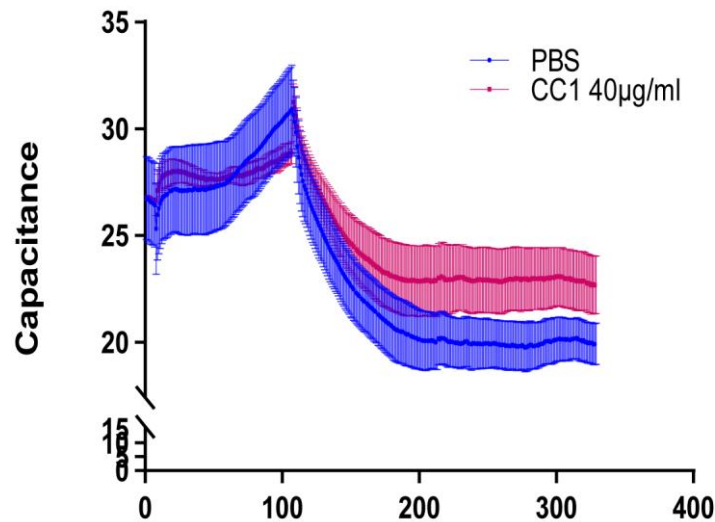


Figure 22 Effects of CEACAM1 in human epithelial cell culture model of barrier function

Electric Cell-substrate Impedance Sensing experiments. Capacitance curves for histone stimulation and subsequent CEACAM1 antibody (CC1) treatment and control (PBS) for human epithelial cells.

3.10 CEACAM1 effects on Anti-GBM disease are likely mediated by expression on endothelial cells

3.10.1 CEACAM1 increases endothelial cell loss in anti-GBM mouse model

Glomerular capillary loop endothelial cells are a vital part within the filtration barrier and can prevent the passage of large molecules, such as albumin. In this regard, it was known before that CEACAM1 can regulate glomerular capillary loop endothelial cells through VEGF and VEGF receptor [53], [103]. To test, whether CEACAM1 also influences endothelial cells in the Anti-GBM mouse model, endothelial cells were stained for CD31⁺ and the stained area was quantified. Indeed, while a decrease of CD31⁺ stained area was seen on day 1 irrespective of *Ceacam1* genotype, on day 7 there was a significantly larger area of CD31⁺ stained cells in *Ceacam1*-deficient mice compared to wild-type controls (Figure 23).

Further evidence for a role of endothelial CEACAM1 was found performing electron microscopy (Figure 24): while all mice showed ultrastructural evidence of foot process effacement, no endothelial cell swelling or luminal thrombosis formation were found in *Ceacam1*^{-/-} mice, whereas these findings were clearly present in wild-type controls after GN induction.

Taken together, CEACAM1 induces endothelial cell swelling, luminal thrombosis and subsequent endothelial cell loss in the anti-GBM disease mouse model.

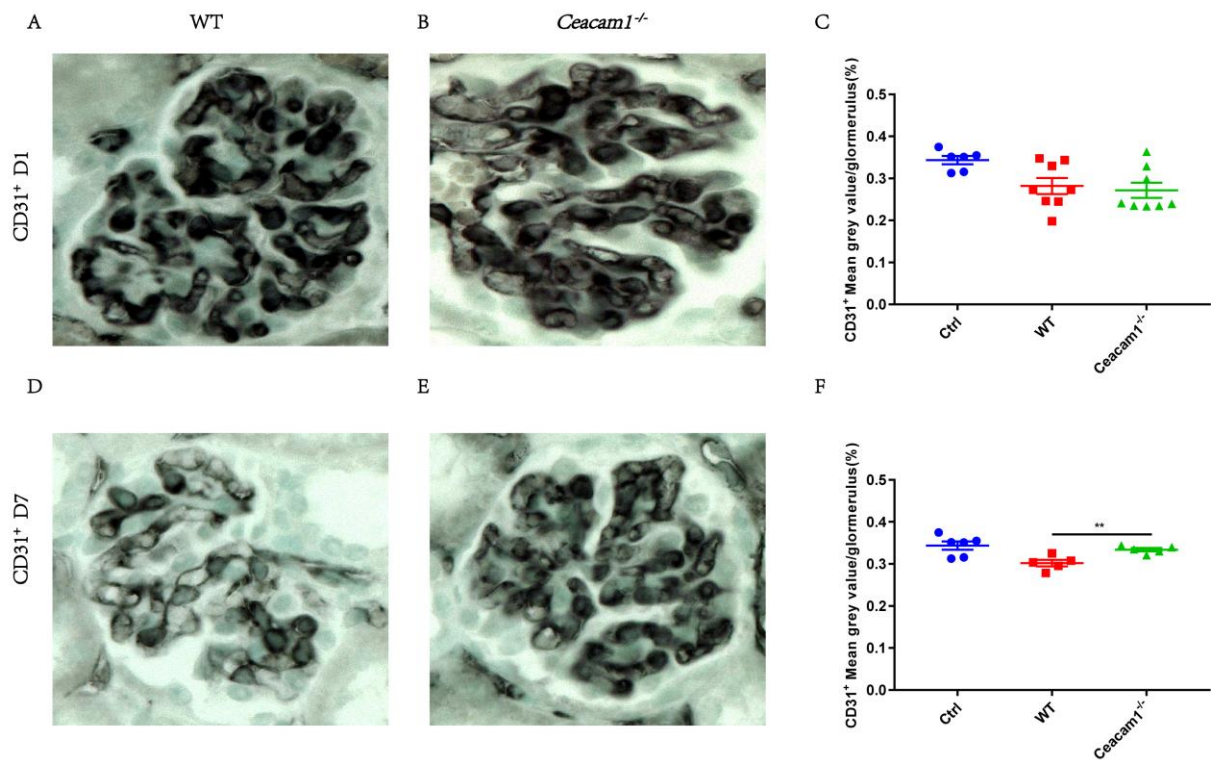


Figure 23 CD31⁺ staining for endothelial cells after induced in Anti-GBM disease in mice

(A, B, C and D) CD31⁺ staining for endothelial cells of WT day 1, *Ceacam1*^{-/-} day 1, WT day 7 and *Ceacam1*^{-/-} day 7, respectively. (C and F) quantitation data of those section. **p<0.01.

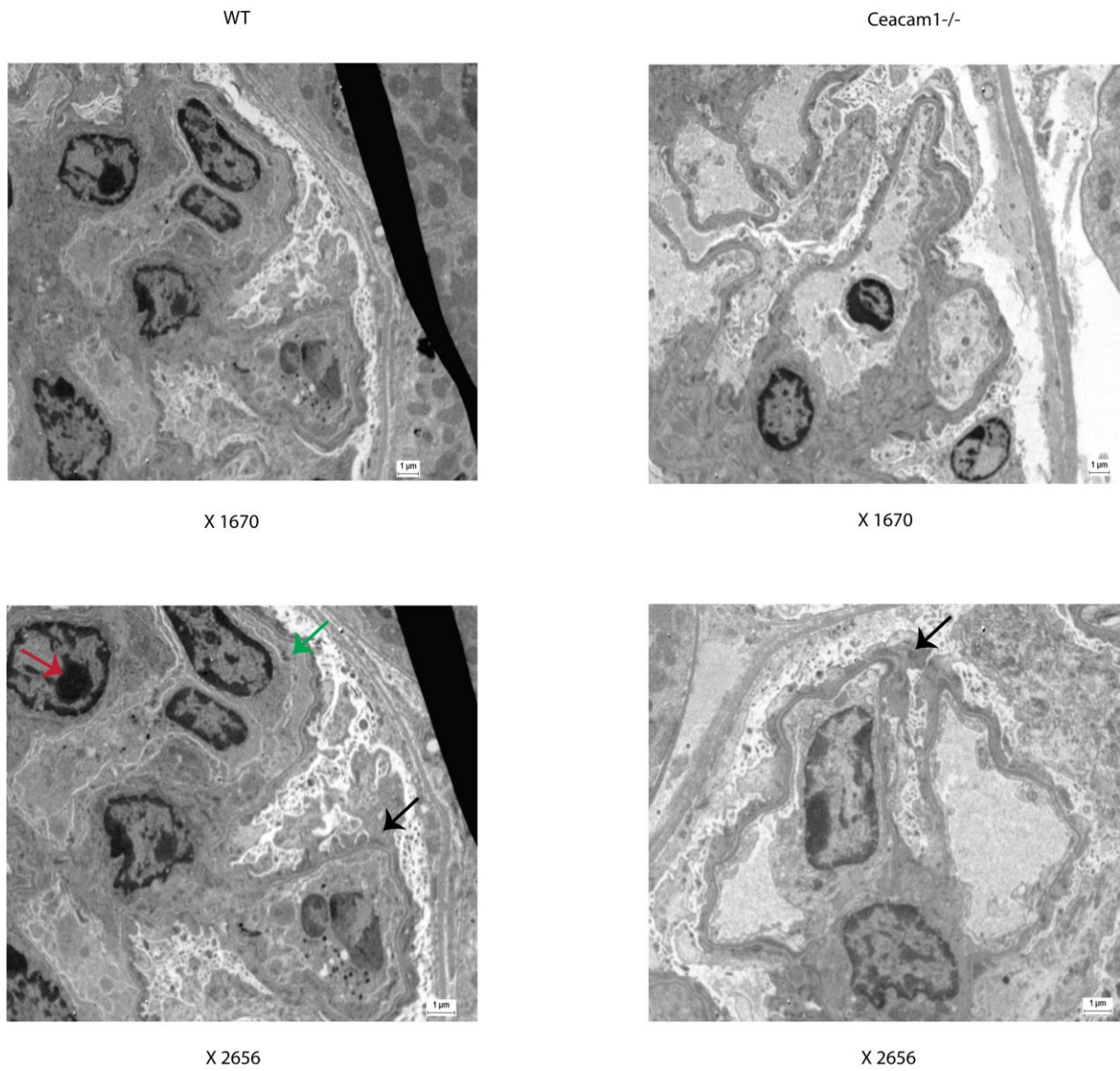


Figure 24 Image from electron microscopy of anti-GBM nephritis

Luminal thrombosis formation (red arrow), endothelial cell swelling (green arrow) and foot process effacement (black arrow).

3.10.2 *Ceacam1* deficiency attenuates glomerular endothelial cell death

In addition to the aforementioned effects on endothelial cells, and also *Ceacam1*^{-/-} mice showed less cell death (indicated by TUNEL⁺) in their glomeruli in GN at both day 1 and day 7 (Figure 25 A-F). To identify the specific cell type affected by cell death, kidney sections were co-stained with TUNEL (green) and CD31 (red), a co-staining identifying the dead cells as endothelial cells (Figure 25G). As there are many types of cell death, RIP3 phosphorylation was checked by western blot to identify necroptotic cell death. Figure 26 shows more RIP3 phosphorylation in wild-type mice compared to *Ceacam1*^{-/-} mice at day 1 but not day 7. In summary, CEACAM1 mediates endothelial cell death during GN at least partly by necroptosis induction.

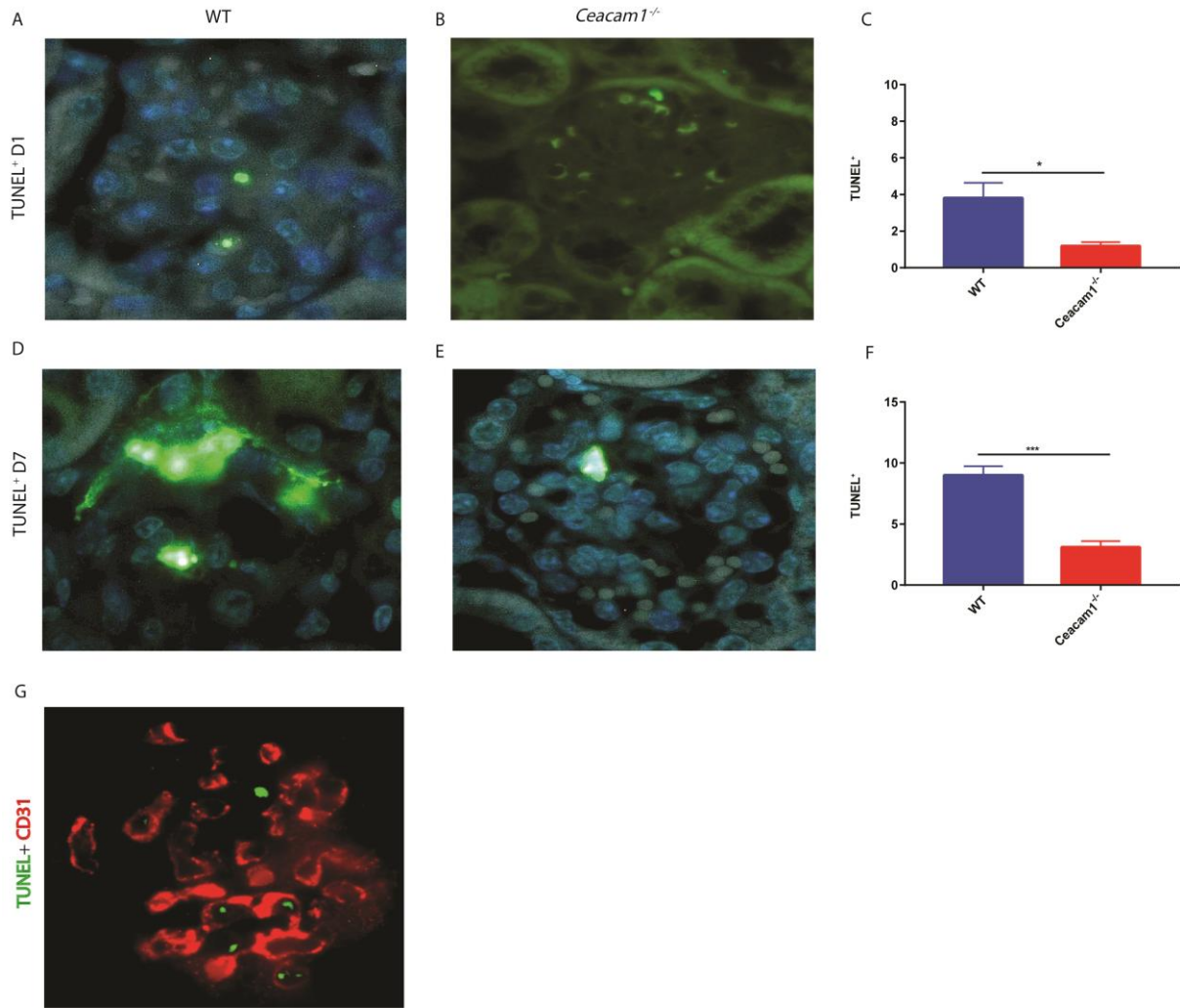


Figure 25 Endothelial cell death in nephritis

Immunofluorescence staining and quantitation of endothelial cell death with TUNEL (TdT-mediated dUTP-biotin nick end labeling) and CD31 (cluster of differentiation 31) staining in GN. Section for TUNEL staining (A, B, D, E) and quantitation of section (C, F), section for TUNEL and CD31 co-staining (G). *p<0.05, ***p<0.001.

3.10.3 CEACAM1 expression is upregulated in endothelial cells after stimulation with lipopolysaccharide or histones

As most of CEACAM1 is expressed by endothelial cells and there is an upregulation upon injury, cell culture experiments using murine endothelial cells were performed to identify possible triggers and mechanisms for upregulation. Endothelial cells were exposed to lipopolysaccharide (LPS) or histones for 6 h, supernatant free DNA concentration was measured and surviving cells were harvested for RNA isolation and *Ceacam1* gene expression analysis. As expected, endothelial cell death was observed after stimulation with histones alone, and this was amplified by LPS pre-stimulation (Figure 27). The results show that after stimulated with LPS or histone for 6 h (Figure 28), *Ceacam1* expression was significantly enhanced on endothelial cells compared with unstimulated cells. Taken together, while murine endothelial cells express low levels of CEACAM1 at baseline, there is a histone- and LPS-induced upregulation and this CEACAM1 upregulation is associated with histone-induced cell death.

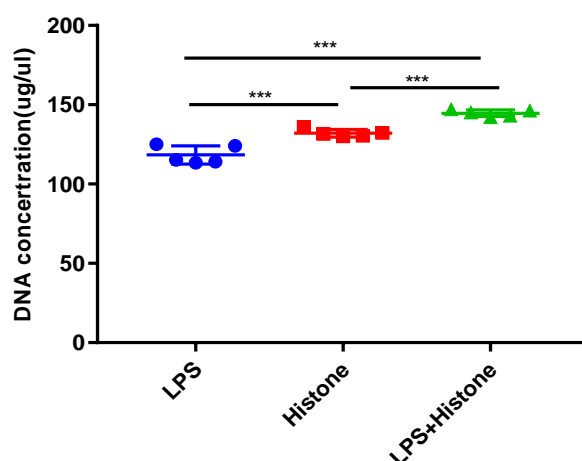


Figure 27 Endothelial cell death after stimulated with LPS and histone

Endothelial cells are stimulated 6h with LPS first and then stimulated with histone for another 6h.***p<0.001.

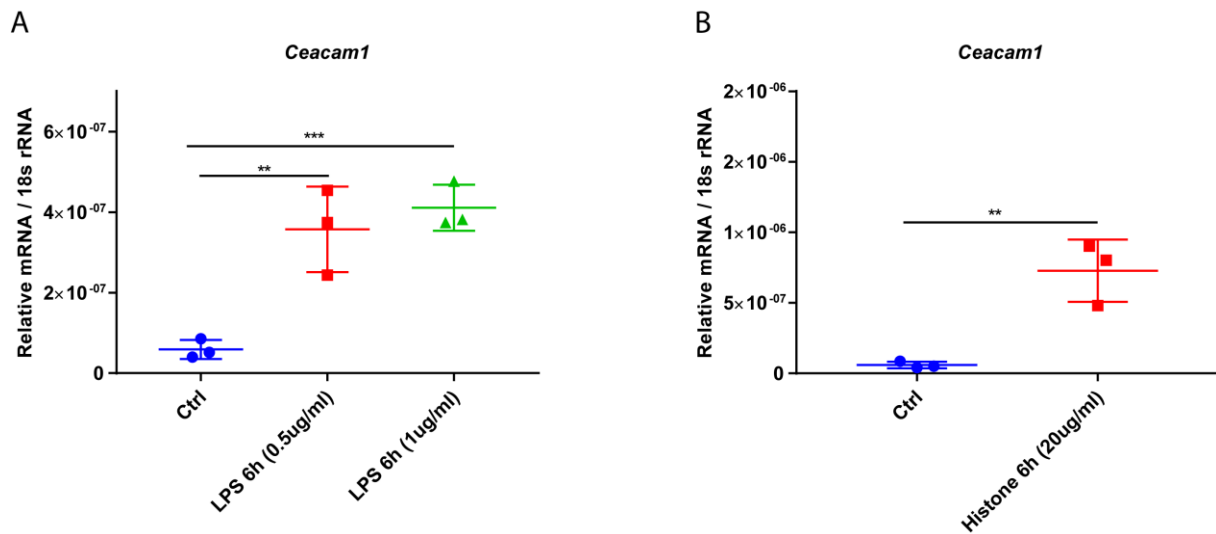


Figure 28 *Ceacam1* expression on endothelial cell after stimulated with LPS and histone

Ceacam1 expression significant upregulate after exposed to LPS for 6 h at different concentration (0,5ug/ml and 1ug/ml), n= 3 (A). *Ceacam1* expression increased after stimulated with histone (20ug/ml) n=3. *p<0.05, **p<0.01, ***p<0.001 (B).

3.10.4 Endothelial cell death leads to increased permeability *in vitro*

To investigate whether the endothelial cell death and the subsequent GBM permeability observed *in vivo* can be observed also *in vitro*, transwell permeability assays were performed using murine endothelial cells after stimulation with LPS or histone. The results (Figure 29) shown that endothelial cell death can lead to permeability after damage by histone. This demonstrates that increased endothelial cell death leads to increased endothelial permeability. Thus, consistent with the *in vivo* data, CEACAM1 is upregulated upon injury and associated with an increase in endothelial permeability after stimulation with histone.

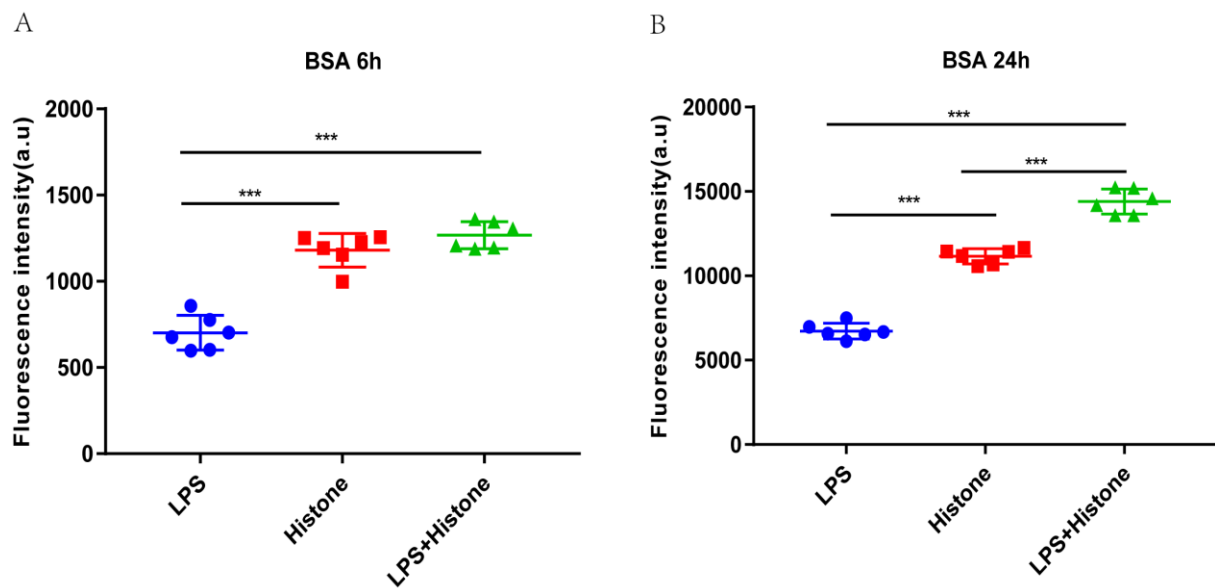


Figure 29 Transwell permeability assay with bovine serum albumin

Endothelial cells are stimulated for 6h (Left of the panel) or 24 h (Right of the panel) with LPS and histone. bovine serum albumin (BSA) was detected by ELISA reader. ***p<0.001.

3.10.5 Endothelial cell death activates vascular endothelial growth factor and AKT signaling pathways leading to vascular permeability

A powerful angiogenic factor that maintains the glomerular and peritubular capillary network is the VEGF. CEACAM1 signaling has been shown relative with the VEGFR2/AKT/eNOS-mediated vascular permeability pathway [65]. In fact, the mRNA level of *Vegf* and *Vegf* receptor were significant increase in wild-type mice at day 7 in GN (Figure 30). Consistent with this, an enhanced phosphorylation of AKT downstream signaling was also been seen in day 7 (Figure 31). Angiopoietins 1 and 2, ligands for receptor kinase Tie-2, are proposed to play vital but opposing function in vascular development with VEGF. *Ang1*, *Ang2*, *Tie1* and *Tie2* were in fact significantly increased in wild-type mice compared to *Ceacam1*^{-/-} mice both at day1 and day 7 (Figure 32). In sum, the above findings suggest that CEACAM1 signaling activates VEGF/VEGFR and AKT signaling pathways to promote vascular permeability upon GN.

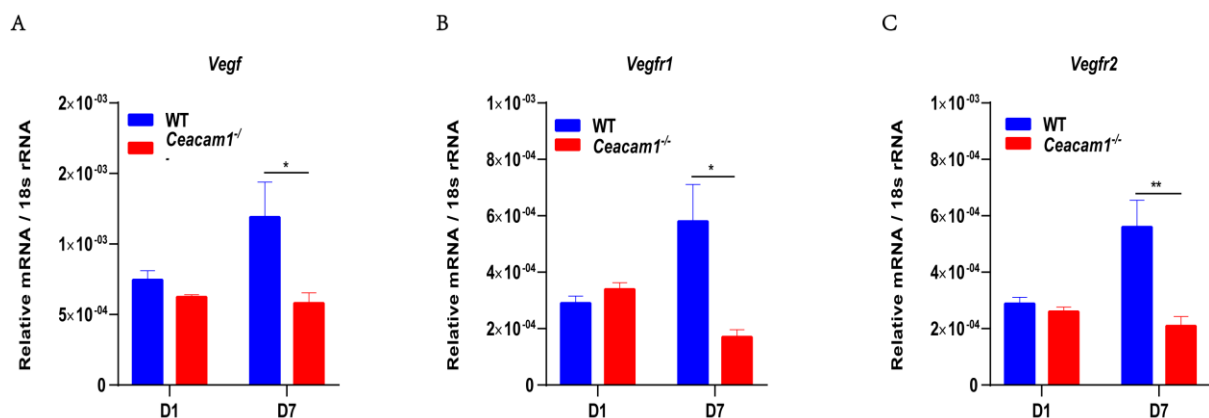


Figure 30 Gene expression of *Vegf* and *Vegf* receptor in GN

Reverse transcriptase quantitative PCR (RT-qPCR) was used to quantitative for *Vegf/Vegfr*. VEGF: Vascular endothelial growth factor, VEGFR: Vascular endothelial growth factor receptor. *p<0.05, **p<0.01.

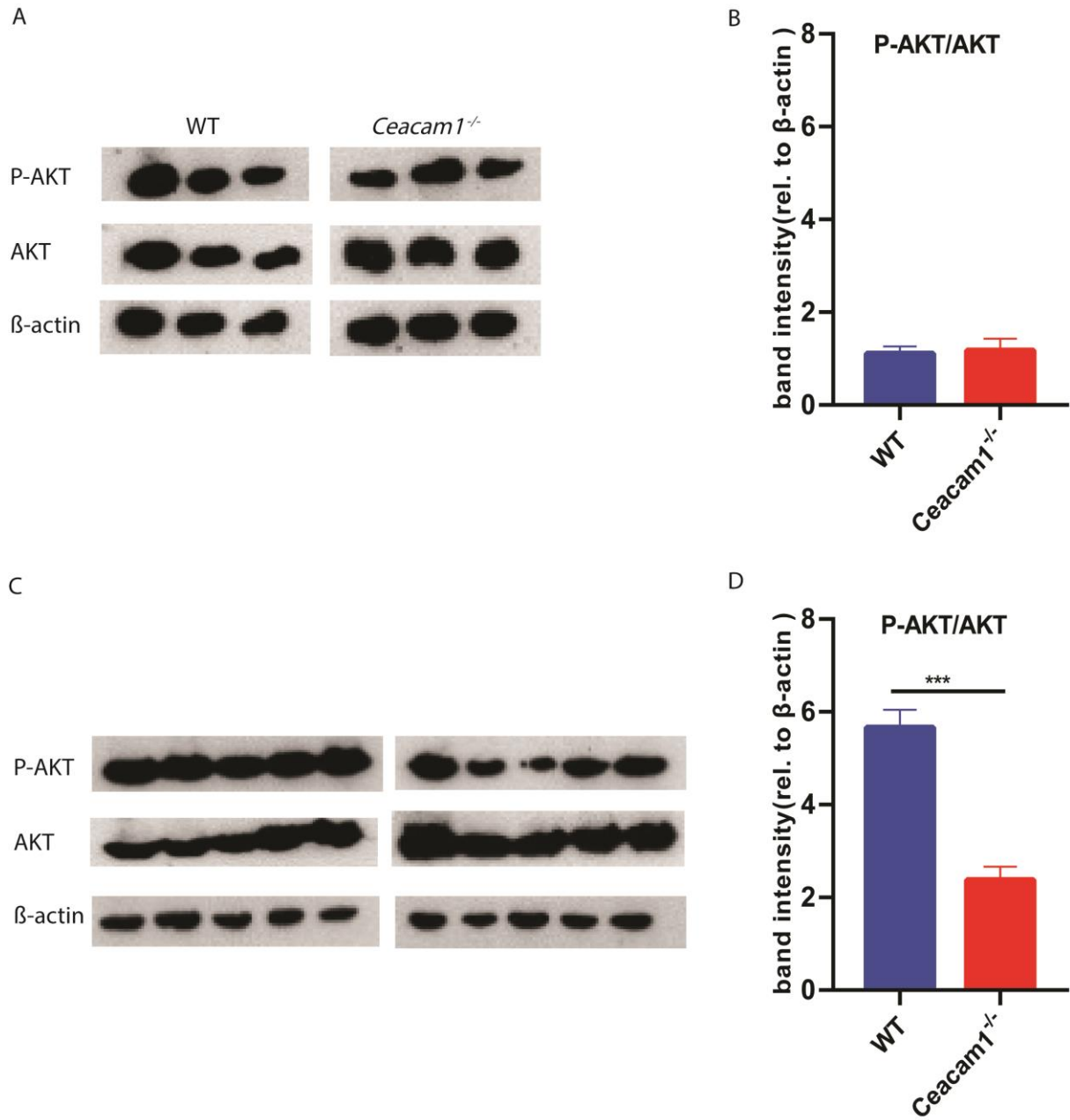


Figure 31 Kidney tissue western blots in WT and *Ceacam1^{-/-}* mice in GN

Western blots gel staining (A, C) and (B, D) staining quantitation for AKT. *** $p < 0.001$.

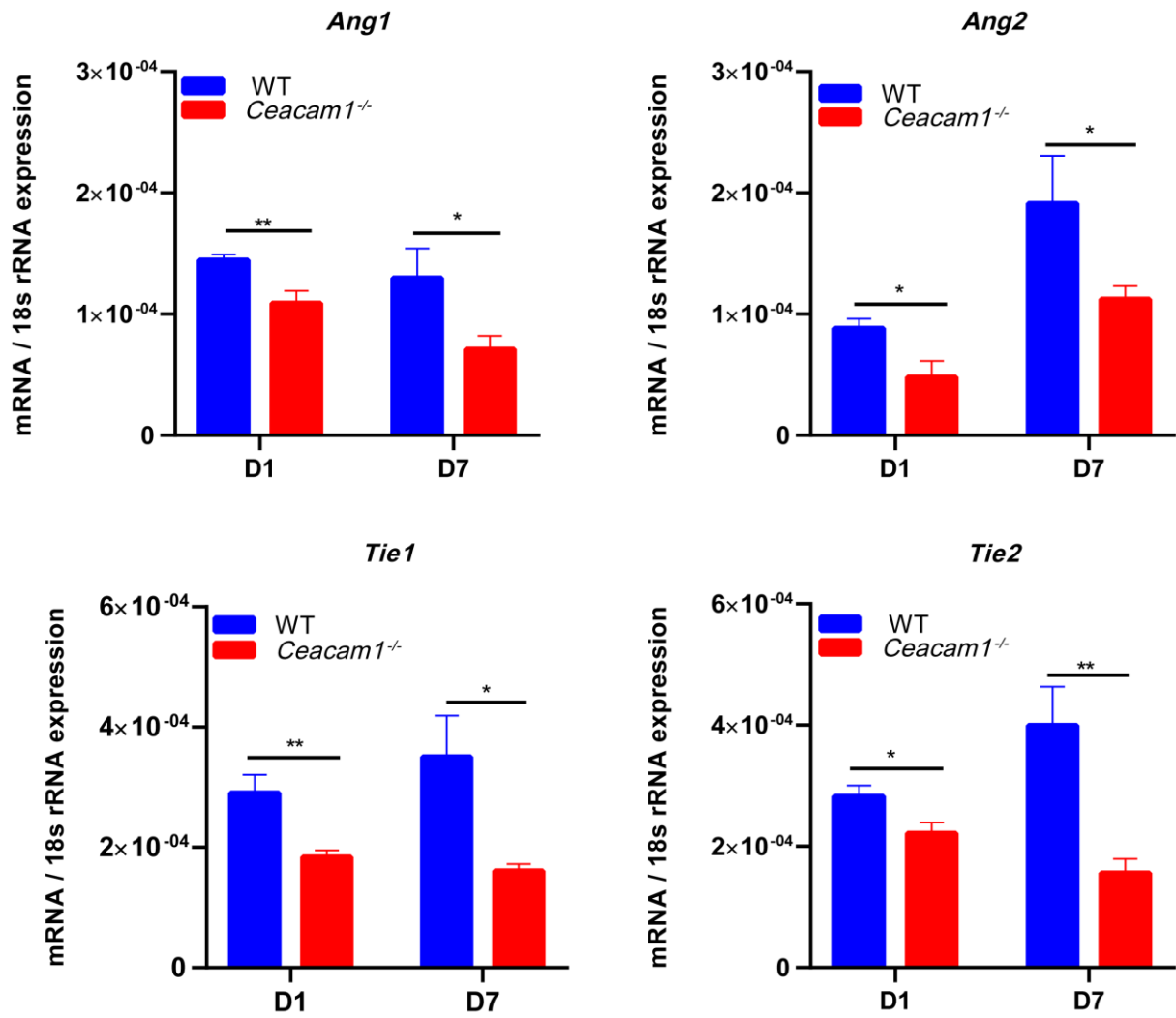


Figure 32 Angiopoietins-1,2 and receptor kinase Tie-1,2 expression on kidney of nephritis

Reverse transcriptase quantitative PCR (RT-qPCR) was used to quantitative for *Ang1*, *Ang2*, *Tie-1* and *Tie-2*.

Angiopoietins-1,2 (*Ang1* and *Ang2*) and receptor kinase Tie-1,2 (*Tie-1* and *Tie-2*), * $p < 0.05$, ** $p < 0.01$.

3.10.6 Tight junction proteins decrease in endothelial cells after stimulation with histone and LPS

The tight junction constitutes the barrier both to the molecules as well as passage of ions. When tight junction proteins are decreased, there is an increase in permeability of endothelial cells [104]. Tight junction proteins were also found to be downregulated after stimulation with histone and LPS (Figure 33). Taken together with the previous data, CEACAM1 can increase the permeability of GBM by various mechanisms leading to albuminuria, for example through downregulation of tight junction proteins between endothelial cells.

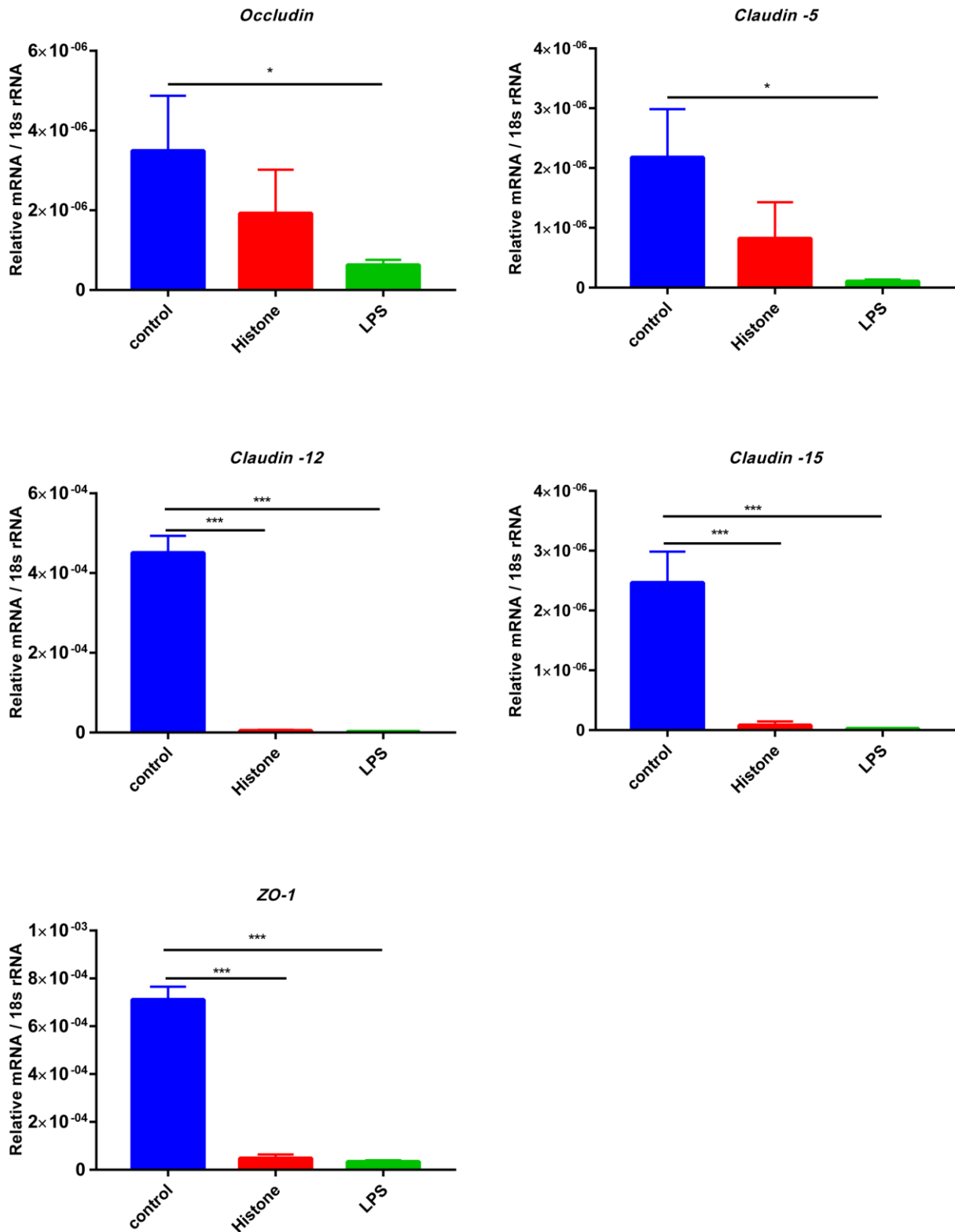


Figure 33 Tight junction proteins expression on endothelial cells

Reverse transcriptase quantitative PCR (RT-qPCR) was used to quantitative for *Occludin*, *Claudin-5*, *Claudin-12*, *Claudin-15* and *Zo-1*. *Zo-1*: Zonula occludens-1, *p<0.05, **p<0.01.

4 Discussion

The goal of our work was to study the role of CEACAM1 in the pathogenesis of glomerulonephritis. I had hypothesized that CEACAM1 aggravates the death of endothelial cells and promote the development of nephritis, hence *Ceacam1* knock-out mice should be protected during Anti-GBM nephritis. To explore the function of CEACAM1 in anti-GBM nephritis, I established an anti-GBM mouse model with *Ceacam1*^{-/-} and wild-type mice. After induction of nephritis, *Ceacam1*^{-/-} mice indeed showed various signs of an ameliorated phenotype: they had less albuminuria, decreased mRNA levels of injury markers as well as markers of inflammation, less podocyte loss and less leukocyte infiltration. These results are all consistent with my hypothesis.

Based on the phenotype observed in human tissue samples and the *Ceacam1*- knockout mouse model of anti-glomerular basement membrane nephritis, the following conclusions arise in detail:

1. CEACAM1 is only expressed at low levels in normal mouse kidney and healthy human kidneys. Upon some, but not all injurious stimuli to the glomerular basement membrane, CEACAM1 is upregulated in the human kidney. CEACAM1 is also upregulated during the cause of anti-GBM disease in mice.
2. In the mouse model, this upregulation of CEACAM1 aggravates the damage to the glomerular basement membrane by first injuring the capillary endothelial cells in the glomeruli, which in turn damages the basement membrane and leads to podocyte loss.

3. CEACAM1 induced endothelial cell injury by regulating at least two pathways: a) the VEGF/AKT signaling pathway leading to downregulation of tight junction molecules, causing increased vascular permeability, and ultimately albuminuria. b) the RIPK1/RIPK3 pathway leading to increased endothelial cell death.

4.1 CEACAM1 is mainly expressed on endothelial cells in the kidney

CEACAM1 is widely expressed in a many organs, tissues and cells, including the liver, colon, lymph nodes, testis, skeletal muscles, bone marrow and peripheral blood cells, (e.g. B and T cells, monocytes, neutrophils) and endothelial cells [42], [53], [64], [105]–[114]. There are tissue-specific differences: in the liver, CEACAM1 is expressed by immune cells and liver epithelial cells. CEACAM1 was first defined as a CEA-like product and a biliary glycoprotein (BGP) in human hepatic bile. Later, a particular correlation between BGP-I/soluble CEACAM1 expression and obstructive liver disease has been recognized in patients [42], [64]. In fact, soluble CEACAM1 expression in rodents with liver disease is also strongly increased [115]. Additionally, in rats CEACAM1 is also expressed during the fetal period [116]. CEACAM1 can be detected in all biliary specimens, not only in malignant diseases [42], [117]. The expression of CEACAM1 major subtypes increased after birth, demonstrated that CEACAM1 is a marker molecule in epithelial cell differentiation process.

CEACAM1 is widely expressed in colitis and colon cancer. A recent study showed that exogenous CEACAM1 ameliorates the inflammatory response, improves epithelial barrier function, promotes recovery of epithelial cells, and effectively alleviates ulcerative colitis symptoms in the mouse model of colitis [109]. CEACAM1 expression defects are associated with early colorectal tumorigenesis [118], and compared with the control group, mice with

Ceacam1 gene deletion are more likely to develop colon tumors after exposure to carcinogens [51]. These results shown that the absence of CEACAM1 is permissive to the development of colon tumors.

CEACAM1 is expressed in a lot of immune cells, for example, B cells, neutrophils, macrophages, T cells as well as Natural Killer cells [68], [119]. Recently studies have indicated CEACAM1-L acts as an inhibitor of T cell activation by its ITIM motif based on a SHP-1-dependent manner [74], [120]–[122]. CEACAM1 has a function in B cell, although some results of the studies are contradictory [77], [78], [123], [124]. The antibody response of B cells to some viral antigens was shown to be CEACAM1-dependent [77], but the role of CEACAM1 in B cell neoplasms is debated. However, CEACAM1 seems to play a vital role in B cells as well as in T cells.

Although CEACAM1 plays a very important role in many organs and tissues, there is little data on CEACAM1 in the kidney. According the KIT database of single-cell RNAseq data, CEACAM1 is mainly expressed on endothelial cells, with weaker expression on podocytes and proximal as well as distal tubular cells. To corroborate the findings on renal CEACAM1 expression, I analyzed kidney tissues of both humans and mice by means of immunohistochemistry and confirmed the CEACAM1 expression to be confined mainly on endothelial cells with a very faint staining on podocytes. In addition, I could show that the relatively low CEACAM1 expression in normal kidneys was significantly upregulated in both human and murine anti-GBM disease. This is in agreement with another study that showed an up-regulation of CEACAM1 expression in renal tubules and/or glomerular cells during acute rejection of human kidney allografts [125]. Interestingly, while I observed an

upregulation of CEACAM1 in human anti-GBM disease, I did not see such an effect in another form of human glomerular disease, namely diabetic nephropathy.

4.2 CEACAM1 aggravates kidney injury in anti-GBM nephritis

CEACAM1 can exert pro- and anti-inflammatory effects in different diseases. For example, CEACAM1 suppresses T-cell function after T-cell activation in colitis as a coinhibitory receptor. One study [126] found that CEACAM1 acts as a heterologous ligand for TIM-3 and mediates T cell suppression through the interaction of highly conserved membrane-distal N-terminal domains of each molecule, promoting TIM-3 maturation and cell surface expression. Additionally, CEACAM1 is expressed on B-cell subsets [77], [127] and Khairnar et al. [77] demonstrated that the intrinsic signaling of CEACAM1 is critical for generating efficient B-cell responses, although CEACAM1 has a limited effect on B cell proliferation. In my study, I found CEACAM1 to be pro-inflammatory after the induction of anti-GBM nephritis: *Ceacam1*-deficient mice produce less inflammatory cytokines (CCL2, CCL5 and TNF- α) leading to less infiltration of macrophages. However, the details about how CEACAM1 acts as an inflammatory factor on B and T cells are not definitively clarified by my work. While I did not observe any difference in intrarenal CD3⁺ or CD19⁺ cells between *Ceacam1*^{-/-} and *Ceacam1*^{+/+} mice, I did not assess B cell and T cell survival or proliferation in the nephritis mouse model. However, my results show that CEACAM1 upregulation aggravates kidney injury in a totally different way, namely by damaging glomerular endothelial cells. Endothelial dysfunction, tubular injury and intrarenal inflammation are common pathophysiologic processes that occur in AKI. I establish here CEACAM1-mediated endothelial cell dysfunction as a driving force in the development of anti-GBM disease (see

below). I also studied tubular injury markers such as NGAL, KIM-1, liver fatty acid-binding protein, as well as the two cell cycle arrest markers TIMP2 and IGFBP7 [128]–[135] and found a significant increase in *Ceacam1*^{-/-} mice, but this tubular phenotype is rather secondary to the primary GBM injury. Conversely, Li et al. [88] demonstrated, that CEACAM1 colocalizes with NLRC5 in proximal renal tubular cells. Interestingly, in their model of primary tubular injury by ischemia-reperfusion, CEACAM1 is downregulated in a NLRC5-dependent manner and the reversal of this downregulation is associated with an ameliorated phenotype mainly driven by anti-apoptotic functions of CEACAM1.

Taken together, this suggests that CEACAM1 has differential, cell-type specific roles within the kidney. Hence, the net effect of CEACAM1 depends on the disease-context and which cell type or compartment (glomerular vs. tubular) is primarily affected.

4.3 The VEGF/AKT pathway in the downstream signaling of CEACAM1 in anti-GBM nephritis

From my previous results, I concluded that CEACAM1 aggravates the inflammation and injury in nephritis through damage the endothelial cell. This is exemplified by decreased glomerular crescent formation and less albuminuria in *Ceacam1*^{-/-} mice. As it was known that in endothelial cells CEACAM1 is involved in VEGF-dependent AKT signaling, AKT and VEGF/VEGFR1/2 levels were detected by WB and RT-qPCR. The observed upregulation during the course of anti-GBM nephritis is consistent with previous research results, showing that VEGF plays a very crucial role in endothelial dysfunction [136]–[138]. Complex local autocrine and paracrine pathways (podocytes and glomerular endothelial cells) are crucial to the filtration barrier homeostasis, where podocytes secrete various factors that directly

affect the glomerular endothelium [139], [140]. Several studies have shown that VEGF has an important function in the maintenance of the glomerular capillary as well as for endothelial permeability [141]–[143]. The imbalance between VEGF and VEGF receptor 1/2 has been mentioned in a variety of diseases, such as kidney disease, in which regulation of VEGF signaling is related to impaired endothelial barrier, endothelial dysfunction, as well as increased proteinuria [144]–[147]. While the contribution to chronic kidney disease progression is unknown, it is saved to say that VEGF/VEGFR takes part in the process of endothelial dysfunction in nephritis. More recently, studies have shown that AKT signaling also participates in VEGF production [148], [149]. So how about the relationship between CEACAM1 and AKT/VEGF pathway in anti-GBM disease? My results show that *Ceacam1*^{-/-} mice have a largely blunted VEGF/VEGFR upregulation upon glomerular injury and hence less AKT phosphorylation. The effect of this should be less vascular permeability, indeed found by the reduced proteinuria *Ceacam1*^{-/-} mice compared wild-type mice. In 2010, one study [65] found that CEACAM1 is essential to maintain vascular integrity in ischemic neovascularization, but in this study the basal vascular permeability of *Ceacam1*^{-/-} mice was significantly increased, which was associated with increased activation of AKT and endothelial nitric oxide synthase in mice lung endothelial cells. While this is in contrast with my findings, in the same study the deletion of *Ceacam1* in lung endothelial cells inhibited VEGF mediated nitric oxide production, consistent with the downstream VEGF signaling defects in my *Ceacam1*^{-/-} mice after anti-GBM disease induction. While it is difficult to explain these partly contrasting phenotypes, the function of CEACAM1 might differ between lung and kidney endothelial cells and their response to injurious stimuli.

Taken together, CEACAM1 aggravates anti-GBM nephritis through activating the VEGF/AKT pathway in glomerular endothelial cells.

4.4 CEACAM1-mediated endothelial cell death in anti-GBM nephritis

Cell death is a part of the normal process of growth as well as maturation, and it is a key and positive process for maintaining tissue homeostasis and eliminating potentially harmful cells in multicellular organisms [150]–[154]. Regulated cell death is already known to take part in the pathogenesis of many different acute kidney diseases [155]. In the past two decades, mainly tubular cell death has been found in preclinical models of AKI and in patients [119], [121], [132], [156]. Glomerular mesangial cells and endothelial cells are the three most important cell types in the glomerulus, and cell death has mostly been studied in endothelial cells [157]–[160]. Glomerular endothelial cell dysfunction and death are involved in the pathogenesis of nephrotic syndrome in general [132]. Necroptosis is a kind of gene-regulated necrotic cell death that has become an vital pathogenic pathway for many diseases of human [161]–[163]. RIPK1 and RIPK3 (receptor-interacting protein kinases 1 and 3) and MLKL (mixed-lineage kinase domain-like pseudo kinase) form a regulatory necrosome complex together induce the necroptosis pathway. MLKL phosphorylation mediated by RIPK3 induces necroptosis. Consistent with previous studies, I found endothelial cell death during the course of anti-GBM disease, shown by TUNEL / CD31 double-positive cells in the glomerulus. Interestingly, a difference in TUNEL staining observed between *Ceacam1*^{-/-} and *Ceacam1*^{+/+} mice was found, with lower numbers of TUNEL+ cells in *Ceacam1*^{-/-} mice. As different routines of regulated cell death can occur in kidney endothelial cells, and TUNEL

staining is not, as previously thought, apoptosis-specific, I investigated this phenotype further. I found increasing levels of phosphorylated RIPK3 during the course of anti-GBM disease, while phosphorylated RIPK3 was reduced in the kidneys of *Ceacam1^{-/-}* mice compared to *Ceacam1^{+/+}* mice on day 1. This suggests two things: i) glomerular endothelial cell necroptosis is involved during the development of anti-GBM nephritis, as already found by others [164]. ii) CEACAM1 regulates this process in a pro-necroptotic fashion.

Recently, one study found RIPK3 to be strongly expressed in human chronic kidney disease (CKD) [165]. Another study found that up-regulation and interaction of RIPK3 and MLKL induce necroptosis of renal proximal tubule cells under renal ischemia-reperfusion injury (IRI) conditions [166]. Necrosis can trigger inflammation, which enhances the positive feedback loop of necrosis, which in turn triggers more inflammation, called necrotic inflammation. However, the mechanism of necrosis-induced inflammation caused by renal tubular necroptosis in the progression of AKI to CKD remains unclear. They also found that up-regulation and interaction of RIPK3 and MLKL under IRI conditions induce renal proximal tubule cell necroptosis and promote activation of NLRP3 inflammatory bodies [166]. Most of them found is that necroptosis happens in kidney tubular cells, not endothelial cells. Except one study reveals that anti-neutrophil cytoplasmic antibody (ANCA) stimulated neutrophils induced endothelial cell damage via RIPK1/3 and MLKL-dependent necroptosis. This further proves that my findings are correct.

4.5 Limitations of this study

To study the effect of CEACAM1 on Anti-GBM nephritis, I used *Ceacam1* knockout mice and the mouse model of anti-GBM disease. While this allowed me for detailed analysis and the assessment of causation (rather than association), the research presented here has several important limitations: First and foremost, my study is based on conclusions of mouse experiments. The results presented here are therefore not necessarily representative of human renal biology and pathogenesis. Although most scientists use mice for experimental research [167], [168], there are big differences between the human body environment and the mouse environment. It takes a certain amount of time to transform from scientific research results to clinical applications. It is however promising, that at least the upregulation of CEACAM1, that is observed in the mouse model, is mirrored in the corresponding human disease.

Second, the way I induced Anti-GBM nephritis leads to a heterologous nephritis. While this method has previously been described [94] and is widely applied, it has certain shortcomings. The serum is not identical between different product batches, which can affect the reproducibility of mouse model. I had to use 200 μ l serum to induce glomerulonephritis, while previous researchers from our group [94] only used a 100 μ l serum to successfully induce anti-GBM disease. An alternative to the heterologous model is the use of the autologous model, where generally lower doses of serum are necessary, as the host is actively being immunized.

Third, many additional experiments could be envisioned to further characterize the phenotype of *Ceacam1*^{-/-} mice in more detail: while I analyzed bulk RNA isolated from whole

kidneys, this analysis could be strengthened by microdissection the kidneys and separating the glomerular and the tubular compartment, or ideally by single-cell RNA sequencing. This would allow for a detailed cell-type specific analysis of downstream effects of the *Ceacam1* knock-effect. Also, the use of bone-marrow chimeras or ideally conditional, i.e. cell-type specific knock-out mice (e.g. via crossing *Ceacam1*^{fl^{ox}/fl^{ox}} mice with endothelial cell promotor-specific cre-expressing mice) would be needed to definitively proof the suggested endothelial cell specific effects of CEACAM1.

Fourth, in the necroptosis experiments I did not check the MLKL phosphorylation levels which is today considered the only definitive prove of necroptotic cell death.

5 Summary

Glomerulonephritis is characterized by increasing membrane permeability due to impaired glomerular basement membrane eventually leads to hyperplasia of the basement membrane to form a crescent. the antibody will bind to the membrane then activate the immune system. previous study has shown that endothelial cell death plays a key role in nephritis, other studies already demonstrated that CEACAM1 regulates the endothelial barrier function in vasculogenesis and angiogenesis. But there is no published paper reveal the relationship between the function of CEACAM1 and glomerulonephritis. In this thesis, I investigated whether CEACAM1 produces similar effects during glomerulonephritis. CEACAM1 knockout mice were used during this experiment, and glomerulonephritis was induced by injection of 200 ul sheep anti-GBM serum.

To observe the function of CEACAM1 in nephritis, the phenotype between wild-type mice and CEACAM1^{-/-} mice were compared. Mice treated with Anti-GBM serum showed increased BUN and proteinuria levels, this because the lost endothelial cells and podocytes of GBM, increased glomerular crescent formation and basement membrane permeability. In my results, CEACAM1 expression is significant upregulate after induce nephritis. CEACAM1 deficient mice shown less kidney injury and infiltration of inflammatory factors, reduced endothelial cell death, decreased AKT phosphorylation and VEGF/VEGFR RNA levels. This is consistent with my hypothesis that CEACAM1 plays a pathogenic role in the heterologous anti GBM disease mouse model of crescentic nephritis.

In summary, CEACAM1 aggravates nephritis through the endothelial cell by activating AKT/VEGF pathway in heterologous glomerulonephritis.

6 Zusammenfassung

In der Pathogenese der Glomerulonephritis kommt es durch entzündungsbedingte Schädigung der glomerulären Basalmembran zur Permeabilitätserhöhung, die zu Proteinurie, Aktivierung der Parietalzellen („Halbmondbildung“), Vernarbung und letztlich renalem Funktionsverlust führt. In diesem Prozess spielen Wachstumsfaktoren (z.B. VEGF) und Zell-Zell-Verbindungen (tight junctions) ebenso eine Rolle wie die Induktion regulierten Zelltods. CEACAM1 ist ein wichtiger Regulator der Endothelbarrierefunktion, die Rolle von CEACAM1 in der Pathogenese der Glomerulonephritis war bislang aber unbekannt.

Um die Funktion von CEACAM1 in der Pathogenese der Glomerulonephritis zu beobachten, wurde der Phänotyp zwischen *Ceacam1*^{+/+} und *Ceacam1*^{-/-} Mäusen nach der Induktion einer Glomerulonephritis verglichen. Während die CEACAM1 Expression während der Pathogenese der Glomerulonephritis signifikant ansteigt, zeigen *Ceacam1*^{-/-} Mäuse einen deutlich milderen Phänotyp: sie haben niedrigere Serumretentionsparameter, weniger Albuminurie, weniger intrarenale Entzündung und weniger endothelialen Zelltod. Dieser Phänotyp ist mit einer deutlich geringeren Aktivierung des VEGF/AKT Signalwegs *in vivo* assoziiert. Zusammenfassend verschlimmert CEACAM1 den Verlauf der Glomerulonephritis durch vermehrten Endothelzellschaden via VEGF/AKT- und RIPK1/RIPK3-Signalweginduktion.

7 List of abbreviations

CEACAM1	Carcinoembryonic antigen-related cell adhesion molecule 1
Anti-GBM	Anti-glomerular basement membrane
GN	Glomerulonephritis
AKI	Acute kidney injury
CEACAM1-4L	Namely Carcinoembryonic antigen-related cell adhesion molecule 1 1-4 longer
CEACAM1-4S	Namely Carcinoembryonic antigen-related cell adhesion molecule 1 1-4 short
VEGF	Vascular endothelial growth factor
VEGFR1	Vascular endothelial growth factorreceptor1
VEGFR2	Vascular endothelial growth factorreceptor2
eNOS	Endothelial nitric oxide synthase
cDNA	Complementary desoxyribonucleic acid
ITIMs	Immunoreceptor tyrosine receptor inhibition motifs
COL1A1	Collagen type I alpha 1 chain
TIM-3	T-cell immunoglobulin and mucin-domain containing-3
NK	Natural killer
AKT	Protein kinase B
DMEM	Dulbecco's modified Eagle media
PI3K	Phosphoinositide 3-kinases
ECIS	Epithelial barrier testing via electric cell-substrate impedance sensing

RNA	Ribonucleic acid
BUN	Blood urea nitrogen
PAS	Periodic acid–Schiff
SD	Standard deviation
GBM	Glomerular basement membrane
GFR	Glomerular filtration rate
PBS	Phosphate-buffered saline
CD31	Cluster of differentiation 31
TUNEL	Terminal deoxynucleotidyl transferase dUTP nick end labeling
Ctrl	Control
NGAL	Neutrophil gelatinase-associated lipocalin
KIM-1	Kidney Injury Molecule-1
TIMP2	Tissue inhibitor of metalloproteinases 2
IGFBP7	Insulin-like growth factor-binding protein 7
CCL2	Chemokine (C-C motif) ligand 2
TNF-alpha	Tumour Necrosis Factor alpha
CCL5	Chemokine (C-C motif) ligand 5
CXCL1	Chemokine (C-X-C motif) ligand 1
CXCL2	Chemokine (C-X-C motif) ligand 2
LPS	Lipopolysaccharides
qPCR	quantitative polymerase chain reaction
RT	Reverse transcription
G	Germany
C	China

8 References

- [1] S. P. McAdoo and C. D. Pusey, "Anti-glomerular basement membrane disease," *Clin. J. Am. Soc. Nephrol.*, vol. 12, no. 7, pp. 1162–1172, 2017.
- [2] E. E. van Daalen *et al.*, "Predicting outcome in patients with anti-GBM glomerulonephritis," *Clin. J. Am. Soc. Nephrol.*, vol. 13, no. 1, pp. 63–72, 2018.
- [3] T. Hellmark and M. Segelmark, "Diagnosis and classification of Goodpasture's disease (anti-GBM)," *J. Autoimmun.*, vol. 48–49, pp. 108–112, 2014.
- [4] D. J. Wayne and R. J. Porter, "Goodpasture's Syndrome (Pulmonary Hæmorrhage Associated with Glomerulonephritis)," *J. R. Soc. Med.*, vol. 57, no. 7, pp. 590–592, 1964.
- [5] E. W. Goodpasture, "Landmark publication from The American Journal of the Medical Sciences: The significance of certain pulmonary lesions in relation to the etiology of influenza.," *Am. J. Med. Sci.*, vol. 338, no. 2, pp. 148–151, 2009.
- [6] C. Marques *et al.*, "Prognostic Factors in Anti-glomerular Basement Membrane Disease: A Multicenter Study of 119 Patients," *Front. Immunol.*, vol. 10, 2019.
- [7] C. D. Pusey, "Anti-glomerular basement membrane disease CASE PRESENTATION," 2003.
- [8] J. B. Levy, A. N. Turner, A. J. Rees, and C. D. Pusey, "Long-term outcome of anti-glomerular basement membrane antibody disease treated with plasma exchange and immunosuppression," *Ann. Intern. Med.*, vol. 134, no. 11, pp. 1033–1042, 2001.
- [9] J. Saus, J. Wieslander, J. P. M. Langeveld, S. Quinones, and B. G. Hudson, "Identification of the Goodpasture antigen as the $\alpha 3$ (IV) chain of collagen IV," *J. Biol. Chem.*, vol. 263, no. 26, pp. 13374–13380, 1988.
- [10] N. Turner *et al.*, "Molecular cloning of the human goodpasture antigen demonstrates it to Be the $\alpha 3$ chain of type IV collagen," *J. Clin. Invest.*, vol. 89, no. 2, pp. 592–601, 1992.
- [11] T. Hellmark, H. Burkhardt, and J. Wieslander, "Goodpasture disease. Characterization of a single conformational epitope as the target of pathogenic autoantibodies," *J. Biol. Chem.*, vol. 274, no. 36, pp. 25862–25868, 1999.

-
- [12] M. Segelmark and T. Hellmark, "Anti-glomerular basement membrane disease: An update on subgroups, pathogenesis and therapies," *Nephrology Dialysis Transplantation*, vol. 34, no. 11. pp. 1826–1832, 2019.
- [13] A. Greco *et al.*, "Goodpasture's syndrome: A clinical update," *Autoimmunity Reviews*, vol. 14, no. 3. pp. 246–253, 2015.
- [14] A. Nasrullah, Z. Fatima, A. Javed, U. Tariq, and M. S. Saleem, "A Case of Anti-glomerular Basement Disease Without Pulmonary Involvement," *Cureus*, 2019.
- [15] D. M. Taylor, M. Yehia, I. J. Simpson, H. Thein, Y. Chang, and J. R. de Zoysa, "Anti-glomerular basement membrane disease in Auckland," *Intern. Med. J.*, vol. 42, no. 6, pp. 672–676, 2012.
- [16] P. Raval, "Goodpasture's syndrome," in *xPharm: The Comprehensive Pharmacology Reference*, 2007, pp. 1–4.
- [17] L. F.K. *et al.*, "Incidence and outcome of antiglomerular basement membrane disease in Chinese," *Nephrology*, vol. 9, no. 2, pp. 100–104, 2004.
- [18] C. Savage, C. D. Pusey, C. Bowman, A. J. Rees, and C. M. Lockwood, "Antiglomerular basement membrane antibody mediated disease in the British Isles 1980–4," *Br. Med. J. (Clin. Res. Ed.)*, vol. 292, no. 6516, pp. 301–304, 1986.
- [19] C. B. Wilson and R. C. Smith, "Goodpasture's syndrome associated with influenza A2 virus infection.," *Ann. Intern. Med.*, vol. 76, no. 1, pp. 91–94, 1972.
- [20] E. G. Fischer and D. J. Lager, "Anti-glomerular basement membrane glomerulonephritis: A morphologic study of 80 cases," *Am. J. Clin. Pathol.*, vol. 125, no. 3, pp. 445–450, 2006.
- [21] G. O. Perez, S. Bjornsson, A. H. Ross, J. Aamato, and N. Rothfield, "A mini epidemic of Goodpasture's syndrome. Clinical and immunological studies," *Nephron*, vol. 13, no. 2, pp. 161–173, 1974.
- [22] S. P. McAdoo and C. D. Pusey, "Clustering of anti-GBM disease: Clues to an environmental trigger?," *Clinical Journal of the American Society of Nephrology*, vol. 11, no. 8, pp. 1324–1326, 2016.
- [23] X. jie Zhou *et al.*, "Copy number variation of FCGR3A rather than FCGR3B and FCGR2B is associated with susceptibility to anti-GBM disease," *Int. Immunol.*, vol. 22, no. 1, pp. 45–51, 2009.

- [24] X. J. Zhou *et al.*, "FCGR2B gene polymorphism rather than FCGR2A, FCGR3A and FCGR3B is associated with anti-GBM disease in Chinese," *Nephrol. Dial. Transplant.*, vol. 25, no. 1, pp. 97–101, 2010.
- [25] M. Fisher, C. D. Pusey, R. W. Vaughan, and A. J. Rees, "Susceptibility to anti-glomerular basement membrane disease is strongly associated with HLA-DRB1 genes," *Kidney Int.*, vol. 51, no. 1, pp. 222–229, 1997.
- [26] C. Benchimol, "Anti-glomerular basement membrane disease," in *Glomerulonephritis*, 2019, pp. 359–366.
- [27] R. N. Srivastava and V. P. Choudhry, "Rapidly progressive (crescentic) glomerulonephritis," *Int. J. Pediatr. Nephrol.*, vol. 1, no. 2, pp. 94–96, 1980.
- [28] Z. Ricci and S. Romagnoli, "Acute Kidney Injury: Diagnosis and Classification in Adults and Children," *Contrib. Nephrol.*, 2018.
- [29] Z. Cui *et al.*, "Anti-glomerular basement membrane disease: Outcomes of different therapeutic regimens in a large single-center chinese cohort study," *Medicine (Baltimore)*, vol. 90, no. 5, pp. 303–311, 2011.
- [30] S. R. Henderson and A. D. Salama, "Diagnostic and management challenges in Goodpasture's (anti-glomerular basement membrane) disease," *Nephrology Dialysis Transplantation*. 2018.
- [31] R. A. Sinico, A. Radice, C. Corace, E. Sabadini, and B. Bollini, "Anti-glomerular basement membrane antibodies in the diagnosis of Goodpasture syndrome: A comparison of different assays," *Nephrol. Dial. Transplant.*, 2006.
- [32] S. P. McAdoo and C. D. Pusey, "Antiglomerular Basement Membrane Disease," *Seminars in respiratory and critical care medicine*. 2018.
- [33] C. M. Lockwood, T. A. Pearson, A. J. Rees, D. J. Evans, D. K. Peters, and C. B. Wilson, "IMMUNOSUPPRESSION AND PLASMA-EXCHANGE IN THE TREATMENT OF GOODPASTURE'S SYNDROME," *Lancet*, vol. 307, no. 7962, pp. 711–715, 1976.
- [34] K. J. M. Assmann, M. M. Tangelder, W. P. J. Lange, G. Schrijver, and R. A. Koene, "Anti-GBM nephritis in the mouse: severe proteinuria in the heterologous phase," *Virchows Arch. A Pathol. Anat. Histopathol.*, 1985.
- [35] J. M. Hoppe and V. Vielhauer, "Induction and Analysis of Nephrotoxic Serum Nephritis in Mice," *Methods Mol. Biol.*, 2014.

- [36] D. Nakazawa *et al.*, “Histones and neutrophil extracellular traps enhance tubular necrosis and remote organ injury in ischemic AKI,” *J. Am. Soc. Nephrol.*, vol. 28, no. 6, pp. 1753–1768, 2017.
- [37] Y. Chen, L. Lin, X. Tao, Y. Song, J. Cui, and J. Wan, “The role of podocyte damage in the etiology of ischemia-reperfusion acute kidney injury and post-injury fibrosis,” *BMC Nephrol.*, 2019.
- [38] P. Mundel and S. J. Shankland, “Podocyte biology and response to injury,” *Journal of the American Society of Nephrology*. 2002.
- [39] T. A. Sutton, “Alteration of microvascular permeability in acute kidney injury,” *Microvasc. Res.*, 2009.
- [40] H. Yasuda, P. S. T. Yuen, X. Hu, H. Zhou, and R. A. Star, “Simvastatin improves sepsis-induced mortality and acute kidney injury via renal vascular effects,” *Kidney Int.*, 2006.
- [41] Y. Sato and M. Yanagita, “Immune cells and inflammation in AKI to CKD progression,” *American Journal of Physiology - Renal Physiology*. 2018.
- [42] A. K. Horst, S. M. Najjar, C. Wagener, and G. Tiegs, “CEACAM1 in liver injury, metabolic and immune regulation,” *International Journal of Molecular Sciences*, vol. 19, no. 10. 2018.
- [43] Y. Hinoda *et al.*, “Molecular cloning of a cDNA coding biliary glycoprotein I: Primary structure of a glycoprotein immunologically crossreactive with carcinoembryonic antigen,” *Proc. Natl. Acad. Sci. U. S. A.*, vol. 85, no. 18, pp. 6959–6963, 1988.
- [44] M. Aurivillius, O. C. Hansen, M. B. S. Lazrek, E. Bock, and B. Öbrink, “The cell adhesion molecule Cell-CAM 105 is an ecto-ATPase and a member of the immunoglobulin superfamily,” *FEBS Lett.*, vol. 264, no. 2, pp. 267–269, 1990.
- [45] U. Rueckschloss, S. Kuerten, and S. Ergün, “The role of CEA-related cell adhesion molecule-1 (CEACAM1) in vascular homeostasis,” *Histochemistry and Cell Biology*, vol. 146, no. 6. pp. 657–671, 2016.
- [46] N. Beauchemin *et al.*, “Redefined nomenclature for members of the carcinoembryonic antigen family,” *Experimental Cell Research*, vol. 252, no. 2. pp. 243–249, 1999.
- [47] R. Kammerer and W. Zimmermann, “Coevolution of activating and inhibitory receptors within mammalian carcinoembryonic antigen families,” *BMC Biol.*, vol. 8, 2010.

- [48] C. Ueshima *et al.*, "CEACAM1 long isoform has opposite effects on the growth of human mastocytosis and medullary thyroid carcinoma cells," *Cancer Med.*, vol. 6, no. 4, pp. 845–856, 2017.
- [49] S. D. Gray-Owen and R. S. Blumberg, "CEACAM1: Contact-dependent control of immunity," *Nature Reviews Immunology*, vol. 6, no. 6, pp. 433–446, 2006.
- [50] A.-L. Nouvion and N. Beauchemin, "[CEACAM1 as a central modulator of metabolism, tumor progression, angiogenesis and immunity].," *Med. Sci. (Paris)*., vol. 25, no. 3, pp. 247–52, 2009.
- [51] N. Leung, C. Turbide, M. Olson, V. Marcus, S. Jothy, and N. Beauchemin, "Deletion of the carcinoembryonic antigen-related cell adhesion molecule 1 (Ceacam1) gene contributes to colon tumor progression in a murine model of carcinogenesis," *Oncogene*, vol. 25, no. 40, pp. 5527–5536, 2006.
- [52] D. M. Rovituso *et al.*, "CEACAM1 mediates B cell aggregation in central nervous system autoimmunity," *Sci. Rep.*, vol. 6, 2016.
- [53] S. Ghavampour *et al.*, "Endothelial barrier function is differentially regulated by CEACAM1-mediated signaling," *FASEB J.*, vol. 32, no. 10, pp. 5612–5625, 2018.
- [54] W. Staels, Y. Heremans, H. Heimberg, and N. De Leu, "VEGF-A and blood vessels: a beta cell perspective," *Diabetologia*, 2019.
- [55] N. Papadopoulos *et al.*, "Binding and neutralization of vascular endothelial growth factor (VEGF) and related ligands by VEGF Trap, ranibizumab and bevacizumab," *Angiogenesis*, vol. 15, no. 2, pp. 171–185, 2012.
- [56] H. Sawa *et al.*, "C-CAM expression in the developing rat central nervous system," *Dev. Brain Res.*, vol. 78, no. 1, pp. 35–43, 1994.
- [57] S. Ergün *et al.*, "CEA-related cell adhesion molecule 1: A potent angiogenic factor and a major effector of vascular endothelial growth factor," *Mol. Cell*, vol. 5, no. 2, pp. 311–320, 2000.
- [58] L. Oliveira-Ferrer *et al.*, "Dual role of carcinoembryonic antigen-related cell adhesion molecule 1 in angiogenesis and invasion of human urinary bladder cancer," *Cancer Res.*, vol. 64, no. 24, pp. 8932–8938, 2004.

- [59] A. Gu, W. Tsark, K. V. Holmes, and J. E. Shively, "Role of Ceacam1 in VEGF induced vasculogenesis of murine embryonic stem cell-derived embryoid bodies in 3D culture," *Exp. Cell Res.*, vol. 315, no. 10, pp. 1668–1682, 2009.
- [60] J. Long *et al.*, "Vascular endothelial growth factor (VEGF) impairs the motility and immune function of human mature dendritic cells through the VEGF receptor 2-RhoA-cofilin1 pathway," *Cancer Sci.*, 2019.
- [61] F. Zhu *et al.*, "Effects of cooking oil fume derived fine particulate matter on blood vessel formation through the VEGF/VEGFR2/MEK1/2/ERK1/2/mTOR pathway in human umbilical vein endothelial cells," *Environ. Toxicol. Pharmacol.*, vol. 69, pp. 112–119, 2019.
- [62] S. Dango *et al.*, "Elevated expression of carcinoembryonic antigen-related cell adhesion molecule 1 (CEACAM-1) is associated with increased angiogenic potential in non-small-cell lung cancer," *Lung Cancer*, vol. 60, no. 3, pp. 426–433, 2008.
- [63] A. K. Horst *et al.*, "Carcinoembryonic antigen-related cell adhesion molecule 1 modulates vascular remodeling in vitro and in vivo," *J. Clin. Invest.*, vol. 116, no. 6, pp. 1596–1605, 2006.
- [64] N. Kilic *et al.*, "Pro-angiogenic signaling by the endothelial presence of CEACAM1," *J. Biol. Chem.*, vol. 280, no. 3, pp. 2361–2369, 2005.
- [65] A. L. Nouvion *et al.*, "CEACAM1: A key regulator of vascular permeability," *J. Cell Sci.*, vol. 123, no. 24, pp. 4221–4230, 2010.
- [66] V. Khairnar *et al.*, "CEACAM1 promotes CD8+ T cell responses and improves control of a chronic viral infection," *Nat. Commun.*, vol. 9, no. 1, 2018.
- [67] A. K. Horst *et al.*, "Carcinoembryonic antigen-related cell adhesion molecule 1 controls IL-2-dependent regulatory T-cell induction in immune-mediated hepatitis in mice," *Hepatology*, vol. 68, no. 1, pp. 200–214, 2018.
- [68] M. Dankner, S. D. Gray-Owen, Y. H. Huang, R. S. Blumberg, and N. Beauchemin, "CEACAM1 as a multi-purpose target for cancer immunotherapy," *Oncoimmunology*, vol. 6, no. 7, 2017.
- [69] Y. Zhang *et al.*, "Co-expression of TIM-3 and CEACAM1 promotes T cell exhaustion in colorectal cancer patients," *Int. Immunopharmacol.*, vol. 43, pp. 210–218, 2017.

- [70] R. Kammerer, S. Hahn, B. B. Singer, J. S. Luo, and S. Von Kleist, "Biliary glycoprotein (CD66a), a cell adhesion molecule of the immunoglobulin superfamily, on human lymphocytes: Structure, expression and involvement in T cell activation," *Eur. J. Immunol.*, vol. 28, no. 11, pp. 3664–3674, 1998.
- [71] A. Nakajima *et al.*, "Activation-Induced Expression of Carcinoembryonic Antigen-Cell Adhesion Molecule 1 Regulates Mouse T Lymphocyte Function," *J. Immunol.*, vol. 168, no. 3, pp. 1028–1035, 2002.
- [72] V. M. Morales *et al.*, "Regulation of human intestinal intraepithelial lymphocyte cytolytic function by biliary glycoprotein (CD66a).," *J. Immunol.*, vol. 163, no. 3, pp. 1363–70, 1999.
- [73] D. Chen *et al.*, "Carcinoembryonic Antigen-Related Cellular Adhesion Molecule 1 Isoforms Alternatively Inhibit and Costimulate Human T Cell Function," *J. Immunol.*, vol. 172, no. 6, pp. 3535–3543, 2004.
- [74] E. Staub, A. Rosenthal, and B. Hinzmann, "Systematic identification of immunoreceptor tyrosine-based inhibitory motifs in the human proteome," *Cell. Signal.*, vol. 16, no. 4, pp. 435–456, 2004.
- [75] Y. H. Huang *et al.*, "CEACAM1 regulates TIM-3-mediated tolerance and exhaustion," *Nature*, vol. 517, no. 7534, pp. 386–390, 2015.
- [76] Z. Chen *et al.*, "CEACAM1 dampens antitumor immunity by down-regulating NKG2D ligand expression on tumor cells," *J. Exp. Med.*, vol. 208, no. 13, pp. 2633–2640, 2011.
- [77] V. Khairnar *et al.*, "CEACAM1 induces B-cell survival and is essential for protective antiviral antibody production," *Nat. Commun.*, vol. 6, 2015.
- [78] E. O. Lobo, Z. Zhang, and J. E. Shively, "Pivotal Advance: CEACAM1 is a negative coreceptor for the B cell receptor and promotes CD19-mediated adhesion of B cells in a PI3K-dependent manner," *J. Leukoc. Biol.*, vol. 86, no. 2, pp. 205–218, 2009.
- [79] G. Greicius, E. Severinson, N. Beauchemin, B. Öbrink, and B. B. Singer, "CEACAM1 is a potent regulator of B cell receptor complex-induced activation," *J. Leukoc. Biol.*, vol. 74, no. 1, pp. 126–134, 2003.
- [80] L. Chen *et al.*, "The Short Isoform of the CEACAM1 Receptor in Intestinal T Cells Regulates Mucosal Immunity and Homeostasis via Tfh Cell Induction," *Immunity*, vol. 37, no. 5, pp. 930–946, 2012.

- [81] T. P. Ducker and K. M. Skubitz, "Subcellular localization of CD66, CD67, and NCA in human neutrophils," *J. Leukoc. Biol.*, vol. 52, no. 1, pp. 11–16, 1992.
- [82] S. D. Gray-Owen, C. Dehio, A. Haude, F. Grunert, and T. F. Meyer, "CD66 carcinoembryonic antigens mediate interactions between Opa-expressing *Neisseria gonorrhoeae* and human polymorphonuclear phagocytes," *EMBO J.*, vol. 16, no. 12, pp. 3435–3445, 1997.
- [83] N. Wang *et al.*, "Carcinoembryonic antigen cell adhesion molecule 1 inhibits the antitumor effect of neutrophils in tongue squamous cell carcinoma," *Cancer Sci.*, vol. 110, no. 2, pp. 519–529, 2019.
- [84] F. Prall *et al.*, "Cd66a (BGP), an adhesion molecule of the carcinoembryonic antigen family, is expressed in epithelium, endothelium, and myeloid cells in a wide range of normal human tissues," *J. Histochem. Cytochem.*, vol. 44, no. 1, pp. 35–41, 1996.
- [85] R. Kammerer, R. Riesenberger, C. Weiler, J. Lohrmann, J. Schleypen, and W. Zimmermann, "The tumour suppressor gene CEACAM1 is completely but reversibly downregulated in renal cell carcinoma," *J. Pathol.*, 2004.
- [86] M. S. Gordon, "The Tumour Suppressor Gene CEACAM1 Is Completely but Reversibly Downregulated in Renal Cell Carcinoma," *Yearb. Oncol.*, 2006.
- [87] T. K., L. Y., S. D., and S. J., "Carcinoembryonic-antigen-related cell adhesion molecule 1 inhibits natural killer cell cytotoxicity in head and neck squamous cell carcinoma," *Otolaryngol. - Head Neck Surg. (United States)*, vol. 157, no. 1, p. P67, 2017.
- [88] Q. Li *et al.*, "NLRC5 deficiency protects against acute kidney injury in mice by mediating carcinoembryonic antigen-related cell adhesion molecule 1 signaling," *Kidney Int.*, vol. 94, no. 3, pp. 551–566, 2018.
- [89] Y. M. Li *et al.*, "Soluble Tim-3 and Gal-9 are associated with renal allograft dysfunction in kidney transplant recipients: A cross-sectional study," *Int. Immunopharmacol.*, 2018.
- [90] S. S. Ghanem *et al.*, "Age-dependent insulin resistance in male mice with null deletion of the carcinoembryonic antigen-related cell adhesion molecule 2 gene," *Diabetologia*, 2017.
- [91] C. Li *et al.*, "High-fat diet amplifies renal renin angiotensin system expression, blood pressure elevation, and renal dysfunction caused by Ceacam1 null deletion," *Am. J. Physiol. - Endocrinol. Metab.*, 2015.

- [92] J. Huang, K. J. Ledford, W. B. Pitkin, L. Russo, S. M. Najjar, and H. M. Siragy, "Targeted deletion of murine CEACAM 1 activates PI3K-Akt signaling and contributes to the expression of (pro)renin receptor via CREB family and NF- κ B transcription factors," *Hypertension*, 2013.
- [93] V. Liévin-Le Moal *et al.*, "Apical expression of human full-length hCEACAM1-4L protein renders the Madin Darby Canine Kidney cells responsive to lipopolysaccharide leading to TLR4-dependent Erk1/2 and p38 MAPK signalling," *Cell. Microbiol.*, 2011.
- [94] S. V. R. Kumar *et al.*, "Neutrophil extracellular trap-related extracellular histones cause vascular necrosis in severe GN," *J. Am. Soc. Nephrol.*, vol. 26, no. 10, pp. 2399–2413, 2015.
- [95] A. Bideak *et al.*, "The atypical chemokine receptor 2 limits renal inflammation and fibrosis in murine progressive immune complex glomerulonephritis," *Kidney Int.*, 2018.
- [96] T. Guidance, D. Analysis, and B. C. Moore, "Introduction to Western Blotting Western Blotting," *MorphoSys UK Ltd*, 2009.
- [97] S. S. Krajewski, M. M. Tsukamoto, X. Huang, and S. B. Krajewski, "Nonstripping 'Rainbow' and multiple antigen detection (MAD) Western blotting," in *Methods in Molecular Biology*, 2015.
- [98] S. R. Mulay *et al.*, "Murine Double Minute-2 Inhibition Ameliorates Established Crescentic Glomerulonephritis," *Am. J. Pathol.*, 2016.
- [99] N. R. Zerounian and M. C. Linder, "Effects of copper and ceruloplasmin on iron transport in the Caco 2 cell intestinal model," *J. Nutr. Biochem.*, 2002.
- [100] C. C. Uphoff and H. G. Drexler, "Detection of mycoplasma contamination in cell cultures," *Curr. Protoc. Mol. Biol.*, 2014.
- [101] M. A. Ferguson, V. S. Vaidya, and J. V. Bonventre, "Biomarkers of nephrotoxic acute kidney injury," *Toxicology*, vol. 245, no. 3, pp. 182–193, 2008.
- [102] A. Kubiak and Z. I. Niemir, "The role of podocytes in normal glomerular function and in the pathogenesis of glomerulonephritis. Part I. Phenotypic and functional characteristics of podocytes during their differentiation and maturity," *Postepy Hig. Med. Dosw.*, vol. 60, pp. 248–258, 2006.

- [103] Q. Xie, X. Chen, Y. Xu, J. Liang, F. Wang, and J. Liu, "CEACAM1 resists hypoxia-induced inhibition of tube formation of human dermal lymphatic endothelial cells," *Cell. Signal.*, vol. 45, pp. 145–152, 2018.
- [104] R. Li *et al.*, "Primary tumor-secreted VEGF induces vascular hyperpermeability in premetastatic lung via the occludin phosphorylation/ubiquitination pathway," *Mol. Carcinog.*, 2019.
- [105] P. Mach *et al.*, "Soluble CEACAM1 and CEACAM6 are differently expressed in blood serum of pregnant women during normal pregnancy," *Am. J. Reprod. Immunol.*, vol. 78, no. 4, 2017.
- [106] R. L. McLeod *et al.*, "Characterization of murine CEACAM1 in vivo reveals low expression on CD8+ T cells and no tumor growth modulating activity by anti-CEACAM1 mAb CC1," *Oncotarget*, vol. 9, no. 77, pp. 34459–34470, 2018.
- [107] Y. Zhu, D. Song, Y. Song, and X. Wang, "Interferon gamma induces inflammatory responses through the interaction of CEACAM1 and PI3K in airway epithelial cells," *J. Transl. Med.*, vol. 17, no. 1, 2019.
- [108] S. Yamaguchi *et al.*, "CEACAM1 is associated with recurrence after hepatectomy for colorectal liver metastasis," *J. Surg. Res.*, vol. 220, pp. 353–362, 2017.
- [109] Y. Jin, Y. Lin, L. Lin, Y. Sun, and C. Zheng, "Carcinoembryonic antigen related cellular adhesion molecule 1 alleviates dextran sulfate sodium-induced ulcerative colitis in mice," *Life Sci.*, vol. 149, pp. 120–128, 2016.
- [110] D. Zippel, H. Barlev, R. Ortenberg, I. Barshack, J. Schachter, and G. Markel, "A longitudinal study of CEACAM1 expression in melanoma disease progression," *Oncol. Rep.*, vol. 33, no. 3, pp. 1314–1318, 2015.
- [111] E. Han *et al.*, "Differences in tissue-specific and embryonic expression of mouse Ceacam1 and Ceacam2 genes," *Biochem. J.*, vol. 355, no. 2, pp. 417–423, 2001.
- [112] H. Lauke *et al.*, "Expression of carcinoembryonic antigen-related cell adhesion molecule-1 (CEACAM1) in normal human Sertoli cells and its up-regulation in impaired spermatogenesis," *Mol. Hum. Reprod.*, vol. 10, no. 4, pp. 247–252, 2004.
- [113] Z. Zhang, C. Long, X. Li, Q. Xie, M. Song, and Y. Zhang, "CEACAM-1 promotes myocardial injury following coxsackievirus infection by regulating the coxsackievirus-adenovirus receptor," *Medicine (Baltimore)*, vol. 98, no. 19, p. e15629, 2019.

- [114] S. X. Lu *et al.*, "Ceacam1 separates graft-versus-host-disease from graft-versus-tumor activity after experimental allogeneic bone marrow transplantation," *PLoS One*, vol. 6, no. 7, 2011.
- [115] L. Lucka, S. Sel, K. Danker, R. Horstkorte, and W. Reutter, "Carcinoembryonic antigen-related cell-cell adhesion molecule C-CAM is greatly increased in serum and urine of rats with liver diseases," *FEBS Lett.*, vol. 438, no. 1–2, pp. 37–40, 1998.
- [116] P. Odin and B. Öbrink, "Dynamic expression of the cell adhesion molecule cell-CAM 105 in fetal and regenerating rat liver," *Exp. Cell Res.*, vol. 164, no. 1, pp. 103–114, 1986.
- [117] R. Uchino, K. Kanemitsu, H. Obayashi, T. Hiraoka, and Y. Miyauchi, "Carcinoembryonic antigen (CEA) and CEA-related substances in the bile of patients with biliary diseases," *Am. J. Surg.*, vol. 167, no. 3, pp. 306–308, 1994.
- [118] S. Nittka, J. Günther, C. Ebisch, A. Erbersdobler, and M. Neumaier, "The human tumor suppressor CEACAM1 modulates apoptosis and is implicated in early colorectal tumorigenesis," *Oncogene*, vol. 23, no. 58, pp. 9306–9313, 2004.
- [119] S. Ashkenazi, R. Ortenberg, M. Besser, J. Schachter, and G. Markel, "SOX9 indirectly regulates CEACAM1 expression and immune resistance in melanoma cells," *Oncotarget*, vol. 7, no. 21, pp. 30166–30177, 2016.
- [120] B. B. Singer, I. Scheffrahn, R. Heymann, K. Sigmundsson, R. Kammerer, and B. Öbrink, "Carcinoembryonic Antigen-Related Cell Adhesion Molecule 1 Expression and Signaling in Human, Mouse, and Rat Leukocytes: Evidence for Replacement of the Short Cytoplasmic Domain Isoform by Glycosylphosphatidylinositol-Linked Proteins in Human Leukocytes," *J. Immunol.*, vol. 168, no. 10, pp. 5139–5146, 2002.
- [121] Z. Chen, L. Chen, S.-W. Qiao, T. Nagaishi, and R. S. Blumberg, "Carcinoembryonic Antigen-Related Cell Adhesion Molecule 1 Inhibits Proximal TCR Signaling by Targeting ZAP-70," *J. Immunol.*, vol. 180, no. 9, pp. 6085–6093, 2008.
- [122] H. S. W. Lee, M. A. Ostrowski, and S. D. Gray-Owen, "CEACAM1 Dynamics during *Neisseria gonorrhoeae* Suppression of CD4 + T Lymphocyte Activation," *J. Immunol.*, vol. 180, no. 10, pp. 6827–6835, 2008.

- [123] W. N. Khan, S. Hammarström, and T. Ramos, "Expression of antigens of the carcinoembryonic antigen family on B cell lymphomas and epstein-barr virus immortalized B cell lines," *Int. Immunol.*, vol. 5, no. 3, pp. 265–270, 1993.
- [124] W. Zhao, Y. Zhang, D. Liu, L. Zhong, Q. He, and Y. Zhao, "Abnormal expression of CD66a promotes proliferation and inhibits apoptosis of human leukemic B cells in vitro," *Leuk. Lymphoma*, vol. 56, no. 1, pp. 202–210, 2015.
- [125] H. B. Sager *et al.*, "Expression of Carcinoembryonic Antigen-Related Cell Adhesion Molecule 1 in Acute Rejection of Human Renal Allografts," *Transplant. Proc.*, vol. 41, no. 5, pp. 1536–1540, 2009.
- [126] G. Manley, J. R. Conn, E. M. Catchpoole, N. Runnegar, S. J. Mapp, and K. A. Markey, "CEACAM1 regulates TIM-3-mediated tolerance and exhaustion," *Nature*, vol. 32, no. 7, pp. 736–740, 2015.
- [127] R. Månsson, A. Lagergren, F. Hansson, E. Smith, and M. Sigvardsson, "The CD53 and CEACAM-1 genes are genetic targets for early B cell factor," *Eur. J. Immunol.*, vol. 37, no. 5, pp. 1365–1376, 2007.
- [128] G. Schley *et al.*, "Comparison of plasma and urine biomarker performance in acute kidney injury," *PLoS One*, vol. 10, no. 12, 2015.
- [129] E. D. Siew, L. B. Ware, and T. A. Ikizler, "Biological markers of acute kidney injury," *Journal of the American Society of Nephrology*, vol. 22, no. 5, pp. 810–820, 2011.
- [130] C. R. Parikh *et al.*, "Postoperative biomarkers predict acute kidney injury and poor outcomes after adult cardiac surgery," *J. Am. Soc. Nephrol.*, vol. 22, no. 9, pp. 1748–1757, 2011.
- [131] J. L. Koyner *et al.*, "Biomarkers predict progression of acute kidney injury after cardiac surgery," *J. Am. Soc. Nephrol.*, vol. 23, no. 5, pp. 905–914, 2012.
- [132] D. P. A. *et al.*, "Acute kidney injury after cardiac surgery: Role of cystatin C and NGAL," *Nephrol. Dial. Transplant.*, vol. 27, p. ii351, 2012.
- [133] A. Spahillari *et al.*, "Serum cystatin C- versus creatinine-based definitions of acute kidney injury following cardiac surgery: A prospective cohort study," *Am. J. Kidney Dis.*, vol. 60, no. 6, pp. 922–929, 2012.

- [134] J. A. Schaub *et al.*, "Perioperative heart-type fatty acid binding protein is associated with acute kidney injury after cardiac surgery," *Kidney Int.*, vol. 88, no. 3, pp. 576–583, 2015.
- [135] K. Kashani *et al.*, "Discovery and validation of cell cycle arrest biomarkers in human acute kidney injury," *Crit. Care*, vol. 17, no. 1, p. R25, 2013.
- [136] S. Sedrakyan *et al.*, "Amniotic fluid stem cell-derived vesicles protect from VEGF-induced endothelial damage," *Sci. Rep.*, vol. 7, no. 1, 2017.
- [137] W. S. Wan Ghazali, R. Iberahim, and N. S. Mohd Ashari, "Serum vascular endothelial growth factor (VEGF) as a biomarker for disease activity in lupus nephritis," *Malaysian J. Med. Sci.*, vol. 24, no. 5, pp. 62–72, 2017.
- [138] W. Deng *et al.*, "CD8+CD103+ iTregs inhibit the progression of lupus nephritis by attenuating glomerular endothelial cell injury," *Rheumatology*, 2019.
- [139] A. B. Fogo and V. Kon, "The glomerulus - a view from the inside - the endothelial cell," *International Journal of Biochemistry and Cell Biology*, vol. 42, no. 9, pp. 1388–1397, 2010.
- [140] H. Cheng and R. C. Harris, "The glomerulus - a view from the outside - the podocyte," *International Journal of Biochemistry and Cell Biology*, vol. 42, no. 9, pp. 1380–1387, 2010.
- [141] C. S. Bartlett, M. Jeansson, and S. E. Quaggin, "Vascular Growth Factors and Glomerular Disease," *Annu. Rev. Physiol.*, vol. 78, no. 1, pp. 437–461, 2016.
- [142] L. Gnudi, S. Benedetti, A. S. Woolf, and D. A. Long, "Vascular growth factors play critical roles in kidney glomeruli," *Clinical Science*, vol. 129, no. 12, pp. 1225–1236, 2015.
- [143] V. Eremina, H. J. Baelde, and S. E. Quaggin, "Role of the VEGF-A signaling pathway in the glomerulus: Evidence for crosstalk between components of the glomerular filtration barrier," *Nephron - Physiol.*, vol. 106, no. 2, 2007.
- [144] V. Eremina *et al.*, "Glomerular-specific alterations of VEGF-A expression lead to distinct congenital and acquired renal diseases," *J. Clin. Invest.*, vol. 111, no. 5, pp. 707–716, 2003.

- [145] Y. L. Zhai, L. Zhu, S. F. Shi, L. J. Liu, J. C. Lv, and H. Zhang, "Elevated soluble VEGF receptor sFlt-1 correlates with endothelial injury in IgA nephropathy," *PLoS One*, vol. 9, no. 7, 2014.
- [146] S. E. Maynard *et al.*, "Excess placental soluble fms-like tyrosine kinase 1 (sFlt1) may contribute to endothelial dysfunction hypertension, and proteinuria in preeclampsia," *J. Clin. Invest.*, vol. 111, no. 5, pp. 649–658, 2003.
- [147] N. H. Kim *et al.*, "Vascular endothelial growth factor (VEGF) and soluble VEGF receptor FLT-1 in diabetic nephropathy," *Kidney Int.*, vol. 67, no. 1, pp. 167–177, 2005.
- [148] J. Zhang, H. Su, Q. Li, J. Li, and Q. Zhao, "Genistein decreases A549 cell viability via inhibition of the PI3K/AKT/HIF-1 α /VEGF and NF- κ B/COX-2 signaling pathways," *Mol. Med. Rep.*, vol. 15, no. 4, pp. 2296–2302, 2017.
- [149] Y. Di and X. L. Chen, "Inhibition of LY294002 in retinal neovascularization via down-regulation the PI3K/AKT-VEGF pathway in vivo and in vitro," *Int. J. Ophthalmol.*, vol. 11, no. 8, pp. 1284–1289, 2018.
- [150] D. R. Green and F. Llambi, "Cell death signaling," *Cold Spring Harb. Perspect. Biol.*, vol. 7, no. 12, 2015.
- [151] D. Kanduc *et al.*, "Cell death: apoptosis versus necrosis (review).," *International journal of oncology*, vol. 21, no. 1. pp. 165–170, 2002.
- [152] E. Farber, "Programmed cell death: necrosis versus apoptosis.," *Modern pathology : an official journal of the United States and Canadian Academy of Pathology, Inc*, vol. 7, no. 5. pp. 605–609, 1994.
- [153] D. V. Krysko, T. Vanden Berghe, K. D'Herde, and P. Vandenabeele, "Apoptosis and necrosis: Detection, discrimination and phagocytosis," *Methods*, vol. 44, no. 3, pp. 205–221, 2008.
- [154] S. Elmore, "Apoptosis: A Review of Programmed Cell Death," *Toxicologic Pathology*, vol. 35, no. 4. pp. 495–516, 2007.
- [155] A. Linkermann, G. Chen, G. Dong, U. Kunzendorf, S. Krautwald, and Z. Dong, "Regulated cell death in AKI," *Journal of the American Society of Nephrology*, vol. 25, no. 12. pp. 2689–2701, 2014.
- [156] J. E. Cooper and A. C. Wiseman, "Acute kidney injury in kidney transplantation," *Current Opinion in Nephrology and Hypertension*, vol. 22, no. 6. pp. 698–703, 2013.

-
- [157] S. Manohar, P. Kompotiatis, C. Thongprayoon, W. Cheungpasitporn, J. Herrmann, and S. M. Herrmann, "Programmed cell death protein 1 inhibitor treatment is associated with acute kidney injury and hypocalcemia: meta-analysis," *Nephrol. Dial. Transplant.*, vol. 34, no. 1, pp. 108–117, 2019.
- [158] R. S. Al-Lamki *et al.*, "Expression of silencer of death domains and death-receptor-3 in normal human kidney and in rejecting renal transplants," *Am. J. Pathol.*, vol. 163, no. 2, pp. 401–411, 2003.
- [159] U. K. Messmer, V. A. Briner, and J. Pfeilschifter, "Basic fibroblast growth factor selectively enhances TNF- α -induced apoptotic cell death in glomerular endothelial cells: Effects on apoptotic signaling pathways," *J. Am. Soc. Nephrol.*, vol. 11, no. 12, pp. 2199–2211, 2000.
- [160] M. O. Hanif and K. Ramphul, *Renal Tubular Necrosis, Acute*. 2018.
- [161] M. E. Choi, D. R. Price, S. W. Ryter, and A. M. K. Choi, "Necroptosis: a crucial pathogenic mediator of human disease," *JCI Insight*, vol. 4, no. 15, 2019.
- [162] W. K. Saeed, D. W. Jun, K. Jang, and D. H. Koh, "Necroptosis signaling in liver diseases: An update," *Pharmacol. Res.*, vol. 148, p. 104439, 2019.
- [163] K. Sai, C. Parsons, J. S. House, S. Kathariou, and J. Ninomiya-Tsuji, "Necroptosis mediators RIPK3 and MLKL suppress intracellular *Listeria* replication independently of host cell killing," *J. Cell Biol.*, vol. 218, no. 6, pp. 1994–2005, 2019.
- [164] M. B. Müller *et al.*, "Exclusive expression of transmembrane TNF aggravates acute glomerulonephritis despite reduced leukocyte infiltration and inflammation," *Kidney Int.*, 2019.
- [165] M. Imamura *et al.*, "RIPK3 promotes kidney fibrosis via AKT-dependent ATP citrate lyase," *JCI insight*, vol. 3, no. 3, 2018.
- [166] H. Chen *et al.*, "RIPK3-MLKL-mediated necroinflammation contributes to AKI progression to CKD," *Cell Death Dis.*, vol. 9, no. 9, 2018.
- [167] N. Toda *et al.*, "Crucial Role of Mesangial Cell-derived Connective Tissue Growth Factor in a Mouse Model of Anti-Glomerular Basement Membrane Glomerulonephritis," *Sci. Rep.*, vol. 7, 2017.

-
- [168] J. H. Kang *et al.*, "Aliskiren Regulates Neonatal Fc Receptor and IgG Metabolism with Attenuation of Anti-GBM Glomerulonephritis in Mice," *Nephron*, vol. 134, no. 4, pp. 272–282, 2016.

9 Acknowledgement

When the collection of the thesis is about to be completed, my mood can't be calm. From the beginning of the entry to the successful completion of the thesis, how many respected teachers, classmates, and friends have given countless help. Please accept my sincere gratitude here, sincerely. thank you.

First, I would like to thank my thesis supervisor Prof. Dr. Markus Wörnle and my co-supervisor Dr. med. Marc Weidenbusch as well as my thesis committee member.

I would like to thank the Ludwig Maximilian University of Munich and the Ludwig Maximilian University of Munich School of Medicine for providing me with such a good working and learning platform, such a good learning resource and an elegant learning environment. I would like to thank all the faculty and staff of the University for their help in work and study.

I also would to thank some who give my more helpful and suggestion during the experiment., namely Dr. Ph.D. Stefanie Steiger, Dr. Ph.D. Mohammad Mohsen Honarpisheh, Dr. Ph.D Julian Marschner, Dr. M.D. Takamasa Iwakura, Janina Mandelbaum and Dan Draganovici, who performed the histological staining.

I would like to give special thanks to cand. med. Tehyung Kim who did ECIS experiment, Arzt John Hoppe who did WB experiment, M. Sc. Vet. Med. Chongxu Shi who took picture for Immunofluorescence staining, MD PhD Viviane Gnemmi who give me the slides of human kidney.

Last, I would like to give thanks to all colleague of my lab, for their daily help and the pleasure brought to me in work, namely, M. Sc. Med. Yutian Lei, cand. med. Nils Krüger, M. Sc. Vet. Med. Qiuyue Ma, MS Bioch. Manga Motrapu, M. Sc. Med. Na Li, M. Sc. Med. Wenkai Xia.

This work can't be done so smoothly, without the enthusiastic help of the tutor and classmates. Once again, I sincerely thank everyone for their meticulous care and help.

Finally, I want to thank the mice who sacrificed for human research and hope that there is no research in heaven.